Title
Dissecting Striosome Circuitry and the Mechanisms of Tardive Dyskinesia

Permalink
https://escholarship.org/uc/item/8dg0r91j

Author
McGregor, Matthew Mark

Publication Date
2022

Peer reviewed|Thesis/dissertation

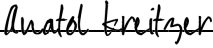Dissecting Striosome Circuitry and the Mechanisms of Tardive Dyskinesia

by
Matt McGregor

DISSERTATION
Submitted in partial satisfaction of the requirements for degree of
DOCTOR OF PHILOSOPHY

in

Neuroscience

in the

GRADUATE DIVISION
of the
UNIVERSITY OF CALIFORNIA, SAN FRANCISCO

Approved:

DocuSigned by:

Anatol Kreitzer
1CD5E76F5308469...

Anatol Kreitzer
_____
Chair

DocuSigned by:

Karunesh Ganguly

Karunesh Ganguly
_____

DocuSigned by: ...407...

Zachary Knight

Zachary Knight
_____

DocuSigned by: ...479...

AB Nelson
12024A1A01564EB...

Alexandra Nelson
_____

_____
Committee Members

Dedications

To my parents, Mark and Gina, and my sister, Molly

For their unwavering love and support of me as person, and for their wonderful combination of wit, crudeness, and absurdity.

To my outstanding mentors: Alexandra Nelson, Robert Edwards, Kevin Bender, Maryka Quik, and Gregory Aponte

For their devoted teaching, enduring support, and inspirational embodiment of all the ways a scientist can kindle joy in this world.

And to anybody in the world who simply reads and runs

For all miles and pages left behind, and many more that lie ahead.

Acknowledgments

First and foremost, I would like to thank my thesis mentor, Alexandra Nelson. Throughout my PhD, she has been the model for what I aspire to be as a scientist and as a human being. Through a combination of incredible intellect, deep compassion, unwavering integrity, and boundless energy, she has acted as a central pillar in the neuroscience community here at UCSF, raising its roof beams high. She has also built a lab that is a perfect home for doing science, or just for any oddball that loves electrodes and funny movements. I owe so much of who I am as a scientist to your mentorship. You have always treated me like I am the scientist I could become, and like I am the best version of myself, even when I have not felt that way. Through heartbreak and panic, celebration and joy, and all the little hills and valleys of doing science each day, you have been there for me. These past seven years have been the best, and I thank you for that. I can't return everything that you have given me, but I hope to pass it on to others. I hope to honor the privilege of having been a member of the Nelson Lab, and to make you proud. Thank you, Alexandra.

While in Alexandra's lab, I have had the privilege of working alongside many wonderful individuals to whom I owe thanks. When I first joined the lab, I started alongside three incredible graduate students: Ally Girasole, Michael Ryan, and Jon Schor. I cannot imagine a better group of students to have done a PhD with. Together, we formed a natural scientific machine and a lab family. My fondest and richest memories are laughing, bantering, theorizing, and problem solving (or occasionally problem creating) together with you. Thank you for your continued friendship, and for so many crazy and amazing memories. In addition to these initial members, I also owe deep gratitude to the "second wave" of the Nelson lab. Emily Twedell, Rose Creed, and Xiaowen Zhuang have moved the lab in exciting new directions. They also continue to make it a joyous and stimulating place of research. Thank you all for maintaining and building upon such a special environment. I would also like to thank the many volunteers and technicians who have assisted in the lab's research. Zoe Boosalis and Xiao Tong were volunteers who played a critical role in

the early stages of project development for investigating tardive dyskinesia. Additionally, I deeply thank Chloe Bair-Marshall, Rea Brakaj, Julia Lemak, and Jasmine Stansil for expertly managing the mouse colony, for keeping me from forgetting my own head, and for constantly making me laugh. (I also thank each of you for helping me to amass cages and for assuaging Alexandra's concerns). I would especially like to thank Jasmine Stansil, who has worked as my right-hand companion on investigating the mechanisms of tardive dyskinesia. It has been such a joy to see each of you blossom into outstanding scientists and professionals.

I also owe deep gratitude to the scientific and professional mentors outside of the lab that offered me their full support. To begin with, I thank my thesis committee. As a researcher, I have had the privilege of Anatol Kreitzer's, Zachary Knight's, and Karunesh Ganguly's keen intellectual insight to guide my thesis work. Each one of them took a genuine interest in all my projects, offering critical, yet supportive feedback that sharpened the work presented here. As a student, I have also had the blessing of their personal and professional support. Throughout graduate school, they acted as guiding lights in the foggiest of times, keeping me on a productive path and moving forward. For this, I am eternally grateful.

In addition to my thesis committee, I must thank the other faculty at UCSF whose mentorship has had an untellable impact on my career. It has been my absolute pleasure to have Kevin Bender and Robert Edwards as scientific uncles. Their fervor for the finest neural processes and for life at large is a constant reminder that science should be fun. Thank you both for your selfless support and for pushing me to grow in unexpected ways. Furthermore, I thank Dorit Ron for being a wonderful scientific colleague, mentor, and lab neighbor.

Next, I would like to thank my collaborators, John Rubenstein and Gabriel McKinsey, for laying the foundations of my thesis research and for their direct contributions. None of this work would have been possible without them, and I could not ask for better collaborators. Thank you for both being a joy to work with and for showing what fruit can come out of unexpected pairings.

Of those at UCSF, I would lastly like to thank my fellow classmates for breathing fun and excitement into my time in San Francisco. Most of all, I would like to thank my dear friend and dedicated running partner—Selin Schamiloglu—and to give her a small piece of the recognition that she deserves. Selin has the all the qualities that make an incredible scientist and the best of friends. She is sharp and creative, never failing to deliver a pun that could not possibly land a laugh (though I am certain she will dispute that). What is beyond dispute, however, is that Selin is honest to fault and relentlessly determined. She is the type of honest that comes from someone so good, that unlike the rest of us, she is unaware of the need to pretend to be better than she really is. Science and friendship are not hobbies that she can drop whenever they stop being enjoyable; they are promises she keeps out of loyalty to those she cares about. Of all the students in neuroscience program that I have known, none has done more to help those around them than Selin. Thank you for being beside me each step of the way, through the ups and downs, the good, bad, and everything in between.

Most of all, I would like to thank my family—my parents Mark McGregor and Gina Devito, and my sister Molly McGregor. Together, you understand me and love me in a way that no else can. It is this understanding and love that has sustained me through life. While others are to thank for this dissertation, you are to thank for the man writing it. You are the ones that read to me at night, taught me to write, coached all my sports teams, brought me to meadows of wildflowers, and made certain my childhood was filled with fun. You bought me a chemistry set, a microscope, countless Kinex, and my first computer. Together we choreographed karate fights, played cops and robbers at Jackson Elementary, waged trench warfare with stuffed animals, and did everything in our kid imaginations (except letting me beat you at Smash or MarioKarts). You were the ones that forgave me when I hurt your feeling, when I kicked a hole in the wall, when I forgot the SAT, when I skipped on chores, and when I did all the things I wish I could take back. Together, you taught me how to be strong, how to enjoy life, and how to be forgiving of others. I am still

learning, but I hope to make each of you proud and to provide you with the same tenacious support in life that you have given me. <u>I love you.</u>

Author Contributions

Chapter 1 of this dissertation was written by Matthew McGregor and Alexandra Nelson.

Chapter 2 of this dissertation was written by Matthew McGregor and Alexandra Nelson was reproduced in its entirety from the published work:

> McGregor M.M., Nelson A.B. (2019) Circuit Mechanisms of Parkinson's Disease. *Neuron* 101(6):1042-1056. doi: 10.1016/j.neuron.2019.03.004.

Chapter 3 was reproduced in its entirety from the published work:

> McGregor M.M., McKinsey G.L., Girasole A.E., Bair-Marshall C.J., Rubenstein J.L.R., and Nelson A.B. (2019) Functionally Distinct Connectivity of Developmentally Targeted Striosome Neurons. *Cell Reports.* 29(6):1419-1428. doi: 10.1016/j.celrep.2019.09.076.

Author contributions: M.M.M., A.B.N., G.L.M., and J.L.R.R. designed experiments. Histological validation of *hs599^{CreER}* mice were performed by G.L.M., M.M.M., and C.J.B.-M. M.M.M., A.E.G., and A.B.N. carried out electrophysiological experiments. The manuscript was prepared by M.M.M. and A.B.N., with input from G.L.M. and J.L.R.R.

Chapter 4 was written by Matthew McGregor and Alexandra Nelson and represents work that is currently in process for the manuscript:

> McGregor M.M., Stansil J.S., Schor J.S., Menon S., and Nelson A.B. Excessive Striatal Dopamine and Altered Direct Pathway Activity Drives Orofacial Movements associated with Tardive Dyskinesia. *In preparation.*

Author contributions: M.M.M and A.B.N. designed experiments. M.M.M. executed experiments involving D2 dopamine receptor knockouts and imaging of dopamine signaling. M.M.M. and A.B.N. carried out slice electrophysiology experiments. J.S. Stansil and M.M.M performed *in vivo* calcium imaging experiments. J.S. Schor design and setup of the selfie-cam recordings. S.M. developed automated detection of orofacial movements. Data was analyzed by M.M.M. The manuscript was written by M.M.M. and A.B.N.

Chapter 5 was written by Matthew McGregor.

All chapters in this dissertation were reviewed and editing by Alexandra Nelson and members of the Nelson Lab.

Dissecting Striosome Circuitry and the Mechanisms of Tardive Dyskinesia

Matthew Mark McGregor

Abstract

The basal ganglia are a group of interconnected, subcortical nuclei that mediate a wide array of behavioral functions. The primary input nucleus of the basal ganglia, the striatum, is a region implicated in behaviors ranging from motor control, reward learning, decision making, habit formation, to social interaction. How these diverse behavioral functions map onto various striatal cell types and circuit connections remains a major question within the basal ganglia field. Classical models of striatal circuitry that divide output neurons into populations called the direct and indirect pathways have proven extremely useful in understanding how the striatum mediates function such as movement initiation and behavioral reinforcement. Furthermore, such models have played a foundational role in understanding the pathophysiology of disorders linked to the basal ganglia, such as Parkinson's disease and Huntington's disease. These models, however, struggle to explain how the striatum mediates other well-established functions, and in other types of disease can even lead to behavioral predictions contrary to what is observed. Here, we began by reviewing foundational models of basal ganglia function and how they informed present understanding of Parkinson's disease mechanisms. Next, we built on this foundation by exploring how alternative models of striatal circuitry might be used to better understand basal ganglia function and dysfunction through two parallel approaches. First, we investigated whether striosome and matrix neurons—an alternative model for dividing striatal neurons—differ in the electrophysiological properties and synaptic connectivity. Early anatomical work suggested that striosome and matrix may represent two parallel circuits, relaying limbic and motor information to downstream nuclei, respectively. However, recent attempts to genetically isolate these population cast doubt upon these earlier findings. Using a developmental approach to isolate striosome and matrix neurons, we found that these population receive differing cortical input consistent with early anatomical

x

studies. Furthermore, we determined that striosome and matrix differ in how they process cortical input and where they project information within the midbrain. Next, we investigated how changes in striatal activity relate to a disorder called tardive dyskinesia (TD). Resulting from chronic administration of antipsychotic medications, TD is characterized by involuntary movements of the face, mouth, and tongue that can be irreversible once developed. Several lines of evidence implicate a causal role for the striatum in TD, and classical models predict that excessive involuntary movements may be driven by hypoactivity of indirect pathway neurons. Unfortunately, little is known about how striatal activity changes over the course of the disease. To address this gap in knowledge, we used a combination of genetic manipulations, in vivo recordings, and slice electrophysiology to determine how striatal activity changes of the development of TD. Currently in progress, our findings indicate that alternative changes outside that predicted by classical models of basal ganglia function likely underlie TD. Mainly, we find that TD may arise as the result of changes in dopaminergic signaling that affect both direct and indirect pathway neurons. In combination, the results of these projects demonstrate that additional models of striatal circuitry are necessary to describe its function, and additionally identify new cellular populations on which to build such models.

Table of Contents

List of Figures

Chapter 4

List of Tables

Chapter 1

CHAPTER 1

Introduction

1.1 Overview of Dissertation

Over the past several decades, a symbiotic relationship between basic, translational, and clinical research has critically shaped our understanding of basal ganglia function. In this dissertation, we continue that tradition by exploring basic models of basal ganglia function and by probing the underlying mechanisms of disorders such as Parkinson's disease and tardive dyskinesia.

In Chapter 1, we begin with a brief overview of the basal ganglia's circuitry and its role in behavior. Next, we introduce several models of basal ganglia function that explore how such circuitry gives rise to these behaviors. We then provide a more extensive review on striosome and matrix, two populations of striatal neurons that form the basis for a largely understudied model of basal ganglia function. Lastly, we provide an overview on a disease called tardive dyskinesia and how basal ganglia dysfunction might contribute to its manifestation.

In Chapter 2, we review the circuit mechanisms of Parkinson's disease, a disorder that fueled decades of discovery within the basal ganglia. In addition to reviewing clinical features of the disease and future directions of the field, we highlight how models of the basal ganglia and findings in Parkinson's disease inform each other.

In Chapter 3, we investigate the function of striosome and matrix neurons. Using a developmental approach to identify striosome and matrix neurons, we find that these populations differ in their upstream and downstream connectivity with other brain regions. Our findings support a model in which striosome neurons exist as part of a limbic loop within the basal ganglia that may play an important role in regulating dopamine, while matrix neurons contribute to the traditional sensorimotor loop.

In Chapter 4, we reveal preliminary findings into the brain regions, cell types, and activity patterns that mediate tardive dyskinesia. To do this, we use a mouse model of the disease in combination with *ex vivo* physiology and *in vivo* optogenetics, imaging of dopamine and neural activity, and a newly developed system for detecting orofacial movements. We find that tardive dyskinesia may result from hyperdopaminergic signaling and its impact on a subset of neurons with the ventrolateral portion of the striatum.

Lastly, we conclude in Chapter 5 by discussing how our findings fit into the current understanding of basal ganglia function. We then speculate on the future directions of research into basal ganglia and diseases such as tardive dyskinesia.

1.2 Introduction to the Basal Ganglia

1.2.1 Summary

To begin, we cover basic information pertinent to understanding the basal ganglia and the major outstanding questions about its function. We begin by detailing the basic anatomy of the basal ganglia, then the specific anatomy of the striatum. Next, we briefly cover some of the major behavioral functions it serves. Lastly, we provide introduction to several prominent models aimed at explaining how the basal ganglia mediates is behavioral functions.

1.2.2 Anatomy of the Basal Ganglia

The basal ganglia is a group of interconnected nuclei whose key parts can be divided like that of a computer into input, intermediate processors, and output. In this analogy, the user of the computer is considered to be the cerebral cortex. Thus, the structure of the basal ganglia is designed to receive information from the cortex, process it, and return some output back (Figure 1.1). Here, we cover the basic regions of the basal ganglia involved in this process.

The primary input nucleus of the basal ganglia is the striatum. Situated beneath the cortex, the striatum receives glutamatergic (excitatory) inputs from nearly every cortical region, as well

the thalamus. These glutamatergic projections are integrated with dopaminergic input from the substantia nigra pars compacta (SNc) and ventral tegmental area (VTA) (Moore and Bloom, 1978). Unlike glutamatergic signals that can directly drive neuronal firing, these dopaminergic inputs plays a modulatory role, adjusting the strength of the glutamatergic projections and the overall output of the striatum to its downstream targets.

The diverse set of synaptic input received by the striatum is next transformed and relayed by two major GABAergic (inhibitory) pathways, the "direct" and "indirect" pathways. Striatal neurons that make up the direct pathway project directly to output nuclei of the basal ganglia, the globus pallidus pars interna (GPi) and the substantia nigra pars reticulata (SNr), both of which are seated at the base of the brain. Conversely, neurons of the indirect pathway project to intermediate basal ganglia nuclei that continue to process information. First, striatal neurons project to the globus pallidus externa (GPe). The GPe then sends GABAergic projections to the only excitatory nucleus in the basal ganglia, the subthalamic nucleus (STN). Named for its position just beneath the thalamus, the STN relays excitatory projections to the GPi and SNr.

The GPi and SNr are the output "devices" of the basal ganglia. They send inhibitory projections to thalamus, which in turn innervates cortex, returning the processed information to complete the "cortico-basal ganglia-thalamo-cortical loop" (Parent and Parent, 2004). Thus, information tends to literally flow down and through the basal ganglia before being sent back up to the cortex. At the top, the cortex projects down to the striatum, which directly and indirectly send information down to the SNr and GPi, two regions that then relay it back up to the cortex through the thalamus. (In humans and other primates, the GPi is the major source of basal ganglia output. In rodents, the SNr is the major source of basal ganglia output and the GPi is referred to as the entopeduncular nucleus. For the purpose of this introduction, we will use GPi and SNr interchangeably to refer to the primary output nucleus of either primates or rodents, respectively).

What is the purpose of this basal ganglia computer within the brain? In the next section, we discuss some of the behavioral functions known to be mediated by the basal ganglia.

1.2.3 Behavioral Roles of the Basal Ganglia

The basal ganglia mediates a diverse range of behavioral functions. Early studies of the basal ganglia were heavily influenced by our understanding of disorders such as Parkinson's and Huntington's disease (DeLong and Wichmann, 2009). Although the non-motor portion of these diseases is increasingly appreciated, they have historically been viewed as movement disorders, and as a consequence the basal ganglia were believed to be primarily a motor circuit. Later, the discovery that midbrain dopamine neurons in the SNc and VTA encode rewarding stimuli expanded the role of the basal ganglia to cognition and learning (Ljungberg et al., 1992; Schultz et al., 1993, 1997). The idea that the basal ganglia updates expectations and behavior based on the outcomes of previous actions quickly emerged as one of its major functions. Since then, the basal ganglia has become well established as a key player in disorders such as addiction and depression, and multiple fields investigating its role in reward and aversion have since emerged. The addition of cognitive functions to the basal ganglia's role in behavior has led to a revised view of its motor function. Rather than simply executing movements, the basal ganglia is now thought to play a critical role in the selection of appropriate actions.

Presently, the list of basal ganglia functions continues to expand. Recent work has shown the basal ganglia is involved in motor learning, habit formation, action selection, socialization, and several forms of decision making (Gremel and Costa, 2013; Friedman et al., 2015; Kawai et al., 2015; Yttri and Dudman, 2016; Walsh et al., 2018; Zalocusky et al., 2016). As the list of basal ganglia functions grows, a major focus of the field has been to explain how these different functions map onto basal ganglia. Such efforts require identification of different cells, mapping of connectivity, and understanding of how activity patterns generate behavior. When combined, these elements come together to form a model of basal ganglia function.

In the next section, we briefly cover prominent models of basal ganglia function. For a more detailed overview of these models and how they fit into our understanding of Parkinson's disease, refer to Chapter 2.

1.2.4 Models of the Basal Ganglia Function

The Parallel Circuit Model

The parallel circuit posits that the different functions of the basal ganglia are organized in parallel lines of information flow organized along anatomical axes. Derived from early anatomical studies of the basal ganglia (Alexander et al., 1986; Alexander and Crutcher, 1990), it was shown that separation of cortical information in the striatum is maintained in subsequent downstream regions. For example, the motor cortex projects to the motor portion of the striatum, which projects to the motor portions of the GPe and GPi. Over the last several decades, the parallel circuit model has largely been confirmed (Foster et al., 2021; Lee et al., 2020), though exceptions have been recently identified (Aoki et al., 2019).

The strength of the parallel circuit model is that it provides a concrete, structural basis for how different types of information are processed within the basal ganglia. Subsequent models have focused on characterizing the processing itself.

Classical Model

The classical model of basal ganglia function focuses on how dopamine modifies the firing rate of the direct and indirect pathway to adjust motor output. In this model (Penney and Young, 1983; Albin et al., 1989; DeLong, 1990), dopamine has two main effects: 1) it increases the firing of direct pathway striatal neurons and 2) decreases the activity of indirect pathway neurons. This function was attributed to the fact that direct pathway neurons express "excitatory" (G_s-coupled) D1-type dopamine receptors (D1Rs), whereas indirect pathway neurons express "inhibitory" (G_i-coupled) D2-type dopamine receptors (D2Rs) (Gerfen and Surmeier, 2011).

Increasing direct pathway activity and decreasing indirect pathway both cause increased movement by reducing firing in the GPi. The direct pathway directly suppresses GPi activity (Freeze et al., 2013; Lee et al., 2016) so increased firing leads to greater inhibition. The indirect pathway acts through a more complicated route: inhibition of indirect pathway neurons in the

striatum 1) disinhibits neurons in the GPe, which 2) suppresses neurons in the STN, leading to 3) reduced excitatory drive to the GPi. Finally, decreases in GPi activity allow for increased activity in the thalamus and cortex that promote movement.

It is important to note that the yin-yang relationship of the direct and indirect pathways applies to other functions beyond movement. For example, the classical model has been used to explain how the basal ganglia mediates reward- and aversion-based learning. Increases in dopamine activate the direct pathway to reinforce behaviors (Matsumoto and Hikosaka, 2009; Tsai et al., 2009; Kravitz et al., 2012), whereas drops in dopamine activate the indirect pathway to inhibit behaviors (Matsumoto and Hikosaka, 2009; Kravitz et al., 2012; Danjo et al., 2014). Thus, the classical model can be nested within the parallel circuit model to understand how the basal ganglia mediates a variety of complementary functions.

A major strength of the classical model is its predictive strength in explaining how manipulations and disorders of the basal ganglia affect overall movement. Studies using optogenetics to either excite or inhibit different parts of the basal ganglia have largely confirmed predictions of the classical model (Kravitz et al., 2010; Freeze et al., 2013; Alcacer et al., 2017; Lee et al., 2016), and its development led directly to the development of deep brain stimulation, a major therapy for the treatment of Parkinson's disease. However, it is important to keep in mind that the classical model oversimplifies both the anatomical and functional connectivity of the basal ganglia, overemphasizes the importance of single-neuron firing rate versus ensemble activity, and fails to explain many behavioral phenomena.

Center Surround Model

The center-surround model aims to explain how the basal ganglia controls specific actions as opposed to overall movement. More conceptually than anatomically based, the model posits that the direct pathway selects specific actions by essentially "hole-punching" activity within the GPi (Mink, 1996). In this model, the STN controls the overall likelihood of actions by broadly

exciting the GPi (Nambu et al., 2000). What motor outputs occur ultimately depend on which portions of the GPi are activated and which parts are "hole-punched" by inhibition. This model also attempts to incorporate the role of convergent versus divergent inputs at different stages of basal ganglia circuitry.

While less well-studied than the parallel circuit or classical model, the center surround model provides a new way to think about action selection within the basal ganglia, and how this process might break down in movement disorders outside Parkinson's and Huntington's, such as those involving dyskinesia or tics. While there is anatomical evidence consistent with the center-surround model, a drawback is that it is more conceptual in nature and more difficult to map onto physical brain structures for hypothesis-testing.

The Striosome and Matrix Model

The striosome and matrix model (discussed extensively in the next section) was originally thought to explain how the basal ganglia can both select a particular action and learn from its outcome in a way that adjusts subsequent actions. Based again on the connectivity and anatomy of the basal ganglia, this model posits that matrix neurons within the striatum receive input from motor regions of the brain and drive motor action. In parallel, striosome neurons in the striatum receive information from limbic brain regions about the value of the action in the present context (i.e. did it result in a rewarding or aversive outcome) (Joel et al., 2002). The striosome neurons then modulate the matrix by controlling dopamine signaling to adjust the likelihood of selecting that action in the future.

1.3 Striosome and Matrix Model of Basal Ganglia Function

1.3.1 Summary

In this section, we provide an overview on striosome and matrix, two striatal populations whose differences have been explored over several decades, and are hypothesized to mediate

distinct basal ganglia functions. We begin by covering basic definitions of striosome and matrix, then touching briefly upon their development. Next, we cover the differences in connectivity between striosome and matrix, focusing on their inputs, local connections, and output. Lastly, we overview the potential behavioral functions of striosomes and future areas of investigation.

1.3.2 Defining Striosome and Matrix Neurons

Anatomically Definition of Striosome and Matrix

A basic understanding of the neurons that comprise the striatum and their traditional classification is necessary to understand striosome and matrix. Here, we begin with a brief overview of the output neurons of the striatum, then discuss how they are divided into striosome and matrix.

The striatum is predominantly composed of GABAergic output cells called medium spiny neurons (MSNs). The classical model of the basal ganglia divides MSNs into two populations based on dopamine receptor expression and output target (Penney and Young, 1983; Albin et al., 1989; Gerfen et al., 1990). Direct pathway MSNs (dMSNs) express D1-type dopamine receptors and project predominantly to the output nuclei of the basal ganglia, the GPi and SNr. Indirect pathway MSNs (iMSNs) express D2-type dopamine receptors and project to the GPe. These two populations are intermixed throughout the striatum in relatively even proportion and largely overlap in the morphology and electrophysiology (Gertler et al., 2008). Both have round somata (deemed "medium" sized in (Kemp and Powell, 1971) with several radial dendrites that extend out in three dimensions (Gerfen, 1988). An abundance of leak channels means that these cells rest at about -90 mV and require substantial excitatory input to spike (Nisenbaum and Wilson, 1995; Mermelstein et al., 1998). *In vivo*, both dMSNs and iMSNs are largely quiescent, typically firing around ~1 Hz, but occasionally showing bursts of activity to relevant events (Hikosaka et al., 1989). The overlapping properties of dMSNs and iMSNs made them difficult to identify, and therefore study, both in *ex vivo* and *in vivo* systems. However, differences in dopamine receptor

expression between these populations enabled development of fluorophore lines to distinguish them, and eventually Cre-recombinase lines to manipulate them (Gerfen, 1988). As a result, understanding of MSNs in terms of direct and indirect pathways has exploded over the last twenty years. Comparatively, the development of similar tools for striosome and matrix divisions lagged, as did our understanding of these divisions.

Striosome and matrix is an alternative method of classifying MSNs in the striatum. Historically, striosome and matrix has divided MSNs based on their anatomical localization within neurochemically distinct compartments within the striatum. Early studies found that post-mortem sections of striatum stained for acetylcholinesterase (a marker of cholinergic neurons) showed an uneven, or "patchy" pattern of labeling (Graybiel and Ragsdale, 1978). While the majority of the striatum densely stained for acetylcholinesterase, small islands of reduced staining appeared scattered throughout the striatum randomly. These islands were referred to as striosomes (and the cells within them striosome neurons), while the surrounding striatal cells became known as matrix neurons. Since then, numerous proteins have been found to preferentially express in either striosome or matrix compartments (see Crittenden & Graybiel, 2011 for a comprehensive overview). Two common striosome-enriched markers are the μ-opioid receptor and prodynorphin, while two common matrix-enriched markers are acetylcholinesterase and calbindin. However, unlike the strict segregation of D1Rs and D2Rs on dMSNs and iMSNs, no single protein or gene is exclusively expressed in either striosome or matrix. As a result, mouse lines and genetic tools for studying striosome and matrix have lagged behind those for the direct and indirect pathway.

It is important to note that striosome and matrix neurons are the same cells as discussed at the beginning of this section, meaning they can also be classified as dMSNs or iMSNs. Both dMSNs and iMSNs are found in striosome and matrix compartments. Thus, striosome and matrix neurons send projections to typical downstream nuclei such as the GPe and GPi. However, striosome and matrix neurons were hypothesized to differ in other forms of connectivity. Whereas dMSNs and iMSNs generally receive similar cortical and thalamic input, striosome and matrix

neurons were hypothesized to receive distinct input, with limbic regions innervating striosomes and sensorimotor regions innervating matrix, based on studies that combined anterograde tracing from cortical regions and histochemical staining in the striatum (Crittenden and Graybiel, 2011). At the same time, similar tracing studies suggested that striosome neurons may uniquely innervate SNc dopamine neurons, which exhibit powerful influence over striatal activity. The differences in striosome and matrix connectivity are discussed in greater detail later, but first we overview the developmental differences of striosome and matrix that also played a key role in defining striosome and matrix neurons.

Developmental Definition of Striosome and Matrix

Development has played an important historic role in understanding striosome and matrix. Striosome compartments were initially identified within the developing striatum as "dopaminergic islands," regions of intense dopamine marker expression (Graybiel et al., 1981; Olson et al., 1972; Tennyson et al., 1972). Subsequent studies identified that these islands were also dense in the expression of cholinergic markers (Butcher and Hodge, 1976; Graybiel and Ragsdale, 1980), and would eventually link these islands to the acetylcholinesterase-poor "patches" in the adult striatum (Graybiel et al., 1981; Nastuk and Graybiel, 1985; Newman-Gage and Graybiel, 1988), unifying them as striosomes. Since then, extensive work has outlined the development of striatal MSNs that arise from radial glial progenitor cells located in the lateral ganglionic eminence (Rubenstein and Campbell, 2013). Birthdating of striatal cells showed that striosome neurons are born and migrate earlier, while matrix neurons arise later (Graybiel and Hickey, 1982; van der Kooy and Fishell, 1987; Newman et al., 2015; Kelly et al., 2018). The regulatory factors that control striosome and matrix development are outside the scope of this introduction, but the finding that striosome and matrix differ in their birthdates is notable, as it provided new ways of identifying, targeting, and investigating striosome neurons in living tissue. Several studies have now used this difference in birthdate in combination with genetic tools for conditionally manipulating neurons

to investigate striosome function (Bloem et al., 2017; Kelly et al., 2018; Matsushima and Graybiel, 2020). In an odd twist, this trend has led the striosome and matrix field full circle. Initially identified developmentally and later defined anatomically, striosomes are once again be viewed as developmentally-defined population of neurons.

1.3.3 Circuitry of Striosomes and Matrix

Inputs to Striosomes and Matrix

Early anatomical tracing studies identified important differences in the inputs between striosome and matrix compartments. Together, these differences led to the idea that striosomes are part of a larger limbic loop within the brain, while the matrix contributes to a sensorimotor loop. Although we will focus on the differences between striosome and matrix, it is important to keep in mind 1) the majority of brain regions project to both striosome and matrix, and 2) the strength of striatal inputs also varies across major anatomical axes, meaning input strength can vary as much within either striosome or matrix compartments as it does between them.

Several cortical and thalamic regions have been identified to preferentially innervate either striosome or matrix compartments. The orbitofrontal, cingulate, and insular cortices preferentially innervate striosomes (Eblen and Graybiel, 1995; Lévesque and Parent, 1998; Ragsdale and Graybiel, 1990), as do paraventricular and rhomboid nuclei of thalamus, regions that are also interconnected with the amygdala (Ragsdale Jr. and Graybiel, 1991). Conversely, the somatosensory, motor, and association cortices preferentially innervate the matrix (Flaherty and Graybiel, 1994; Kincaid and Wilson, 1996), as do intralaminar thalamic nuclei interconnected with sensorimotor regions (Herkenham and Pert, 1981; Ragsdale Jr. and Graybiel, 1991; Sadikot et al., 1992). In addition to these cortical and thalamic regions, several subcortical structures also show biased projections to striosome and matrix compartments. Terminals from the basolateral amygdala largely appear confined to striosomes (Ragsdale and Graybiel, 1988) and more recently the bed nucleus of the stria terminalis (BNST) has been shown (using optogenetics) to

exclusively innervate striosome neurons (Smith et al., 2016). While much of what is known about inputs to striosome and matrix are based on early anatomical tracing, this latter study uses transgenic mouse lines to label striosome and matrix neurons as a means to test the synaptic strength of inputs arriving into each area. While some findings with this transgenic line align with early anatomical work (eg cingulate cortex preferentially innervating the matrix), other findings conflict (eg prelimbic cortex projections showing no preference between areas). Differences between results using anatomical and physiological techniques highlight the need for additional studies to characterize how inputs drive activity in either striosome or matrix compartments. In the next section, we discuss the local circuit elements that further shape striosome and matrix activity.

Local Circuitry of Striosomes and Matrix

The striatal microcircuit is composed of GABAergic MSNs and a variety of local interneurons. With the exception of cholinergic interneurons, all other interneuron populations are GABAergic. These GABAergic interneurons include fast-spiking (FS) interneurons (parvalbumin PV$^+$), neurogliaform-like interneurons (Neuropeptide Y, NPY$^+$), and persistent low-threshold spiking (PLTS) interneurons (NPY/somatostatin, SOM$^+$) (Tepper et al., 2010). Several differences in the microcircuitry of striosome and matrix compartments suggest that they operate as parallel lines with some crosstalk.

First, histological studies demonstrate that MSN morphology is shaped by striosome and matrix compartments. The dendrites of MSNs form radial, star-like arborizations that extend out in all directions (Walker and Graybiel, 1993; Kincaid and Wilson, 1996; Fujiyama et al., 2011). In the matrix, dMSNs have larger arborizations than iMSNs (Gertler et al., 2008). However, striosome dMSNs and iMSNs have reduced arborizations that obey the boundaries of their smaller compartments (Fujiyama et al., 2011). As mentioned above, although most cortices innervate striosome and matrix compartments, individual axons tend to innervate MSNs within a

single compartment (Kincaid and Wilson, 1996). Thus, the morphological boundaries of striosome or matrix may relate to the organization of cortical inputs into the striatum.

Anatomical and functional evidence indicates that lateral connections formed between MSNs tend to obey compartment boundaries. Although typically thought of as the output neurons of the striatum, MSNs form extensive lateral connections within the striatum. The individual strength of these lateral connections is generally low and individual MSNs are thought to make sparse connections (Czubayko and Plenz, 2002; Tunstall et al., 2002). However, the large number of MSNs forming connections means that the total lateral inhibitory input that any one MSN receives can be substantial (Wilson, 2007; Dobbs et al., 2016). Experiments in *ex vivo* slices demonstrate that this laterally connectivity is largely segregated between striosome and matrix compartments (Banghart et al., 2015). Furthermore, this study found that inhibition onto striosome, but not matrix MSNs, is sensitive to neuromodulation (inhibition) by enkephalin (Banghart et al., 2015). The restriction of lateral connectivity between striosome and matrix is notable given that dMSNs and iMSNs form lateral connections within and across pathways (Kawaguchi et al., 1990; Taverna et al., 2004, 2008).

Local interneurons are one potential source of crosstalk between striosome and matrix neurons. Differences in cholinergic markers were instrumental in early identifications of striosome and matrix, with striosome compartments thought to be devoid of cholinergic interneurons (Kubota and Kawaguchi, 1993). However, later work revealed that cholinergic neurons are present in both compartments and that while their dendrites are denser in the matrix, their axons densely innervate both striosome and matrix MSNs (Crittenden et al., 2014). More recent work in *ex vivo* slices suggests cholinergic signaling modulates the activity of both striosome and matrix MSNs (Crittenden et al., 2017). Dendrites and axons of PLTS interneurons were found to cross striosome/matrix boundaries, suggesting they may act a source of cross-communication (Bolam et al., 1988). Conversely, FSI cell bodies appear under-represented within striosomes and seem to provide sparse innervation (Banghart et al., 2015). Taken together, the local circuitry of

striosome and matrix suggests that cortical input and lateral inhibitory connections operate in separate but parallel fashion, while interneurons provide crosstalk or synchronization across compartments.

Outputs from Striosomes and Matrix

Striosome and matrix overlap in their traditional targeting of downstream basal ganglia nuclei. However, early excitement around the striosome and matrix model centered on the possibility that striosome neurons targeted dopamine neurons in the substantia nigra pars compacta (SNc). Retrograde tracing from the SNc revealed preferential labeling of striosomes (Gerfen, 1985; Jiménez-Castellanos and Graybiel, 1989) within the striatum. Later, selective (or presumed selective) toxin-based lesions of striosomes resulted in degenerating terminals within the SNc (Tokuno et al., 2002), consistent with these earlier findings. Almost a decade later, anterograde tracing of axons from single MSNs demonstrated that individual striosome, but not matrix MSNs, innervate SNc dopamine neurons (Fujiyama et al., 2011). Shortly after, development of Cre-dependent modified rabies virus would allow retrograde tracing specifically from dopamine neurons (Watabe-Uchida et al., 2012). This study demonstrated that the majority of striatal neurons innervating SNc dopamine neurons originate within striosomes.

Over the same time period, evidence was emerging that striosome MSNs may indirectly connect to SNc dopamine neurons through an alternative route. Retrograde tracing from the lateral habenula, a region known to receive input from the prefrontal cortex and innervate SNc dopamine neurons, revealed that the region received input from areas of the entopenduclar nucleus (EPN) predominantly innervated by neurons within striosome compartments (Rajakumar et al., 1993). These findings were later confirmed using cell type-specific tracing methods (Wallace et al., 2017) and have been validated *in vivo* in primates (Hong et al., 2019).

The advent of transgenic mouse lines for fluorescently labeling striosome neurons led to the discovery of structures now known as "dendritic bouquets" (Crittenden et al., 2016). Some

SNc dopamine neurons extend long dendrites into the SNr, and in certain cases dendrites from multiple neurons "bundle" together. Fluorescent labeling of striosome neurons revealed that their terminals tightly and densely innervate these dendritic bundles, forming the dendritic bouquets (Crittenden et al., 2016; Davis et al., 2018). The significance of these newly discovered structures is currently unknown, but their discovery highlights just how little is known about how striosomes regulate dopaminergic activity and what influences this connection may have on behavior.

1.3.4 Behavioral Role of Striosomes

Decades of research has explored how striosome and matrix neurons differ, yet their respective roles in shaping basal ganglia output and behavior remains mysterious. Actor-critic models of the basal ganglia posited that striosome neurons play a general role in reward learning (Joel and Weiner, 2000; Joel et al., 2002). Based on their connectivity with other limbic brain regions involved in aversion, and their theorized ability to inhibit dopamine neurons, other hypotheses suggested that striosomes mediated aspects of aversion learning. Several tremendous studies in rats, using optogenetics and behavior, indicate that striosomes may integrate positive and negative outcome information (Friedman et al., 2015, 2017, 2020). These studies found that prefrontal input to the striatum activated during decisions involving conflicting cost-benefit analysis, and activation of these inputs increased firing of striatal FSIs, which in turn inhibit striosome MSNs. Inhibition of this cortical-striosome input led to choices of high-reward / high-cost, while activation promoted choice of low-reward / low cost (Friedman et al., 2015). Furthermore, the activity of these prefrontal inputs was found to be increased by chronic stress, leading to choices of high-reward / high-cost (Friedman et al., 2017). These studies indicate that striosome neurons may play a complex role in integrating reward and punishment to shape decision making.

The recent advent of mouse lines for conditionally identifying and manipulating striosome neurons has lent further evidence that striosome neurons have a dual role in both reward and

aversion. Calcium imaging of striosome and matrix neurons during Pavlovian reward tasks reveal that these two populations respond similarly to reward, reward-predicting stimuli, and licking (Bloem et al., 2017). Deeper analysis revealed that striosome neurons show a stronger response to reward that evolves over learning, whereas matrix neurons have a weaker response to reward that is modulated more by recent reward history. A technically similar study evaluating striosome activity in Pavlovian reward and punishment settings found that some striosome dMSNs (~10%) encode aversive stimuli at some point during learning (Yoshizawa et al., 2018). While this represents only a fraction, the scarce evidence for encoding of aversive stimuli in striatal dMSNs in general suggests that striosomes may be enriched for neurons involved in aversion. Interestingly, a recent study later identified a subset of striosome neurons involved in aversion. This subset of primarily direct pathway striosome neurons are characterized by expression of Teashirt family zinc finger 1 (Tshz1) (Saunders et al., 2018; Zeisel et al., 2018) and encoded both punishing stimuli as well as punishment-predictive stimuli over the course of learning (Xiao et al., 2020). Activation of these neurons was sufficient to drive place aversion. This study provides evidence that the reward and punishment encoding of striosomes may be segregated onto molecularly distinct populations, opening up new possibilities of heterogeneity within striosomes.

1.3.5 Future Directions

A recent trend in neuroscience has been characterizing cellular heterogeneity across lines of molecular identity, connectivity, and activity patterns. Throughout the past, and even in this introduction, striosome and matrix are discussed as two monolithic populations. However, recent research has already identified heterogeneity within these populations in their molecular profiles (Gokce et al., 2016; Miyamoto et al., 2018; Märtin et al., 2019; He et al., 2021), connectivity (Matsushima and Graybiel, 2020), and function (Xiao et al., 2020). Still, little is known about the activity of striosome neurons during behavior, how their activity correlates with other striosome and matrix neurons, and how this is activity is shaped by different inputs. Exploring activity of

striosome neurons with an eye towards potential heterogeneity may reveal insights into their function. It may also address whether striosomes represent multiple pathways or a single functional unit within the striatum.

In the more immediate future, a major question is how striosomes shape the activity of dopamine neurons and dopamine release. While we show that striosome neurons functionally inhibit dopamine neurons, and are the predominant striatal source of such inhibition (see Chapter 3), how this output shapes dopaminergic activity, striatal function, and behavior remains to be seen. Much work remains to be done in terms of understanding striosome and matrix, but the rapid evolution of tools for their study points to a bright and exciting future.

1.4 Clinical Features and Models of Tardive Dyskinesia

1.4.1 Summary

In this section, we cover the clinical features of the disorder tardive dyskinesia (TD), a condition that results from chronically taking antipsychotic medication. We begin with a brief historical overview of psychiatric medications and then explore some of the risk factors and treatments related to TD. Next, we cover several prominent models on the mechanisms underlying TD. Lastly, we provide an introductory background on the animals that have been used to build such models and speculate on future directions of the field.

1.4.2 Clinical Features of Tardive Dyskinesia

Antispychotic Drugs and the Generation of Tardive Dyskinesia

Antipsychotic drugs are the mainstay treatment for diseases such as schizophrenia, bipolar disorder, and Tourette's syndrome. Currently, there are two broad classes of antipsychotic drugs: first generation and second generation. First generation antipsychotics (also known as typical antipsychotics or neuroleptics) were discovered in the 1950s and approved by the FDA over the next three decades (Figure 2.1). Characterized by their antagonism of D2-type dopamine

receptors (D2Rs), these drugs were found to alleviate many of the "positive" symptoms associated with psychosis, including hallucinations, delusion, and paranoia. They were also found to have marked motor effects. Parkinsonian symptoms such as bradykinesia (slowing of movement) and akinesia (lack of movement), as well as other motor symptoms such as dystonia (muscle contractions that cause twisting or repetitive movements) and akathisia (restlessness) were commonly noted. In fact, so tightly intertwined were the motor effects (often referred to as extrapyramidal symptoms) that they were initially considered necessary to achieve therapeutic benefits. However, another motor side effect began to emerge over time, one that presented a more persistent clinical problem. During chronic treatment, patients often developed involuntary movements of the face and mouth, including lip smacking, chewing, tongue protrusions, as well as brow raising and furrowing. Due to its late development (occurring after months to years of treatment), this condition was termed tardive dyskinesia (TD). Several aspects of TD differed from the acute motor effects of antipsychotic drugs. First, TD emerged only after prolonged treatment. Secondly, unlike the acute effects, the involuntary movements of TD were often irreversible once developed, even if the offending medication was discontinued. The observation that antipsychotics could cause an essentially irreversible neurological disorder raised concern and fueled research into new treatments for psychiatric disorders.

The discovery of clozapine opened the door to second generation antipsychotics and the possibility of alleviating symptoms of psychiatric disorders without such severe motor side effects (See Figure A). In contrast to first generation antipsychotics, second generation antipsychotics typically had lower affinity for D2Rs and stronger antagonism at serotonergic receptors (such as 5HT2A). As the motor side-effects of antipsychotics had been linked to their occupancy of D2Rs, second generation antipsychotics were thought to carry lower risk of both acute motor impairment as well as TD. While second generation antipsychotics, especially clozapine, do indeed have a lower risk of acute motor effects and a lower incidence of TD (Casey, 2006; Woods et al., 2010), there is still substantial risk, which has become evident the longer second generation drugs have

been used. Additionally, second generation antipsychotics have been associated with other side effects, such as metabolic alterations (Divac et al., 2014), and have overall comparable tolerability to first generation drugs (Casey, 2006; Jones et al., 2006). As a result, both the acute motor symptoms and the development of TD remain major issues in the treatment of psychiatric illness.

Incidence and Risk Factors of Tardive Dyskinesia

The prevalence and incidence rates of TD have historically been a source of controversy. After the introduction of first generation antipsychotics and the discovery of TD in the 1960s, editorials from psychiatrists downplayed its significance, claiming that the disorder was rare or non-existent (Brandon et al., 1971; Kilpatrick and Whyte, 1965; Kline, 1968; Paulson, 2005; Caroff et al., 2018). Since then, TD has been recognized as major problem, only to be downplayed once again with the introduction of second generation antipsychotics (Divac et al., 2014). Despite these bursts of initial optimism with each generation of antipsychotics, TD remains a problem.

It is estimated that 4-5% of people currently taking antipsychotics will develop TD each year (Caroff, 2019). Prevalence (the number of people on antipsychotics experiencing TD at any one time) is estimated to be ~25% (Carbon et al., 2017; Caroff, 2019). The risk of developing TD depends on several factors, including antipsychotic type, dose, and treatment duration (Miller et al., 2005; Woods et al., 2010; Carbon et al., 2017; Solmi et al., 2018). First generation antipsychotics such as haloperidol have an estimated TD prevalence of 30%, whereas second generation antipsychotics are thought to have prevalence rates around 20%. In addition to these drug-related factors, patient-related aspects such as age, female sex, and Caucasian or African ethnicity have also been identified as potential predictive factors (Morgenstern and Glazer, 1993; Miller et al., 2005; Carbon et al., 2017; Frei, 2019).

Current trends in the prescription of antipsychotic medications suggest that TD is likely to become a growing rather than shrinking problem. Although the global prevalence of psychosis is estimated at 0.7% (Moreno-Küstner et al., 2018), 1.6% of American adults (~3.8 million) are

currently taking antipsychotic medications at a given time (Dennis et al., 2020). This number has been increasing in part due to off-label prescription of antipsychotics for other uses (Comer et al., 2011). Given the shortcomings of second generation antipsychotics and the continued use of first generation drugs, TD is poised to persist as a problem for millions of people.

Genetic Risk Factors in Tardive Dyskinesia

Several genetic polymorphisms have been linked to TD risk, though reports for many have been inconsistent. Generally, these genes fall into two categories: 1) those that function outside of the brain and 2) those directly involved in neural signaling. Expressed in the liver, the enzyme cytochrome P450 family 2 subfamily D member 6 (CYP2D6) is involved in the clearance of antipsychotic drugs, and reduced CYP2D6 function is thought to increase the risk of TD by increasing cumulative drug dose (Patsopoulos et al., 2005; Miksys et al., 2017). Another gene implicated in TD is Heparan sulfate proteoglycan 2 (HSPG 2), which encodes perlecan, a component of the blood-brain barrier. Although it's unclear how changes in perlecan function may relate to the disease (Frei, 2019), this gene has been identified in multiple studies and patient populations (Syu et al., 2010; Greenbaum et al., 2012; Zai et al., 2018a).

Genes affecting neurotransmission and TD risk are typically involved in dopaminergic signaling. Polymorphisms in the DRD2 and DRD3 genes (which encode D2- and D3-type dopamine receptors) appear to increase risk of TD (Hori et al., 2001; Bakker et al., 2006; Mo et al., 2007; Zai et al., 2007, 2009; Koning et al., 2012), though not in all cases (Park et al., 2011; Tsai et al., 2010; Utsunomiya et al., 2012). Polymorphisms in the vesicular monoamine transporter 2 (VMAT 2, see section below for further discussion) have also been linked to TD risk (Zai et al., 2013, 2018b). However, no single gene or mutation has been identified to cause TD, nor predict the likelihood of TD with high confidence. Thus, while genetics may influence the likelihood or severity of TD, they are only one contributing factor.

Available Treatments for Tardive Dyskinesia

There is currently no cure for TD, although recently, two drugs which reduce its severity have been FDA-approved. These compounds are part of a larger group of related drugs that includes tetrabenazine, a competitive inhibitor of the vesicular monoamine transporter 2 (VMAT2). VMAT2 packages dopamine in synaptic vesicles, so tetrabenazine and its relatives lead to synaptic dopamine depletion. Indeed, one theory is that excessive dopamine signaling contributes to TD (see more below). Upon oral administration, tetrabenazine is converted into metabolites ((+)α and (+)ß-dihydrotetrabenazine) that block VMAT2 and therefore prevent the normal release the dopamine (Roberts et al., 1986; Grigoriadis et al., 2017). It is through this mechanism that tetrabenazine is thought to reduce involuntary movements.

Though the parent compound tetrabenazine is approved for treating chorea (involuntary dance-like movements) resulting from Huntington's disease, a long-acting version, deutetrabenazine, is approved for treatment of TD. Deutrabenazine is constructed by replacing six of the hydrogen atoms on tetrabenazine with deuterium (heavy hydrogens), making it more resistant to metabolism (Howland, 2015). As a result, deutrabenazine can be taken once or twice per day, instead of three times per day like tetrabenazine (Koch et al., 2020).

The second drug approved for treatment of TD is valbenazine. This drug is the tetrabenazine metabolite (+)α-dihydrotetrabenazine with a valine attached, which is also meant to delay metabolism. Upon cleavage of the valine ester, valbenazine becomes (+)α-dihydrotetrabenazine, acting just as when derived from tetrabenazine itself. Like deutrabenazine, valbenazine can be taken once a day.

It is critical to note that deutrabenazine and valbenazine are not cures for TD and that their current cost far exceeds the value they provide to patients. According to a study by the Institute or Clinical and Economic Review, these drugs would have to be discounted ~90% to meet thresholds for long-term cost effectiveness (Vesicular Monoamine Transporter 2 Inhibitors for Tardive Dyskinesia: Effectiveness and Value, www.icer-review.org). As a society, we should consider the morality in prescribing drugs known to create a permanent disorder, then prescribing

additional drugs to treat that disorder (all at the expense of patients and towards the profit of pharmaceutical companies). Given the current treatment options for psychiatric disease and TD, new and accessible therapies are urgently needed.

1.4.3 Models of Basal Ganglia Dysfunction in Tardive Dyskinesia

D2R Supersensitivity Hypothesis

The supersensitivity hypothesis adopts from the classical model of basal ganglia function that has proven useful for understanding disorders such as Parkinson's and Huntington's disease. In this model, chronic antagonism of D2Rs on striatal iMSNs is thought to lead to a homeostatic upregulation of D2R signaling. This upregulation is hypothesized to become maladaptive, leading to excessive inhibition of the indirect pathway and excessive motor output.

Many of the acute and chronic motor effects of antipsychotic treatment can be explained using the supersensitivity hypothesis. First, antipsychotics like haloperidol are well known for the ability to acutely induce dose-dependent parkinsonism. Secondly, studies demonstrate that TD severity can transiently worsen if antipsychotics are stopped (Marsden and Jenner, 1980; Peralta and Cuesta, 2010; Peralta et al., 2010). In this case, discontinuation of D2R agonists is thought to restore dopaminergic signaling via sensitized D2R on iMSNs, leading to strong inhibition of these neurons. Based on this theory, one might predict that increasing D2R antagonism might actually relieve TD, despite having initially caused it. Indeed, increasing antipsychotic dose or switching to a drug with more potent D2R antagonism can temporarily suppress TD (Crane, 1973; Marsden and Jenner, 1980). The ability to neatly explain these paradoxes initially made the supersensitivity hypothesis appealing. However, evidence in both animal models of TD and patients has led to a more complicated picture.

Early scientific evidence for the D2R supersensitivity hypothesis arose from studies characterizing the tendency of antipsychotic drugs to enhance the acute motor effects of dopaminergic drugs. Inspired by the discovery that dopaminergic denervation by 6-OHDA led to

an enhanced motor response to dopaminergic agents such as levodopa (Klawans, 1973), several studies in mice and rats found that pretreatment with antipsychotics such as haloperidol, chlorpromazine, and reserpine exacerbated locomotion or stereotypies in response to compounds like apomorphine and methamphetamine (Schelkunov, 1967; Tarsy and Baldessarini, 1973, 1974; Vonvoigtlander et al., 1975; Martres et al., 1977). In line with these findings, biochemical studies later found that antipsychotic treatment also increased D2R mRNA, protein, and binding levels (Burt et al., 1977; Savasta et al., 1988; Rogue et al., 1991; Lévesque et al., 1995; D'Souza et al., 1997; Florijn et al., 1997). Despite these findings, several major observations were not consistent with the supersensitization hypothesis. Increases in D2R binding were not observed in every case (Waddington et al., 1983), and even when increases were found, they were not predictive of whether animals actually developed orofacial dyskinesia (Shirakawa and Tamminga, 1994; Bachus et al., 2012). Additionally, studies testing whether D2R signaling is functionally increased by chronic antipsychotic treatment have found no evidence for enhanced signaling on iMSNs (Jiang et al., 1990; Kruyer et al., 2021).

It is important to note that while the supersensitivity hypothesis is in line with several behavioral effects of antipsychotic drugs, it is less accurate in predicting changes in neural activity. *In vivo* single-unit recordings in rats administered haloperidol found that activity of striatal MSNs was reduced overall compared to baseline (Yael et al., 2013). Given the low firing rates of MSNs (~1 Hz), it is likely that the activity of both direct and indirect pathway neurons is reduced. Additionally, work using conditional knockout of D2Rs to investigate antipsychotic-induced parkinsonism highlighted that D2R signaling on other striatal cell types may play a critical role in motor output (Kharkwal et al., 2016). They found that deletion of D2Rs from striatal cholinergic interneurons blocked drug-induced parkinsonism in response to acute haloperidol, while deletion from iMSNs did not prevent this response to haloperidol. Work such as this highlights the necessary interplay between theoretical models and empirical data on neural activity in understanding disease mechanisms.

Studies from patients with TD have found little evidence for the supersensitivity hypothesis. Positron Emission Tomography (PET) imaging of D2R availability in patients with or without TD have observed no difference in maximum binding or binding sensitivity (Kornhuber et al., 1989; Andersson et al., 1990; Adler et al., 2002). Furthermore, measurement of D2R expression levels in post mortem tissue from patients who have been off medication for several months or more has found similar, or even reduced, D2R levels in TD patients compared to those who received antipsychotics but did not develop TD (Blin et al., 1989; Reynolds et al., 1992). The latter studies also point to another caveat in the supersensitivity hypothesis; while TD persists after cessation of antipsychotic treatment, D2R levels appear to decrease to baseline. It is important note though that alterations in D2R signaling downstream of receptor expression itself could still contribute to the development of TD through altered plasticity. Still, the transience of D2R upregulation, its temporal disconnect from behavior, and the lack of evidence in patients with TD all cast doubt on the supersensitivity hypothesis.

Degeneration Hypothesis

The degeneration hypothesis addresses a major shortcoming of the supersensitivity hypothesis: the persistence of TD after withdrawal from treatment. According to this hypothesis, antipsychotics lead to irreversible neurodegenerative processes that in turn drive TD. Increased turnover of dopamine in response to antipsychotic treatment (See, 1991) has been hypothesized to increase free-radical production, leading to cell damage and cell death (Cho and Lee, 2013). Evidence that such free radicals may contribute to TD come from several studies that have a reduction in TD severity with vitamin E treatment (Cho and Lee, 2013). However, a major caveat to the degeneration hypothesis is the lack of overt degeneration or cell loss within the striatum, where dopamine release and turnover are likely to be highest. Studies of post mortem tissue from TD patients have no overt signs of cell loss in the striatum (Hunter et al., 1968; Christensen et al.,

1970) and multiple computerized tomography (CT) scan studies have identified no difference in striatal volume between patients with or without TD (Swayze et al., 1988).

Others have hypothesized that chronic antipsychotic treatment may lead to selective degeneration of particular cell-types, such as cholinergic interneurons within the striatum, which might not be labeled in standard postmortem analyses, nor significantly contribute to striatal volume on imaging studies. While an early study identified markers of degeneration in putative cholinergic interneurons in the striatum (Miller and Chouinard, 1993) and several studies in rodents have found reduced cholinergic interneurons as identified by choline acetyltransferase (ChAT) staining (Mahadik et al., 1988; Kelley and Roberts, 2004; Angelucci et al., 2000), we can find no additional studies in TD patients investigating loss of cholinergic interneurons.

Aberrant Plasticity Hypothesis

The idea that aberrant plasticity underlies TD was likely born from the shortcomings of the supersensitivity and degeneration hypotheses. Newer and less explored, aberrant plasticity hypotheses aim to explain both how neural activity might change in TD and how such changes could be irreversible (Teo et al., 2012). According to these models, chronic D2R antagonism does not directly modulate neural activity, but alters corticostriatal plasticity to promote unidirectional and/or aberrant motor learning. While few studies have directly tested this hypothesis in TD patients or animal models, aberrant plasticity has been demonstrated in several other disorders involving the striatum (Plotkin and Goldberg, 2019), and a variety of studies have shown that antipsychotics can alter normal plasticity.

Plasticity of excitatory inputs within the striatum is dependent on a complex interaction of various neurotransmitter systems, many of which are altered by antipsychotic drugs. Studies in humans show that antipsychotics can impair plasticity within primary motor cortex (Korchounov and Ziemann, 2011; Nitsche et al., 2009), a major source of excitatory input to the motor portions of the striatum. Additionally, studies in slice have identified a key role of dopamine and D2R

receptors in plasticity of MSNs (Calabresi et al., 1992; Kreitzer and Malenka, 2007; Shen et al., 2008; Iino et al., 2020). High-frequency stimulation paired with depolarization as well as spike-timing dependent plasticity have been shown to induced cannabinoid dependent long-term depression (LTD) in iMSNs (Kreitzer and Malenka, 2007; Shen et al., 2008; Wang et al., 2006). Short-term haloperidol treatment (< 1 month) has been shown to increase glutamatergic synapses in the striatum (Kerns et al., 1992; Meshul et al., 1992) and convert normal LTD in response to high-frequency stimulation into aberrant LTP (Centonze et al., 2004). Furthermore, this aberrant form of plasticity could be replicated by D2R deletion as well (Centonze et al., 2004). In addition to the direct role of D2Rs on iMSNs in corticostriatal plasticity, numerous indirect roles likely exist through modulation of neurotransmitter systems critical for plasticity. Antipsychotics may alter other neurotransmitter systems critical for plasticity indirectly, or act on other cell types such as cholinergic interneurons (Augustin et al., 2018; Calabresi et al., 1992; Wang et al., 2006). Other lines of evidence point to a potential role for pharmacological actions on non-dopamine receptors.

Haloperidol (high risk of TD) and clozapine (low risk of TD) have different effects on NMDA receptors (NMDARs), which has been cited as another piece of indirect evidence supporting the aberrant plasticity hypothesis. First generation antipsychotics like haloperidol have a higher tendency to induce TD compared to second generation antispychotics like clozapine, which has one of the lowest incidence rates (Strous et al., 2006; Novick et al., 2010). Several groups have studied how these two agents differ in order to investigate the role of plasticity in TD. Unlike haloperidol, short-term clozapine treatment was *not* found to increase excitatory synapses within the striatum (Meshul et al., 1992). Additionally, several studies have found that clozapine, but not haloperidol, enhances NMDAR currents through a series of complex mechanisms (Arvanov et al., 1997; Leveque et al., 2000; Wittmann et al., 2005). NMDARs have been shown to play a role in particular types of striatal plasticity (Shen et al., 2008; Yagishita et al., 2014), though the link between their function and TD is more tenuous.

The biggest limitation to the aberrant plasticity hypothesis is a dearth of evidence linking changes in plasticity to the development of TD. This lack of evidence in humans is unsurprising given the difficulty in measuring plasticity within deep structures. However, primate and rodent models of TD have existed for decades (see below). Given the extensive and foundational work on plasticity done in such rodents, these particularly represent an untapped front for investigating the role of aberrant plasticity in TD. In the next section, we review these and other animal models of TD.

1.4.4 Animal Models of Tardive Dyskinesia

Non-human Primate

Studies have used chronic treatment with antipsychotic drugs in combination with several species of non-human primates (NHPs) as potential pre-clinical models of TD with varying success. Direct comparison across species is difficult, in part due to differences in the particular antipsychotic used, dose, administration route, and treatment duration (Table 1.1). Low rates of TD have been observed in rhesus macaque (a common primate choice for preclinical models), with most studies finding no TD (Lidow and Goldman-Rakic, 1994; O'Connor et al., 2006, 2007), and only handful finding TD in any animals (Deneau & Crane, 1969; Paulson et al., 1973; McKinney et al., 1980; Bedard et al., 2011). While potentially reflective of the overall rates of TD observed in human patients, this has made the rhesus macaque model prohibitively costly. Of the several other primate species that have been tested as models of TD (Gunne and Bárány, 1976; Weiss et al., 1977; Bárány et al., 1979; Kovacic and Domino, 1982; Baca-Garcia et al., 1999; Halliday et al., 2002; Klintenberg et al., 2002; Jackson et al., 2004; Dorph-Petersen et al., 2005), capuchins treated with either fluphenazine or haloperidol appear to have the highest rates of TD, though it is worth noting that studies largely come from a single research group several decades ago. In fact, despite NHP models sharing the closest behavioral phenotype to human TD of any animal model, research involving NHP models of TD appear to have declined substantially over

the last decade. This may relate to declining use of NHP models overall, driven in part by the labor-, time- and resource-intensive nature of NHP research, especially with the prolonged drug treatments typically required to induce TD. Still, the decline in NHP models may be in part due to the advantages of other models such as mice and rats, both of which offer increasingly greater toolkits for mechanistic investigations.

Rat

The majority of animal model research in TD has been performed in rats chronically treated with antipsychotic medication. As noted in another excellent review of animal models in TD (Blanchet et al., 2012), early work in rat models of TD has been definitively reviewed previously (Waddington, 1990; Turrone et al., 2002). Here, we review key behavioral features identified in rat models of TD that have laid the groundwork for TD models in mice.

The core behavioral metric of rat TD models is the development of vacuous chewing movements (VCMs). Defined generally as overt chewing movement unrelated to grooming, exploration, or consumption, VCMs can also include tongue protrusions and jaw tremor. VCMs are most commonly scored in 2-5 minute periods, often by a live rater. In certain cases, rats have been restrained to obtain video of the rat's face, with VCMs scored manually by an offline rater. Healthy, wild type animals typical exhibit low, though non-zero, rates of VCMs. Animals treated with high doses of first generation antipsychotics (most commonly haloperidol) for several weeks can begin to display increased VCM frequency. Generally, VCMs that emerge at this early time interval (< 3 months) are not considered a "true" model of the persistent TD seen in patients, as they often resolve after discontinuation of drug. In addition, their frequency can be reduced by treatment with anticholingergics (Waddington, 1990; Egan et al., 1996; Marchese et al., 2004). Generally, a minimum of several months of treatment are considered necessary to induce VCMs that persist even after drug discontinuation in the rat model. However, several other factors affect the development of VCMs, in addition to treatment duration.

The particular antipsychotic drug, delivery route, and dose are also believed to influence the development of VCMs. Haloperidol carries a relatively high risk of TD in patients and has commonly been used in rats for this reason, though it is not the only drug found to induce persistent VCMs (Waddington et al., 1983). Continuous routes of administration (minipumps, slow-release pellets, depot injections) are considered to produce more robust VCMs than intermittent routes such as daily intraperitoneal or subcutaneous injections (Turrone et al., 2002). Lastly, as in TD patients, higher doses are thought to increase the likelihood of developing VCMs. Interestingly though, even with continuous administration of high dose haloperidol over several months, the proportion of animals that develop VCM frequencies above those observed in healthy animals generally ranges between 30-50% (Blanchet et al., 2012). While a substantially higher rate than for patients treated over the same time period, the rat model does recapitulate the incomplete penetrance of TD seen in human patients chronically treated with antipsychotics. In combination with their convenience and reduced cost, the ability of rats to 1) partially recapitulate the orofacial dyskinesia observed in TD and 2) mimic the persistence of the disease has made them popular as an animal model.

Mouse

Use of mice in modeling TD has been historically rarer than that of rats, despite their ability to recapitulate many of the same features. Administration of antipsychotics at high doses over several months has remained a standard, and like rats, mice typically develop increased VCMs with 3-4 weeks of treatment (Carvalho et al., 2003; Ceretta et al., 2018). As in rats, a handful of studies in mice have been used to investigate the role of specific genes or potential treatments in modulating VCMs (Crowley et al., 2013; Ceretta et al., 2018; Sonego et al., 2018). Of note, multiple studies have characterized genetic factors across mouse strains relating to development of VCMs (Crowley et al., 2012; Giusti-Rodríguez et al., 2020). In addition to highlighting genes and inheritable factors that may relate to TD, these studies also provide an excellent

characterization for modeling TD across mouse strains and should serve as a tool in expanding TD research.

In addition to the genetic work being done in mice, several studies have recently highlighted the use of mice to study cellular and circuit mechanisms relating to TD. One study used a combination of transgenic mice and optogenetics to highlight the potential of cholinergic interneurons in alleviating TD (Bordia et al., 2016), while another used a combination of calcium-imaging, transgenic mice, and exogenous channel overexpression to test how short-term antipsychotic activity impacts D2R sensitivity and striatal activity (Kruyer et al., 2021). With genetic toolskits increasing alongside methods for measuring population activity and finer quantification of behavior, these studies highlight exciting uses for mice in the research and understanding of TD.

1.4.5 Conclusion

People treated with antipsychotic medications continue to suffer from the development of TD. While certain risk factors of TD can be mitigated, others are unavoidable, and no patient on antipsychotic medications for prolonged periods is safe from developing TD. With few treatment options available, and the high cost of currently approved treatments, there is a critical need for the development of new approaches to resolving TD. Better understanding of the mechanisms underlying TD will likely be key in these efforts. Previous models have fueled essential research into mechanisms of TD, but additional models and more evidence are needed before a coherent picture can be painted. Most critically, changes at the molecular and cellular level need to be linked to changes in neural activity and behavior in animal models of TD. Fortunately, decades of research have established TD models in non-human primates, rats, and mice. With these tools, the foundational knowledge of prior work, and the rapid emergence of tools for understanding the brain, current researchers are poised to advance our understanding and treatment of TD.

Although just a small step in curing psychiatric disease, such advances could represent leaps for

the well-being and happiness of patients.

1.5 Tables

Table 1.1: Overview of studies involving non-human primate models of tardive dyskinesia.
List of species, antipsychotic drug, dose, administration route, treatment duration, dyskinesia rate, delay until dyskinesia onset, and reference.

Species	Drug	Route	Duration (months)	Dose (mg/kg*day)	TD Rate	Induction Delay	Reference
Macaca mulatta (Rhesus macaque)	Chlorpromazine	oral	20	30	0/17	-	Deneau, 1938
	Chlorpromazine	oral	3-9	30	4/10	9 months	Paulson, 1973
	Chlorpromazine	oral	6	8 to 40	4/4	uncertain	McKinney, 1980
	Clozapine	oral	6	5.2	0/4	-	Lidow, 1994
	Clozapine	oral	6	5.2	0/5	-	O'Connor, 2006a
	Clozapine	oral	6	5.2	0/5	-	O'Connor, 2006b
	Haloperidol	oral	4-9	0.5	0/15	-	Paulson, 1973
	Haloperidol	oral	3-9	0.25	1/6	2 months	Bédard , 1977
	Haloperidol	oral	28	0.2	0/4	-	Lidow, 1994
	Haloperidol	oral	6	0.14	0/5	-	O'Connor, 2006a
	Haloperidol	oral	6	0.14	0/5	-	O'Connor, 2006b
	Remoxipride	oral	6	3.7	0/4	-	Lidow, 1994
Macaca Speciosa (Stump-tailed macaque)	Fluphenazine Haloperidol	intramuscular	60	1.0 & 6.0	1/8	After withdrawal	Baca-Garcia, 1999
Macaca Fascicularis (Cynomolgus macaque)	Haloperidol	oral	17-27	0/6		-	Dorph-Peterson 2005
	Olanzapine	oral	17-27	0/6		-	Dorph-Peterson 2005
Papio Ursinus (Baboon)	Haloperidol	intramuscular	11		4/4	4 months	Halliday, 1999
Saimiri sciureus (Squirrel monkey)	Haloperidol	oral	8-13	0.5	0/5	-	Weiss, 1977
Cebus apella (Capuchin)	Fluphenazine	intramuscular	12	~0.007-0.22	3/3	12 months	Kovacic, 1982
	Fluphenazine	intramuscular	36-48	~1.2-3.3	3/3	24-36 months	Gunne, 1984
	Fluphenazine	intramuscular	12	~0.01	6/19	after withdrawal	Lifshitz, 1991
	Haloperidol	oral	4-16	0.5	2/3	3-12 months	Gunne, 1976
	Haloperidol	oral	12	0.1-0.5	2/2	12 months	Gunne, 1979
	Haloperidol	oral	8-32	0.5-1.0	2/3	14-28 month	Weiss, 1977
	Haloperidol	oral	3-35	0.05-1.0	4/11	3-34 months	Barany, 1979
	Haloperidol	intramuscular	36-48	~0.25-3.3	3/3	24-36 months	Gunne, 1984
Callithri jacchus (Marmoset)	Haloperidol	intramuscular	12	~0.15-0.45	12/13	3-14 months	Klintenberg, 2002
	Haloperidol	oral	24	0.25-3.0	0/4	-	Jackson, 2004

1.6 Figures
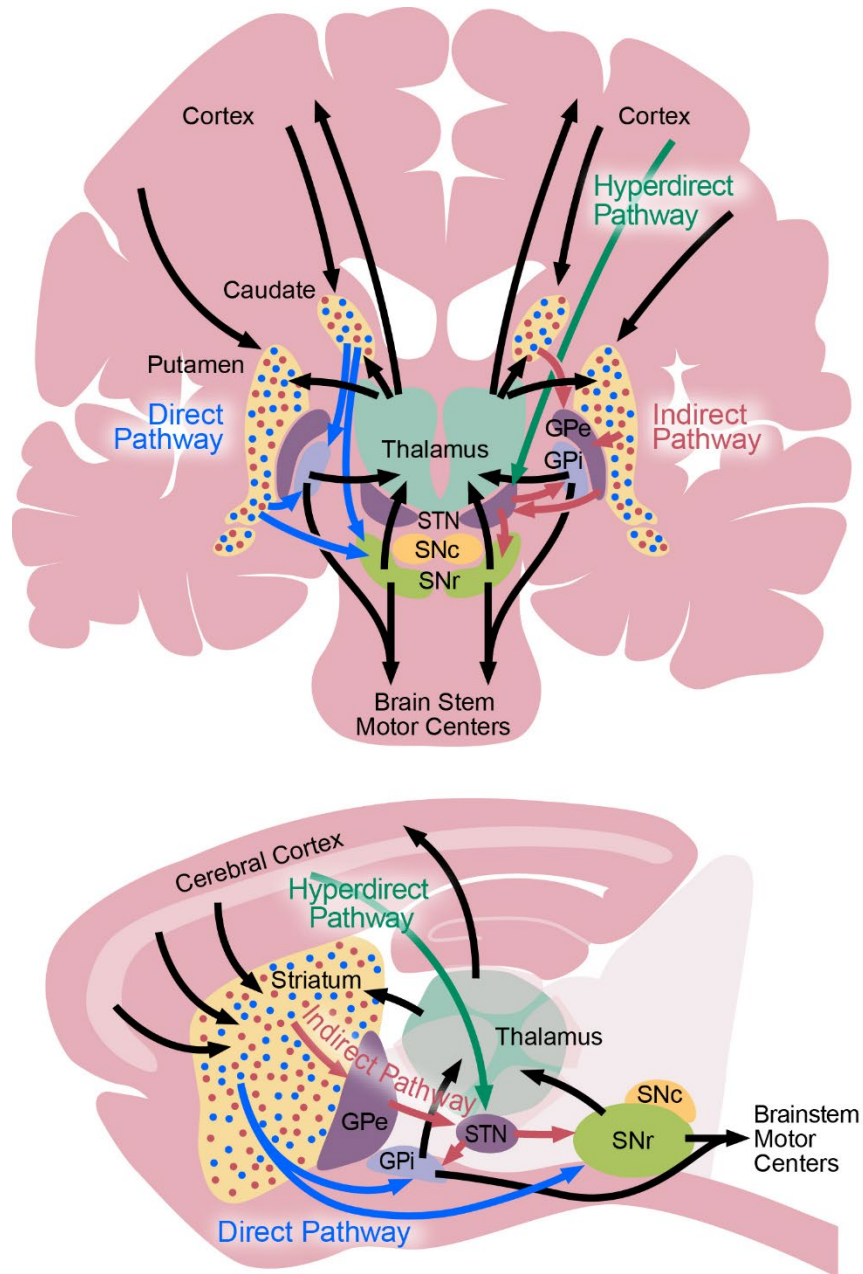
Figure 1.1: Anatomy of the basal ganglia. Above: Coronal section of the human basal ganglia. Below: Sagittal section of the rodent basal ganglia. Abbreviations: GPe = globus pallidus externa, GPi = globus pallidus interna, SNc = substantia nigra pars compacta, SNr = substantia nigra pars reticulata, STN = subthalamic nucleus

.

History of Antipsychotics and Tardive Dyskinesia
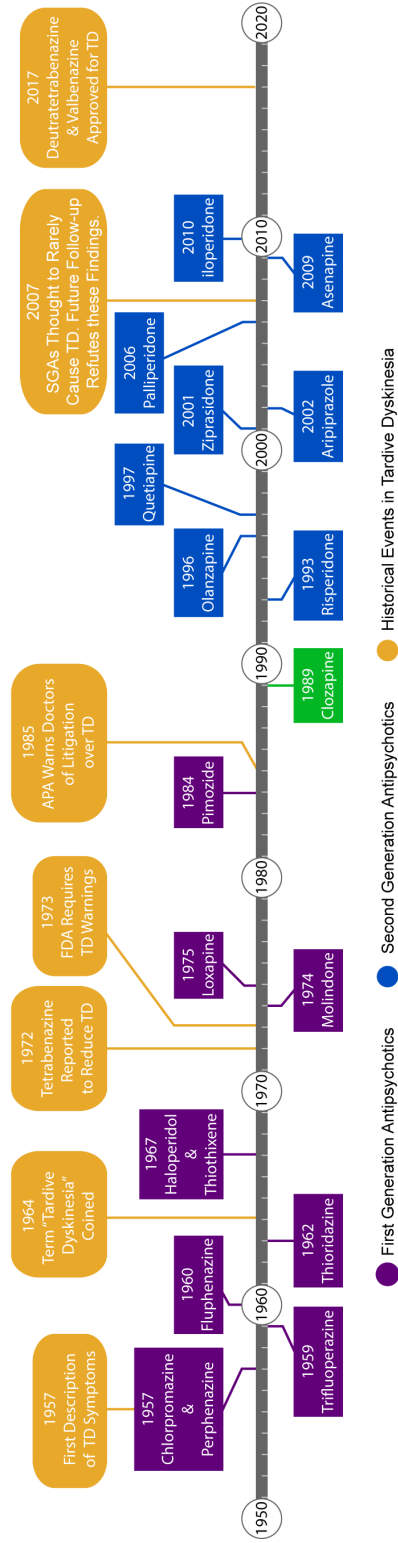
Figure 1.2: Timeline of FDA approved antipsychotic medications. First generation antipsychotics are shown in purple while second generation are shown in blue with the exception of clozapine, which is shown in green to highlight it unique characteristics compared to other antipsychotic drugs. Events in TD history are shown in gold.

1.7 References

Adler, C.M., Malhotra, A.K., Elman, I., Pickar, D., and Breier, A. (2002). Amphetamine-induced dopamine release and post-synaptic specific binding in patients with mild tardive dyskinesia. Neuropsychopharmacol. Off. Publ. Am. Coll. Neuropsychopharmacol. *26*, 295–300.

Albin, R.L., Young, A.B., and Penney, J.B. (1989). The functional anatomy of basal ganglia disorders. Trends Neurosci. *12*, 366–375.

Alcacer, C., Andreoli, L., Sebastianutto, I., Jakobsson, J., Fieblinger, T., and Cenci, M.A. Chemogenetic stimulation of striatal projection neurons modulates responses to Parkinson's disease therapy. J. Clin. Invest. *127*, 720–734.

Alexander, G.E., and Crutcher, M.D. (1990). Functional architecture of basal ganglia circuits: neural substrates of parallel processing. Trends Neurosci. *13*, 266–271.

Alexander, G.E., DeLong, M.R., and Strick, P.L. (1986). Parallel organization of functionally segregated circuits linking basal ganglia and cortex. Annu. Rev. Neurosci. *9*, 357–381.

Andersson, U., Eckernäs, S.A., Hartvig, P., Ulin, J., Långström, B., and Häggström, J.E. (1990). Striatal binding of 11C-NMSP studied with positron emission tomography in patients with persistent tardive dyskinesia: no evidence for altered dopamine D2 receptor binding. J. Neural Transm. Gen. Sect. *79*, 215–226.

Angelucci, F., Aloe, L., Gruber, S.H.M., Fiore, M., and Mathé, A.A. (2000). Chronic antipsychotic treatment selectively alters nerve growth factor and neuropeptide Y immunoreactivity and the distribution of choline acetyl transferase in rat brain regions. Int. J. Neuropsychopharmacol. *3*, 13–25.

Aoki, S., Smith, J.B., Li, H., Yan, X., Igarashi, M., Coulon, P., Wickens, J.R., Ruigrok, T.J., and Jin, X. (2019). An open cortico-basal ganglia loop allows limbic control over motor output via the nigrothalamic pathway. ELife *8*, e49995.

Arvanov, V.L., Liang, X., Schwartz, J., Grossman, S., and Wang, R.Y. (1997). Clozapine and

haloperidol modulate N-methyl-D-aspartate- and non-N-methyl-D-aspartate receptor-mediated neurotransmission in rat prefrontal cortical neurons in vitro. J. Pharmacol. Exp. Ther. *283*, 226–234.

Augustin, S.M., Chancey, J.H., and Lovinger, D.M. (2018). Dual Dopaminergic Regulation of Corticostriatal Plasticity by Cholinergic Interneurons and Indirect Pathway Medium Spiny Neurons. Cell Rep. *24*, 2883–2893.

Baca-Garcia, E., Stanilla, J.K., Büchel, C., Gattaz, W.F., and de Leon, J. (1999). Diurnal variability of orofacial dyskinetic movements. Pharmacopsychiatry *32*, 73–75.

Bachus, S.E., Yang, E., McCloskey, S.S., and Minton, J.N. (2012). Parallels between behavioral and neurochemical variability in the rat vacuous chewing movement model of tardive dyskinesia. Behav. Brain Res. *231*, 323–336.

Bakker, P.R., van Harten, P.N., and van Os, J. (2006). Antipsychotic-induced tardive dyskinesia and the Ser9Gly polymorphism in the DRD3 gene: A meta analysis. Schizophr. Res. *83*, 185–192.

Banghart, M.R., Neufeld, S.Q., Wong, N.C., and Sabatini, B.L. (2015). Enkephalin disinhibits mu opioid receptor rich striatal patches via delta opioid receptors. Neuron *88*, 1227–1239.

Bárány, S., Ingvast, A., and Gunne, L.M. (1979). Development of acute dystonia and tardive dyskinesia in cebus monkeys. Res. Commun. Chem. Pathol. Pharmacol. *25*, 269–279.

Bedard, C., Wallman, M.J., Pourcher, E., Gould, P.V., Parent, A., and Parent, M. (2011). Serotonin and dopamine striatal innervation in Parkinson's disease and Huntington's chorea. Park. Relat Disord *17*, 593–598.

Blanchet, P.J., Parent, M.-T., Rompré, P.H., and Lévesque, D. (2012). Relevance of animal models to human tardive dyskinesia. Behav. Brain Funct. BBF *8*, 12.

Blin, J., Baron, J.C., Cambon, H., Bonnet, A.M., Dubois, B., Loc'h, C., Mazière, B., and Agid, Y. (1989). Striatal dopamine D2 receptors in tardive dyskinesia: PET study. J. Neurol. Neurosurg. Psychiatry *52*, 1248–1252.

Bloem, B., Huda, R., Sur, M., and Graybiel, A.M. (2017). Two-photon imaging in mice shows

    striosomes and matrix have overlapping but differential reinforcement-related responses.

    ELife *6*, e32353.

Bolam, J.P., Izzo, P.N., and Graybiel, A.M. (1988). Cellular substrate of the histochemically

    defined striosome/matrix system of the caudate nucleus: a combined Golgi and

    immunocytochemical study in cat and ferret. Neuroscience *24*, 853–875.

Bordia, T., Zhang, D., Perez, X.A., and Quik, M. (2016). Striatal cholinergic interneurons and D2

    receptor-expressing GABAergic medium spiny neurons regulate tardive dyskinesia. Exp.

    Neurol. *286*, 32–39.

Brandon, S., McClelland, H.A., and Protheroe, C. (1971). A Study of Facial Dyskinesia in a Mental

    Hospital Population. Br. J. Psychiatry *118*, 171–184.

Burt, D.R., Creese, I., and Snyder, S.H. (1977). Antischizophrenic drugs: chronic treatment

    elevates dopamine receptor binding in brain. Science *196*, 326–328.

Butcher, L.L., and Hodge, G.K. (1976). Postnatal development of acetylcholinesterase in the

    caudate-putamen nucleus and substantia nigra of rats. Brain Res. *106*, 223–240.

Calabresi, P., Maj, R., Pisani, A., Mercuri, N.B., and Bernardi, G. (1992). Long-term synaptic

    depression in the striatum: physiological and pharmacological characterization. J.

    Neurosci. *12*, 4224–4233.

Carbon, M., Hsieh, C.-H., Kane, J.M., and Correll, C.U. (2017). Tardive Dyskinesia Prevalence in

    the Period of Second-Generation Antipsychotic Use: A Meta-Analysis. J. Clin. Psychiatry

    78, 20738.

Caroff, S.N. (2019). Overcoming barriers to effective management of tardive dyskinesia.

    Neuropsychiatr. Dis. Treat. *15*, 785–794.

Caroff, S.N., Ungvari, G.S., and Cunningham Owens, D.G. (2018). Historical perspectives on

    tardive dyskinesia. J. Neurol. Sci. *389*, 4–9.

Carvalho, R.C., Silva, R.H., Abílio, V.C., Barbosa, P.N., and Frussa-Filho, R. (2003).

Antidyskinetic effects of risperidone on animal models of tardive dyskinesia in mice. Brain Res. Bull. *60*, 115–124.

Casey, D.E. (2006). Implications of the CATIE Trial on Treatment: Extrapyramidal Symptoms. CNS Spectr. *11*, 25–31.

Centonze, D., Usiello, A., Costa, C., Picconi, B., Erbs, E., Bernardi, G., Borrelli, E., and Calabresi, P. (2004). Chronic haloperidol promotes corticostriatal long-term potentiation by targeting dopamine D2L receptors. J. Neurosci. Off. J. Soc. Neurosci. *24*, 8214–8222.

Ceretta, A.P.C., de Freitas, C.M., Schaffer, L.F., Reinheimer, J.B., Dotto, M.M., de Moraes Reis, E., Scussel, R., Machado-de-Ávila, R.A., and Fachinetto, R. (2018). Gabapentin reduces haloperidol-induced vacuous chewing movements in mice. Pharmacol. Biochem. Behav. *166*, 21–26.

Cho, C.-H., and Lee, H.-J. (2013). Oxidative stress and tardive dyskinesia: pharmacogenetic evidence. Prog. Neuropsychopharmacol. Biol. Psychiatry *46*, 207–213.

Christensen, E., Møller, J.E., and Faurbye, A. (1970). Neuropathological Investigation of 28 Brains from Patients with Dyskinesia. Acta Psychiatr. Scand. *46*, 14–23.

Comer, J.S., Mojtabai, R., and Olfson, M. (2011). National Trends in the Antipsychotic Treatment of Psychiatric Outpatients With Anxiety Disorders. Am. J. Psychiatry *168*, 1057–1065.

Crane, G.E. (1973). Persistent dyskinesia. Br. J. Psychiatry *122*, 395–405.

Crittenden, J.R., and Graybiel, A.M. (2011). Basal Ganglia disorders associated with imbalances in the striatal striosome and matrix compartments. Front. Neuroanat. *5*, 59.

Crittenden, J.R., Lacey, C.J., Lee, T., Bowden, H.A., and Graybiel, A.M. (2014). Severe drug-induced repetitive behaviors and striatal overexpression of VAChT in ChAT-ChR2-EYFP BAC transgenic mice. Front. Neural Circuits *8*.

Crittenden, J.R., Tillberg, P.W., Riad, M.H., Shima, Y., Gerfen, C.R., Curry, J., Housman, D.E.,

Nelson, S.B., Boyden, E.S., and Graybiel, A.M. (2016). Striosome-dendron bouquets highlight a unique striatonigral circuit targeting dopamine-containing neurons. Proc. Natl. Acad. Sci. U. S. A. *113*, 11318–11323.

Crittenden, J.R., Lacey, C.J., Weng, F.-J., Garrison, C.E., Gibson, D.J., Lin, Y., and Graybiel, A.M. (2017). Striatal Cholinergic Interneurons Modulate Spike-Timing in Striosomes and Matrix by an Amphetamine-Sensitive Mechanism. Front. Neuroanat. *11*.

Crowley, J.J., Kim, Y., Szatkiewicz, J.P., Pratt, A.L., Quackenbush, C.R., Adkins, D.E., van den Oord, E., Bogue, M.A., Yang, H., Wang, W., et al. (2012). Genome-wide association mapping of loci for antipsychotic-induced extrapyramidal symptoms in mice. Mamm. Genome Off. J. Int. Mamm. Genome Soc. *23*, 322–335.

Crowley, J.J., Ashraf-Khorassani, M., Castagnoli, N., and Sullivan, P.F. (2013). Brain levels of the neurotoxic pyridinium metabolite HPP+ and extrapyramidal symptoms in haloperidol-treated mice. Neurotoxicology *39*, 153–157.

Czubayko, U., and Plenz, D. (2002). Fast synaptic transmission between striatal spiny projection neurons. Proc Natl Acad Sci U A *99*, 15764–15769.

Danjo, T., Yoshimi, K., Funabiki, K., Yawata, S., and Nakanishi, S. (2014). Aversive behavior induced by optogenetic inactivation of ventral tegmental area dopamine neurons is mediated by dopamine D2 receptors in the nucleus accumbens. Proc. Natl. Acad. Sci. *111*, 6455–6460.

Davis, M.I., Crittenden, J.R., Feng, A.Y., Kupferschmidt, D.A., Naydenov, A., Stella, N., Graybiel, A.M., and Lovinger, D.M. (2018). The cannabinoid-1 receptor is abundantly expressed in striatal striosomes and striosome-dendron bouquets of the substantia nigra. PloS One *13*, e0191436.

DeLong, M.R. (1990). Primate models of movement disorders of basal ganglia origin. Trends Neurosci. *13*, 281–285.

DeLong, M., and Wichmann, T. (2009). Update on models of basal ganglia function and

dysfunction. Parkinsonism Relat. Disord. *15*, S237–S240.

Dennis, J.A., Gittner, L.S., Payne, J.D., and Nugent, K. (2020). Characteristics of U.S. adults taking prescription antipsychotic medications, National Health and Nutrition Examination Survey 2013–2018. BMC Psychiatry *20*, 483.

Divac, N., Prostran, M., Jakovcevski, I., and Cerovac, N. (2014). Second-Generation Antipsychotics and Extrapyramidal Adverse Effects. BioMed Res. Int. *2014*, e656370.

Dobbs, L.K., Kaplan, A.R., Lemos, J.C., Matsui, A., Rubinstein, M., and Alvarez, V.A. (2016). Dopamine Regulation of Lateral Inhibition between Striatal Neurons Gates the Stimulant Actions of Cocaine. Neuron *90*, 1100–1113.

Dorph-Petersen, K.-A., Pierri, J.N., Perel, J.M., Sun, Z., Sampson, A.R., and Lewis, D.A. (2005). The influence of chronic exposure to antipsychotic medications on brain size before and after tissue fixation: a comparison of haloperidol and olanzapine in macaque monkeys. Neuropsychopharmacol. Off. Publ. Am. Coll. Neuropsychopharmacol. *30*, 1649–1661.

D'Souza, U., McGuffin, P., and Buckland, P.R. (1997). Antipsychotic regulation of dopamine D1, D2 and D3 receptor mRNA. Neuropharmacology *36*, 1689–1696.

Eblen, F., and Graybiel, A.M. (1995). Highly restricted origin of prefrontal cortical inputs to striosomes in the macaque monkey. J. Neurosci. *15*, 5999–6013.

Egan, M.F., Hurd, Y., Ferguson, J., Bachus, S.E., Hamid, E.H., and Hyde, T.M. (1996). Pharmacological and neurochemical differences between acute and tardive vacuous chewing movements induced by haloperidol. Psychopharmacology (Berl.) *127*, 337–345.

Flaherty, A.W., and Graybiel, A.M. (1994). Input-output organization of the sensorimotor striatum in the squirrel monkey. J. Neurosci. *14*, 599–610.

Florijn, W.J., Tarazi, F.I., and Creese, I. (1997). Dopamine receptor subtypes: differential regulation after 8 months treatment with antipsychotic drugs. J. Pharmacol. Exp. Ther. *280*, 561–569.

Foster, N.N., Barry, J., Korobkova, L., Garcia, L., Gao, L., Becerra, M., Sherafat, Y., Peng, B., Li,

X., Choi, J.-H., et al. (2021). The mouse cortico–basal ganglia–thalamic network. Nature *598*, 188–194.

Freeze, B.S., Kravitz, A.V., Hammack, N., Berke, J.D., and Kreitzer, A.C. (2013). Control of Basal Ganglia Output by Direct and Indirect Pathway Projection Neurons. J. Neurosci. *33*, 18531–18539.

Frei, K. (2019). Tardive dyskinesia: Who gets it and why. Parkinsonism Relat. Disord. *59*, 151–154.

Friedman, A., Homma, D., Gibb, L.G., Amemori, K., Rubin, S.J., Hood, A.S., Riad, M.H., and Graybiel, A.M. (2015). A Corticostriatal Path Targeting Striosomes Controls Decision-Making under Conflict. Cell *161*, 1320–1333.

Friedman, A., Homma, D., Bloem, B., Gibb, L.G., Amemori, K., Hu, D., Delcasso, S., Truong, T.F., Yang, J., Hood, A.S., et al. (2017). Chronic Stress Alters Striosome-Circuit Dynamics, Leading to Aberrant Decision-Making. Cell *171*, 1191-1205.e28.

Friedman, A., Hueske, E., Drammis, S.M., Toro Arana, S.E., Nelson, E.D., Carter, C.W., Delcasso, S., Rodriguez, R.X., Lutwak, H., DiMarco, K.S., et al. (2020). Striosomes Mediate Value-Based Learning Vulnerable in Age and a Huntington's Disease Model. Cell *183*, 918-934.e49.

Fujiyama, F., Sohn, J., Nakano, T., Furuta, T., Nakamura, K.C., Matsuda, W., and Kaneko, T. (2011). Exclusive and common targets of neostriatofugal projections of rat striosome neurons: a single neuron-tracing study using a viral vector. Eur. J. Neurosci. *33*, 668–677.

Gerfen, C.R. (1985). The neostriatal mosaic. I. compartmental organization of projections from the striatum to the substantia nigra in the rat. J. Comp. Neurol. *236*, 454–476.

Gerfen, C.R. (1988). Synaptic organization of the striatum. J. Electron Microsc. Tech. *10*, 265–281.

Gerfen, C.R., and Surmeier, D.J. (2011). Modulation of striatal projection systems by dopamine. Annu. Rev. Neurosci. *34*, 441–466.

Gerfen, C.R., Engber, T.M., Mahan, L.C., Susel, Z., Chase, T.N., Monsma, F.J., and Sibley, D.R. (1990). D1 and D2 dopamine receptor-regulated gene expression of striatonigral and striatopallidal neurons. Science *250*, 1429–1432.

Gertler, T.S., Chan, C.S., and Surmeier, D.J. (2008). Dichotomous Anatomical Properties of Adult Striatal Medium Spiny Neurons. J. Neurosci. *28*, 10814–10824.

Giusti-Rodríguez, P., Xenakis, J.G., Crowley, J.J., Nonneman, R.J., DeCristo, D.M., Ryan, A., Quackenbush, C.R., Miller, D.R., Shaw, G.D., Zhabotynsky, V., et al. (2020). Antipsychotic Behavioral Phenotypes in the Mouse Collaborative Cross Recombinant Inbred Inter-Crosses (RIX). G3 Bethesda Md *10*, 3165–3177.

Gokce, O., Stanley, G.M., Treutlein, B., Neff, N.F., Camp, J.G., Malenka, R.C., Rothwell, P.E., Fuccillo, M.V., Südhof, T.C., and Quake, S.R. (2016). Cellular Taxonomy of the Mouse Striatum as Revealed by Single-Cell RNA-Seq. Cell Rep. *16*, 1126–1137.

Graybiel, A.M., and Hickey, T.L. (1982). Chemospecificity of ontogenetic units in the striatum: demonstration by combining [3H]thymidine neuronography and histochemical staining. Proc. Natl. Acad. Sci. *79*, 198–202.

Graybiel, A.M., and Ragsdale, C.W. (1980). Clumping of acetylcholinesterase activity in the developing striatum of the human fetus and young infant. Proc. Natl. Acad. Sci. U. S. A. *77*, 1214–1218.

Graybiel, A.M., and Ragsdale, C.W., Jr. (1978). Histochemically distinct compartments in the striatum of human, monkeys, and cat demonstrated by acetylthiocholinesterase staining. Proc Natl Acad Sci U A *75*, 5723–5726.

Graybiel, A.M., Pickel, V.M., Joh, T.H., Reis, D.J., and Ragsdale, C.W. (1981). Direct demonstration of a correspondence between the dopamine islands and acetylcholinesterase patches in the developing striatum. Proc. Natl. Acad. Sci. U. S. A. *78*, 5871–5875.

Greenbaum, L., Alkelai, A., Zozulinsky, P., Kohn, Y., and Lerer, B. (2012). Support for association

of HSPG2 with tardive dyskinesia in Caucasian populations. Pharmacogenomics J. *12*, 513–520.

Gremel, C.M., and Costa, R.M. (2013). Orbitofrontal and striatal circuits dynamically encode the shift between goal-directed and habitual actions. Nat. Commun. *4*, 2264.

Grigoriadis, D.E., Smith, E., Hoare, S.R.J., Madan, A., and Bozigian, H. (2017). Pharmacologic Characterization of Valbenazine (NBI-98854) and Its Metabolites. J. Pharmacol. Exp. Ther. *361*, 454–461.

Gunne, L.M., and Bárány, S. (1976). Haloperidol-induced tardive dyskinesia in monkeys. Psychopharmacology (Berl.) *50*, 237–240.

Halliday, J., Farrington, S., Macdonald, S., MacEwan, T., Sharkey, V., and McCreadie, R. (2002). Nithsdale Schizophrenia Surveys 23: movement disorders. 20-year review. Br. J. Psychiatry J. Ment. Sci. *181*, 422–427.

He, J., Kleyman, M., Chen, J., Alikaya, A., Rothenhoefer, K.M., Ozturk, B.E., Wirthlin, M., Bostan, A.C., Fish, K., Byrne, L.C., et al. (2021). Transcriptional and anatomical diversity of medium spiny neurons in the primate striatum. Curr. Biol. CB *31*, 5473-5486.e6.

Herkenham, M., and Pert, C.B. (1981). Mosaic distribution of opiate receptors, parafascicular projections and acetylcholinesterase in rat striatum. Nature *291*, 415–418.

Hikosaka, O., Sakamoto, M., and Usui, S. (1989). Functional properties of monkey caudate neurons. I. Activities related to saccadic eye movements. J. Neurophysiol. *61*, 780–798.

Hong, S., Amemori, S., Chung, E., Gibson, D.J., Amemori, K., and Graybiel, A.M. (2019). Predominant Striatal Input to the Lateral Habenula in Macaques Comes from Striosomes. Curr. Biol. *29*, 51-61.e5.

Hori, H., Ohmori, O., Shinkai, T., Kojima, H., and Nakamura, J. (2001). Association between three functional polymorphisms of dopamine D2 receptor gene and tardive dyskinesia in schizophrenia. Am. J. Med. Genet. *105*, 774–778.

Howland, R.H. (2015). Deuterated Drugs. J. Psychosoc. Nurs. Ment. Health Serv. *53*, 13–16.

Hunter, R., Blackwood, W., Smith, M.C., and Cumings, J.N. (1968). Neuropathological findings in three cases of persistent dyskinesia following phenothiazine medication. J. Neurol. Sci. *7*, 263–273.

Iino, Y., Sawada, T., Yamaguchi, K., Tajiri, M., Ishii, S., Kasai, H., and Yagishita, S. (2020). Dopamine D2 receptors in discrimination learning and spine enlargement. Nature *579*, 555–560.

Jackson, M.J., Al-Barghouthy, G., Pearce, R.K.B., Smith, L., Hagan, J.J., and Jenner, P. (2004). Effect of 5-HT1B/D receptor agonist and antagonist administration on motor function in haloperidol and MPTP-treated common marmosets. Pharmacol. Biochem. Behav. *79*, 391–400.

Jiang, L.H., Kasser, R.J., Altar, C.A., and Wang, R.Y. (1990). One year of continuous treatment with haloperidol or clozapine fails to induce a hypersensitive response of caudate putamen neurons to dopamine D1 and D2 receptor agonists. J. Pharmacol. Exp. Ther. *253*, 1198–1205.

Jiménez-Castellanos, J., and Graybiel, A.M. (1989). Compartmental origins of striatal efferent projections in the cat. Neuroscience *32*, 297–321.

Joel, D., and Weiner, I. (2000). The connections of the dopaminergic system with the striatum in rats and primates: an analysis with respect to the functional and compartmental organization of the striatum. Neuroscience *96*, 451–474.

Joel, D., Niv, Y., and Ruppin, E. (2002). Actor-critic models of the basal ganglia: new anatomical and computational perspectives. Neural Netw. Off. J. Int. Neural Netw. Soc. *15*, 535–547.

Jones, P.B., Barnes, T.R.E., Davies, L., Dunn, G., Lloyd, H., Hayhurst, K.P., Murray, R.M., Markwick, A., and Lewis, S.W. (2006). Randomized Controlled Trial of the Effect on Quality of Life of Second- vs First-Generation Antipsychotic Drugs in Schizophrenia: Cost Utility of the Latest Antipsychotic Drugs in Schizophrenia Study (CUtLASS 1). Arch. Gen. Psychiatry *63*, 1079–1087.

Kapur, S., Zipursky, R., Jones, C., Shammi, C.S., Remington, G., and Seeman, P. (2000). A Positron Emission Tomography Study of Quetiapine in Schizophrenia: A Preliminary Finding of an Antipsychotic Effect With Only Transiently High Dopamine D2 Receptor Occupancy. Arch. Gen. Psychiatry *57*, 553–559.

Kasper, S., Tauscher, J., Küfferle, B., Barnas, C., Pezawas, L., and Quiner, S. (1999). Dopamine- and serotonin-receptors in schizophrenia: results of imaging-studies and implications for pharmacotherapy in schizophrenia. Eur. Arch. Psychiatry Clin. Neurosci. *249*, S83–S89.

Kawaguchi, Y., Wilson, C.J., and Emson, P.C. (1990). Projection subtypes of rat neostriatal matrix cells revealed by intracellular injection of biocytin. J. Neurosci. Off. J. Soc. Neurosci. *10*, 3421–3438.

Kawai, R., Markman, T., Poddar, R., Ko, R., Fantana, A.L., Dhawale, A.K., Kampff, A.R., and Ölveczky, B.P. (2015). Motor cortex is required for learning but not for executing a motor skill. Neuron *86*, 800–812.

Kelley, J.J., and Roberts, R.C. (2004). Effects of haloperidol on cholinergic striatal interneurons: relationship to oral dyskinesias. J. Neural Transm. Vienna Austria 1996 *111*, 1075–1091.

Kelly, S.M., Raudales, R., He, M., Lee, J.H., Kim, Y., Gibb, L.G., Wu, P., Matho, K., Osten, P., Graybiel, A.M., et al. (2018). Radial Glial Lineage Progression and Differential Intermediate Progenitor Amplification Underlie Striatal Compartments and Circuit Organization. Neuron *99*, 345-361.e4.

Kemp, J.M., and Powell, T.P. (1971). The termination of fibres from the cerebral cortex and thalamus upon dendritic spines in the caudate nucleus: a study with the Golgi method. Philos Trans R Soc Lond B Biol Sci *262*, 429–439.

Kerns, J.M., Sierens, D.K., Kao, L.C., Klawans, H.L., and Carvey, P.M. (1992). Synaptic plasticity in the rat striatum following chronic haloperidol treatment. Clin. Neuropharmacol. *15*, 488–500.

Kharkwal, G., Brami-Cherrier, K., Lizardi-Ortiz, J.E., Nelson, A.B., Ramos, M., Del Barrio, D.,

Sulzer, D., Kreitzer, A.C., and Borrelli, E. (2016). Parkinsonism Driven by Antipsychotics Originates from Dopaminergic Control of Striatal Cholinergic Interneurons. Neuron *91*, 67–78.

Kilpatrick, R., and Whyte, J.H.S. (1965). Side-effects of Phenothiazine Drugs. Br. Med. J. *1*, 316.

Kincaid, A.E., and Wilson, C.J. (1996). Corticostriatal innervation of the patch and matrix in the rat neostriatum. J. Comp. Neurol. *374*, 578–592.

Klawans, H.L. (1973). The pharmacology of tardive dyskinesias. Am. J. Psychiatry *130*, 82–86.

Kline, N.S. (1968). On the Rarity of "Irreversible" Oral Dyskinesias Following Phenothiazines. Am. J. Psychiatry *124*, 48–54.

Klintenberg, R., Gunne, L., and Andrén, P.E. (2002). Tardive dyskinesia model in the common marmoset. Mov. Disord. Off. J. Mov. Disord. Soc. *17*, 360–365.

Koch, J., Shi, W.-X., and Dashtipour, K. (2020). VMAT2 inhibitors for the treatment of hyperkinetic movement disorders. Pharmacol. Ther. *212*, 107580.

Koning, J.P., Vehof, J., Burger, H., Wilffert, B., Al Hadithy, A., Alizadeh, B., van Harten, P.N., Snieder, H., and Genetic Risk and Outcome in Psychosis (GROUP) investigators (2012). Association of two DRD2 gene polymorphisms with acute and tardive antipsychotic-induced movement disorders in young Caucasian patients. Psychopharmacology (Berl.) *219*, 727–736.

van der Kooy, D., and Fishell, G. (1987). Neuronal birthdate underlies the development of striatal compartments. Brain Res. *401*, 155–161.

Korchounov, A., and Ziemann, U. (2011). Neuromodulatory Neurotransmitters Influence LTP-Like Plasticity in Human Cortex: A Pharmaco-TMS Study. Neuropsychopharmacology *36*, 1894–1902.

Kornhuber, J., Riederer, P., Reynolds, G.P., Beckmann, H., Jellinger, K., and Gabriel, E. (1989).

3H-spiperone binding sites in post-mortem brains from schizophrenic patients: relationship to neuroleptic drug treatment, abnormal movements, and positive symptoms. J. Neural Transm. *75*, 1–10.

Kovacic, B., and Domino, E.F. (1982). A monkey model of tardive dyskinesia (TD): evidence that reversible TD may turn into irreversible TD. J. Clin. Psychopharmacol. *2*, 305–307.

Kravitz, A.V., Freeze, B.S., Parker, P.R., Kay, K., Thwin, M.T., Deisseroth, K., and Kreitzer, A.C. (2010). Regulation of parkinsonian motor behaviours by optogenetic control of basal ganglia circuitry. Nature *466*, 622–626.

Kravitz, A.V., Tye, L.D., and Kreitzer, A.C. (2012). Distinct roles for direct and indirect pathway striatal neurons in reinforcement. Nat. Neurosci. *15*, 816–818.

Kreitzer, A.C., and Malenka, R.C. (2007). Endocannabinoid-mediated rescue of striatal LTD and motor deficits in Parkinson's disease models. Nature *445*, 643–647.

Kruyer, A., Parrilla-Carrero, J., Powell, C., Brandt, L., Gutwinski, S., Angelis, A., Chalhoub, R.M., Jhou, T.C., Kalivas, P.W., and Amato, D. (2021). Accumbens D2-MSN hyperactivity drives antipsychotic-induced behavioral supersensitivity. Mol. Psychiatry *26*, 6159–6169.

Kubota, Y., and Kawaguchi, Y. (1993). Spatial distributions of chemically identified intrinsic neurons in relation to patch and matrix compartments of rat neostriatum. J. Comp. Neurol. *332*, 499–513.

Lee, H.J., Weitz, A.J., Bernal-Casas, D., Duffy, B.A., Choy, M., Kravitz, A.V., Kreitzer, A.C., and Lee, J.H. (2016). Activation of Direct and Indirect Pathway Medium Spiny Neurons Drives Distinct Brain-wide Responses. Neuron *91*, 412–424.

Lee, J., Wang, W., and Sabatini, B.L. (2020). Anatomically segregated basal ganglia pathways allow parallel behavioral modulation. Nat. Neurosci. *23*, 1388–1398.

Leveque, J.C., Macías, W., Rajadhyaksha, A., Carlson, R.R., Barczak, A., Kang, S., Li, X.M.,

Coyle, J.T., Huganir, R.L., Heckers, S., et al. (2000). Intracellular modulation of NMDA receptor function by antipsychotic drugs. J. Neurosci. Off. J. Soc. Neurosci. *20*, 4011–4020.

Lévesque, M., and Parent, A. (1998). Axonal arborization of corticostriatal and corticothalamic fibers arising from prelimbic cortex in the rat. Cereb. Cortex *8*, 602–613.

Lévesque, D., Martres, M.P., Diaz, J., Griffon, N., Lammers, C.H., Sokoloff, P., and Schwartz, J.C. (1995). A paradoxical regulation of the dopamine D3 receptor expression suggests the involvement of an anterograde factor from dopamine neurons. Proc. Natl. Acad. Sci. U. S. A. *92*, 1719–1723.

Lidow, M.S., and Goldman-Rakic, P.S. (1994). A common action of clozapine, haloperidol, and remoxipride on D1- and D2-dopaminergic receptors in the primate cerebral cortex. Proc. Natl. Acad. Sci. U. S. A. *91*, 4353–4356.

Ljungberg, T., Apicella, P., and Schultz, W. (1992). Responses of monkey dopamine neurons during learning of behavioral reactions. J. Neurophysiol. *67*, 145–163.

Mahadik, S.P., Laev, H., Korenovsky, A., and Karpiak, S.E. (1988). Haloperidol alters rat CNS cholinergic system: Enzymatic and morphological analyses. Biol. Psychiatry *24*, 199–217.

Marchese, G., Bartholini, F., Casu, M.A., Ruiu, S., Casti, P., Congeddu, E., Tambaro, S., and Pani, L. (2004). Haloperidol versus risperidone on rat "early onset" vacuous chewing. Behav. Brain Res. *149*, 9–16.

Marsden, C.D., and Jenner, P. (1980). The pathophysiology of extrapyramidal side-effects of neuroleptic drugs. Psychol. Med. *10*, 55–72.

Märtin, A., Calvigioni, D., Tzortzi, O., Fuzik, J., Wärnberg, E., and Meletis, K. (2019). A Spatiomolecular Map of the Striatum. Cell Rep. *29*, 4320-4333.e5.

Martres, M.P., Costentin, J., Baudry, M., Marcais, H., Protais, P., and Schwartz, J.C. (1977). Long-term changes in the sensitivity of pre-and postsynaptic dopamine receptors in mouse striatum evidenced by behavioural and biochemical studies. Brain Res. *136*, 319–337.

Matsumoto, M., and Hikosaka, O. (2009). Two types of dopamine neuron distinctly convey positive and negative motivational signals. Nature *459*, 837–841.

Matsushima, A., and Graybiel, A.M. (2020). Combinatorial Developmental Controls on Striatonigral Circuits. Cell Rep. *31*, 107778.

McKinney, W.T., Moran, E.C., Kraemer, G.W., and Prange, A.J. (1980). Long-term chlorpromazine in rhesus monkeys: production of dyskinesias and changes in social behavior. Psychopharmacology (Berl.) *72*, 35–39.

Mermelstein, P.G., Song, W.-J., Tkatch, T., Yan, Z., and Surmeier, D.J. (1998). Inwardly Rectifying Potassium (IRK) Currents Are Correlated with IRK Subunit Expression in Rat Nucleus Accumbens Medium Spiny Neurons. J. Neurosci. *18*, 6650–6661.

Meshul, C.K., Janowsky, A., Casey, D.E., Stallbaumer, R.K., and Taylor, B. (1992). Effect of haloperidol and clozapine on the density of "perforated" synapses in caudate, nucleus accumbens, and medial prefrontal cortex. Psychopharmacology (Berl.) *106*, 45–52.

Miksys, S., Wadji, F.B., Tolledo, E.C., Remington, G., Nobrega, J.N., and Tyndale, R.F. (2017). Rat brain CYP2D enzymatic metabolism alters acute and chronic haloperidol side-effects by different mechanisms. Prog. Neuropsychopharmacol. Biol. Psychiatry *78*, 140–148.

Miller, R., and Chouinard, G. (1993). Loss of striatal cholinergic neurons as a basis for tardive and L-dopa-induced dyskinesias, neuroleptic-induced supersensitivity psychosis and refractory schizophrenia. Biol. Psychiatry *34*, 713–738.

Miller, D.D., McEvoy, J.P., Davis, S.M., Caroff, S.N., Saltz, B.L., Chakos, M.H., Swartz, M.S., Keefe, R.S.E., Rosenheck, R.A., Stroup, T.S., et al. (2005). Clinical correlates of tardive dyskinesia in schizophrenia: Baseline data from the CATIE schizophrenia trial. Schizophr. Res. *80*, 33–43.

Mink, J.W. (1996). THE BASAL GANGLIA: FOCUSED SELECTION AND INHIBITION OF COMPETING MOTOR PROGRAMS. Prog. Neurobiol. *50*, 381–425.

Miyamoto, Y., Katayama, S., Shigematsu, N., Nishi, A., and Fukuda, T. (2018). Striosome-based

map of the mouse striatum that is conformable to both cortical afferent topography and uneven distributions of dopamine D1 and D2 receptor-expressing cells. Brain Struct. Funct.

Mo, G.-H., Liao, D.-L., Lai, I.-C., Wang, Y.-C., Chen, J.-Y., Lin, C.-Y., Chen, T.-T., Chen, M.-L., Bai, Y.-M., Lin, C.-C., et al. (2007). Support for an association of the C939T polymorphism in the human DRD2 gene with tardive dyskinesia in schizophrenia. Schizophr. Res. *97*, 302–304.

Moore, R.Y., and Bloom, F.E. (1978). Central Catecholamine Neuron Systems: Anatomy and Physiology of the Dopamine Systems. Annu. Rev. Neurosci. *1*, 129–169.

Moreno-Küstner, B., Martín, C., and Pastor, L. (2018). Prevalence of psychotic disorders and its association with methodological issues. A systematic review and meta-analyses. PLOS ONE *13*, e0195687.

Morgenstern, H., and Glazer, W.M. (1993). Identifying Risk Factors for Tardive Dyskinesia Among Long-term Outpatients Maintained With Neuroleptic Medications: Results of the Yale Tardive Dyskinesia Study. Arch. Gen. Psychiatry *50*, 723–733.

Nambu, A., Tokuno, H., Hamada, I., Kita, H., Imanishi, M., Akazawa, T., Ikeuchi, Y., and Hasegawa, N. (2000). Excitatory Cortical Inputs to Pallidal Neurons Via the Subthalamic Nucleus in the Monkey. J. Neurophysiol. *84*, 289–300.

Nastuk, M.A., and Graybiel, A.M. (1985). Patterns of muscarinic cholinergic binding in the striatum and their relation to dopamine islands and striosomes. J. Comp. Neurol. *237*, 176–194.

Newman, H., Liu, F.-C., and Graybiel, A.M. (2015). Dynamic ordering of early generated striatal cells destined to form the striosomal compartment of the striatum. J. Comp. Neurol. *523*, 943–962.

Newman-Gage, H., and Graybiel, A.M. (1988). Expression of calcium/calmodulin-dependent protein kinase in relation to dopamine islands and synaptic maturation in the cat striatum. J. Neurosci. Off. J. Soc. Neurosci. *8*, 3360–3375.

Nisenbaum, E.S., and Wilson, C.J. (1995). Potassium currents responsible for inward and outward rectification in rat neostriatal spiny projection neurons. J. Neurosci. *15*, 4449–4463.

Nitsche, M.A., Kuo, M.-F., Grosch, J., Bergner, C., Monte-Silva, K., and Paulus, W. (2009). D1-Receptor Impact on Neuroplasticity in Humans. J. Neurosci. *29*, 2648–2653.

Novick, D., Haro, J.M., Bertsch, J., and Haddad, P.M. (2010). Incidence of extrapyramidal symptoms and tardive dyskinesia in schizophrenia: thirty-six-month results from the European schizophrenia outpatient health outcomes study. J. Clin. Psychopharmacol. *30*, 531–540.

O'Connor, J.A., Hasenkamp, W., Horman, B.M., Muly, E.C., and Hemby, S.E. (2006). Region specific regulation of NR1 in rhesus monkeys following chronic antipsychotic drug administration. Biol. Psychiatry *60*, 659–662.

O'Connor, J.A., Muly, E.C., Arnold, S.E., and Hemby, S.E. (2007). AMPA receptor subunit and splice variant expression in the DLPFC of schizophrenic subjects and rhesus monkeys chronically administered antipsychotic drugs. Schizophr. Res. *90*, 28–40.

Olson, L., Seiger, A., and Fuxe, K. (1972). Heterogeneity of striatal and limbic dopamine innervation: highly fluorescent islands in developing and adult rats. Brain Res. *44*, 283–288.

Parent, M., and Parent, A. (2004). The pallidofugal motor fiber system in primates. Parkinsonism Relat. Disord. *10*, 203–211.

Park, Y.-M., Kang, S.-G., Choi, J.-E., Kim, Y.-K., Kim, S.-H., Park, J.-Y., Kim, L., and Lee, H.-J. (2011). No Evidence for an Association between Dopamine D2 Receptor Polymorphisms and Tardive Dyskinesia in Korean Schizophrenia Patients. Psychiatry Investig. *8*, 49–54.

Patsopoulos, N.A., Ntzani, E.E., Zintzaras, E., and Ioannidis, J.P.A. (2005). CYP2D6 polymorphisms and the risk of tardive dyskinesia in schizophrenia: a meta-analysis. Pharmacogenet. Genomics *15*, 151–158.

Paulson, G.W. (2005). Historical Comments on Tardive Dyskinesia: A Neurologist's Perspective. J. Clin. Psychiatry *66*, 8251.

Penney, J.B., and Young, A.B. (1983). Speculations on the Functional Anatomy of Basal Ganglia Disorders. Annu. Rev. Neurosci. *6*, 73–94.

Peralta, V., and Cuesta, M.J. (2010). The effect of antipsychotic medication on neuromotor abnormalities in neuroleptic-naive nonaffective psychotic patients: a naturalistic study with haloperidol, risperidone, or olanzapine. Prim. Care Companion J. Clin. Psychiatry *12*, PCC.09m00799.

Peralta, V., Campos, M.S., De Jalón, E.G., and Cuesta, M.J. (2010). Motor behavior abnormalities in drug-naïve patients with schizophrenia spectrum disorders. Mov. Disord. *25*, 1068–1076.

Plotkin, J.L., and Goldberg, J.A. (2019). Thinking Outside the Box (and Arrow): Current Themes in Striatal Dysfunction in Movement Disorders. Neurosci. Rev. J. Bringing Neurobiol. Neurol. Psychiatry *25*, 359–379.

Ragsdale, C.W., and Graybiel, A.M. (1988). Fibers from the basolateral nucleus of the amygdala selectively innervate striosomes in the caudate nucleus of the cat. J. Comp. Neurol. *269*, 506–522.

Ragsdale, C.W., and Graybiel, A.M. (1990). A simple ordering of neocortical areas established by the compartmental organization of their striatal projections. Proc. Natl. Acad. Sci. *87*, 6196–6199.

Ragsdale Jr., C.W., and Graybiel, A.M. (1991). Compartmental organization of the thalamostriatal connection in the cat. J. Comp. Neurol. *311*, 134–167.

Rajakumar, N., Elisevich, K., and Flumerfelt, B.A. (1993). Compartmental origin of the striato-entopeduncular projection in the rat. J. Comp. Neurol. *331*, 286–296.

Remington, G., and Kapur, S. (1999). D2 and 5-HT2 receptor effects of antipsychotics: bridging basic and clinical findings using PET. J. Clin. Psychiatry *60 Suppl 10*, 15–19.

Reynolds, G.P., Brown, J.E., McCall, J.C., and Mackay, A.V. (1992). Dopamine receptor abnormalities in the striatum and pallidum in tardive dyskinesia: a post mortem study. J. Neural Transm. Gen. Sect. *87*, 225–230.

Roberts, M.S., McLean, S., Millingen, K.S., and Galloway, H.M. (1986). The pharmacokinetics of tetrabenazine and its hydroxy metabolite in patients treated for involuntary movement disorders. Eur. J. Clin. Pharmacol. *29*, 703–708.

Rogue, P., Hanauer, A., Zwiller, J., Malviya, A.N., and Vincendon, G. (1991). Up-regulation of dopamine D2 receptor mRNA in rat striatum by chronic neuroleptic treatment. Eur. J. Pharmacol. *207*, 165–168.

Rubenstein, J.L.R., and Campbell, K. (2013). Chapter 24 - Neurogenesis in the Basal Ganglia. In Patterning and Cell Type Specification in the Developing CNS and PNS, J.L.R. Rubenstein, and P. Rakic, eds. (Oxford: Academic Press), pp. 455–473.

Sadikot, A.F., Parent, A., Smith, Y., and Bolam, J.P. (1992). Efferent connections of the centromedian and parafascicular thalamic nuclei in the squirrel monkey: A light and electron microscopic study of the thalamostriatal projection in relation to striatal heterogeneity. J. Comp. Neurol. *320*, 228–242.

Saunders, A., Macosko, E.Z., Wysoker, A., Goldman, M., Krienen, F.M., de Rivera, H., Bien, E., Baum, M., Bortolin, L., Wang, S., et al. (2018). Molecular Diversity and Specializations among the Cells of the Adult Mouse Brain. Cell *174*, 1015-1030.e16.

Savasta, M., Dubois, A., Benavidès, J., and Scatton, B. (1988). Different plasticity changes in D1 and D2 receptors in rat striatal subregions following impairment of dopaminergic transmission. Neurosci. Lett. *85*, 119–124.

Schelkunov, E.L. (1967). Adrenergic Effect of Chronic Administration of Neuroleptics. Nature *214*, 1210–1212.

Schultz, W., Apicella, P., and Ljungberg, T. (1993). Responses of monkey dopamine neurons to

reward and conditioned stimuli during successive steps of learning a delayed response task. J. Neurosci. *13*, 900–913.

Schultz, W., Dayan, P., and Montague, P.R. (1997). A Neural Substrate of Prediction and Reward. Science *275*, 1593–1599.

See, R.E. (1991). Striatal dopamine metabolism increases during long-term haloperidol administration in rats but shows tolerance in response to acute challenge with raclopride. Neurosci. Lett. *129*, 265–268.

Shen, W., Flajolet, M., Greengard, P., and Surmeier, D.J. (2008). Dichotomous dopaminergic control of striatal synaptic plasticity. Science *321*, 848–851.

Shirakawa, O., and Tamminga, C.A. (1994). Basal ganglia GABAA and dopamine D1 binding site correlates of haloperidol-induced oral dyskinesias in rat. Exp. Neurol. *127*, 62–69.

Smith, J.B., Klug, J.R., Ross, D.L., Howard, C.D., Hollon, N.G., Ko, V.I., Hoffman, H., Callaway, E.M., Gerfen, C.R., and Jin, X. (2016). Genetic-Based Dissection Unveils the Inputs and Outputs of Striatal Patch and Matrix Compartments. Neuron *91*, 1069–1084.

Solmi, M., Pigato, G., Kane, J.M., and Correll, C.U. (2018). Clinical risk factors for the development of tardive dyskinesia. J. Neurol. Sci. *389*, 21–27.

Sonego, A.B., Prado, D.S., Vale, G.T., Sepulveda-Diaz, J.E., Cunha, T.M., Tirapelli, C.R., Del Bel, E.A., Raisman-Vozari, R., and Guimarães, F.S. (2018). Cannabidiol prevents haloperidol-induced vacuos chewing movements and inflammatory changes in mice via PPARγ receptors. Brain. Behav. Immun. *74*, 241–251.

Strous, R.D., Kupchik, M., Roitman, S., Schwartz, S., Gonen, N., Mester, R., Weizman, A., and Spivak, B. (2006). Comparison between risperidone, olanzapine, and clozapine in the management of chronic schizophrenia: a naturalistic prospective 12-week observational study. Hum. Psychopharmacol. *21*, 235–243.

Swayze, V.W., Yates, W.R., Andreasen, N.C., and Alliger, R.J. (1988). CT abnormalities in tardive dyskinesia. Psychiatry Res. *26*, 51–58.

Syu, A., Ishiguro, H., Inada, T., Horiuchi, Y., Tanaka, S., Ishikawa, M., Arai, M., Itokawa, M., Niizato, K., Iritani, S., et al. (2010). Association of the HSPG2 Gene with Neuroleptic-Induced Tardive Dyskinesia. Neuropsychopharmacology *35*, 1155–1164.

Tarsy, D., and Baldessarini, R.J. (1973). Pharmacologically induced behavioural supersensitivity to apomorphine. Nature. New Biol. *245*, 262–263.

Tarsy, D., and Baldessarini, R.J. (1974). Behavioural supersensitivity to apomorphine following chronic treatment with drugs which interfere with the synaptic function of catecholamines. Neuropharmacology *13*, 927–940.

Taverna, S., van Dongen, Y.C., Groenewegen, H.J., and Pennartz, C.M. (2004). Direct physiological evidence for synaptic connectivity between medium-sized spiny neurons in rat nucleus accumbens in situ. J Neurophysiol *91*, 1111–1121.

Taverna, S., Ilijic, E., and Surmeier, D.J. (2008). Recurrent collateral connections of striatal medium spiny neurons are disrupted in models of Parkinson's disease. J. Neurosci. Off. J. Soc. Neurosci. *28*, 5504–5512.

Tennyson, V.M., Barrett, R.E., Cohen, G., Côté, L., Heikkila, R., and Mytilineou, C. (1972). The developing neostriatum of the rabbit: correlation of fluorescence histochemistry, electron microscopy, endogenous dopamine levels, and (3 H)dopamine uptake. Brain Res. *46*, 251–285.

Teo, J.T., Edwards, M.J., and Bhatia, K. (2012). Tardive dyskinesia is caused by maladaptive synaptic plasticity: A hypothesis. Mov. Disord. *27*, 1205–1215.

Tepper, J.M., Tecuapetla, F., Koos, T., and Ibanez-Sandoval, O. (2010). Heterogeneity and diversity of striatal GABAergic interneurons. Front Neuroanat *4*, 150.

Tokuno, H., Chiken, S., Kametani, K., and Moriizumi, T. (2002). Efferent projections from the striatal patch compartment: anterograde degeneration after selective ablation of neurons expressing μ-opioid receptor in rats. Neurosci. Lett. *332*, 5–8.

Tsai, H.-C., Zhang, F., Adamantidis, A., Stuber, G.D., Bonci, A., de Lecea, L., and Deisseroth, K.

(2009). Phasic firing in dopaminergic neurons is sufficient for behavioral conditioning. Science *324*, 1080–1084.

Tsai, H.-T., North, K.E., West, S.L., and Poole, C. (2010). The DRD3 rs6280 polymorphism and prevalence of tardive dyskinesia: A meta-analysis. Am. J. Med. Genet. B Neuropsychiatr. Genet. *153B*, 57–66.

Tunstall, M.J., Oorschot, D.E., Kean, A., and Wickens, J.R. (2002). Inhibitory interactions between spiny projection neurons in the rat striatum. J. Neurophysiol. *88*, 1263–1269.

Turrone, P., Remington, G., and Nobrega, J.N. (2002). The vacuous chewing movement (VCM) model of tardive dyskinesia revisited: is there a relationship to dopamine D(2) receptor occupancy? Neurosci. Biobehav. Rev. *26*, 361–380.

Utsunomiya, K., Shinkai, T., Sakata, S., Yamada, K., Chen, H.-I., De Luca, V., Hwang, R., Ohmori, O., and Nakamura, J. (2012). Genetic association between the dopamine D3 receptor gene polymorphism (Ser9Gly) and tardive dyskinesia in patients with schizophrenia: A reevaluation in East Asian populations. Neurosci. Lett. *507*, 52–56.

Vonvoigtlander, P.F., Losey, E.G., and Triezenberg, H.J. (1975). Increased sensitivity to dopaminergic agents after chronic neuroleptic treatment. J. Pharmacol. Exp. Ther. *193*, 88–94.

Waddington, J.L. (1990). Spontaneous orofacial movements induced in rodents by very long-term neuroleptic drug administration: phenomenology, pathophysiology and putative relationship to tardive dyskinesia. Psychopharmacology (Berl.) *101*, 431–447.

Waddington, J.L., Cross, A.J., Gamble, S.J., and Bourne, R.C. (1983). Spontaneous orofacial dyskinesia and dopaminergic function in rats after 6 months of neuroleptic treatment. Science *220*, 530–532.

Walker, R.H., and Graybiel, A.M. (1993). Dendritic arbors of spiny neurons in the primate striatum are directionally polarized. J. Comp. Neurol. *337*, 629–639.

Wallace, M.L., Saunders, A., Huang, K.W., Philson, A.C., Goldman, M., Macosko, E.Z., McCarroll,

S.A., and Sabatini, B.L. (2017). Genetically Distinct Parallel Pathways in the Entopeduncular Nucleus for Limbic and Sensorimotor Output of the Basal Ganglia. Neuron *94*, 138-152.e5.

Walsh, J.J., Christoffel, D.J., Heifets, B.D., Ben-Dor, G.A., Selimbeyoglu, A., Hung, L.W., Deisseroth, K., and Malenka, R.C. (2018). 5-HT release in nucleus accumbens rescues social deficits in mouse autism model. Nature *560*, 589–594.

Wang, Z., Kai, L., Day, M., Ronesi, J., Yin, H.H., Ding, J., Tkatch, T., Lovinger, D.M., and Surmeier, D.J. (2006). Dopaminergic control of corticostriatal long-term synaptic depression in medium spiny neurons is mediated by cholinergic interneurons. Neuron *50*, 443–452.

Watabe-Uchida, M., Zhu, L., Ogawa, S.K., Vamanrao, A., and Uchida, N. (2012). Whole-Brain Mapping of Direct Inputs to Midbrain Dopamine Neurons. Neuron *74*, 858–873.

Weiss, B., Santelli, S., and Lusink, G. (1977). Movement disorders induced in monkeys by chronic haloperidol treatment. Psychopharmacology (Berl.) *53*, 289–293.

Wilson, C.J. (2007). GABAergic inhibition in the neostriatum. Prog. Brain Res. *160*, 91–110.

Wittmann, M., Marino, M.J., Henze, D.A., Seabrook, G.R., and Conn, P.J. (2005). Clozapine Potentiation of N-Methyl-d-aspartate Receptor Currents in the Nucleus Accumbens: Role of NR2B and Protein Kinase A/Src Kinases. J. Pharmacol. Exp. Ther. *313*, 594–603.

Woods, S.W., Morgenstern, H., Saksa, J.R., Walsh, B.C., Sullivan, M.C., Money, R., Hawkins, K.A., Gueorguieva, R.V., and Glazer, W.M. (2010). Incidence of Tardive Dyskinesia With Atypical Versus Conventional Antipsychotic Medications: A Prospective Cohort Study. J. Clin. Psychiatry *71*, 8896.

Xiao, X., Deng, H., Furlan, A., Yang, T., Zhang, X., Hwang, G.-R., Tucciarone, J., Wu, P., He, M., Palaniswamy, R., et al. (2020). A Genetically Defined Compartmentalized Striatal Direct Pathway for Negative Reinforcement. Cell *183*, 211-227.e20.

Yael, D., Zeef, D.H., Sand, D., Moran, A., Katz, D.B., Cohen, D., Temel, Y., and Bar-Gad, I.

(2013). Haloperidol-induced changes in neuronal activity in the striatum of the freely moving rat. Front. Syst. Neurosci. *7*, 110.

Yagishita, S., Hayashi-Takagi, A., Ellis-Davies, G.C.R., Urakubo, H., Ishii, S., and Kasai, H. (2014). A critical time window for dopamine actions on the structural plasticity of dendritic spines. Science *345*, 1616–1620.

Yoshizawa, T., Ito, M., and Doya, K. (2018). Reward-Predictive Neural Activities in Striatal Striosome Compartments. ENeuro *5*.

Yttri, E.A., and Dudman, J.T. (2016). Opponent and bidirectional control of movement velocity in the basal ganglia. Nature *533*, 402–406.

Zai, C.C., Hwang, R.W., De Luca, V., Müller, D.J., King, N., Zai, G.C., Remington, G., Meltzer, H.Y., Lieberman, J.A., Potkin, S.G., et al. (2007). Association study of tardive dyskinesia and twelve DRD2 polymorphisms in schizophrenia patients. Int. J. Neuropsychopharmacol. *10*, 639–651.

Zai, C.C., Tiwari, A.K., De Luca, V., Müller, D.J., Bulgin, N., Hwang, R., Zai, G.C., King, N., Voineskos, A.N., Meltzer, H.Y., et al. (2009). Genetic study of BDNF, DRD3, and their interaction in tardive dyskinesia. Eur. Neuropsychopharmacol. *19*, 317–328.

Zai, C.C., Tiwari, A.K., Mazzoco, M., de Luca, V., Müller, D.J., Shaikh, S.A., Lohoff, F.W., Freeman, N., Voineskos, A.N., Potkin, S.G., et al. (2013). Association study of the vesicular monoamine transporter gene SLC18A2 with tardive dyskinesia. J. Psychiatr. Res. *47*, 1760–1765.

Zai, C.C., Lee, F.H., Tiwari, A.K., Lu, J.Y., Luca, V. de, Maes, M.S., Herbert, D., Shahmirian, A., Cheema, S.Y., Zai, G.C., et al. (2018a). Investigation of the HSPG2 Gene in Tardive Dyskinesia – New Data and Meta-Analysis. Front. Pharmacol. *9*.

Zai, C.C., Maes, M.S., Tiwari, A.K., Zai, G.C., Remington, G., and Kennedy, J.L. (2018b). Genetics of tardive dyskinesia: Promising leads and ways forward. J. Neurol. Sci. *389*, 28–34.

Zalocusky, K.A., Ramakrishnan, C., Lerner, T.N., Davidson, T.J., Knutson, B., and Deisseroth, K.

    (2016). Nucleus accumbens D2R cells signal prior outcomes and control risky decision-

    making. Nature *531*, 642–646.

Zeisel, A., Hochgerner, H., Lönnerberg, P., Johnsson, A., Memic, F., van der Zwan, J., Häring,

    M., Braun, E., Borm, L.E., La Manno, G., et al. (2018). Molecular Architecture of the Mouse

    Nervous System. Cell *174*, 999-1014.e22.

CHAPTER 2

Circuit Mechanisms of Parkinson's Disease

2.1 Abstract

Parkinson's disease (PD) is a complex, multi-system neurodegenerative disorder. The second most common neurodegenerative disorder after Alzheimer's Disease, it affects approximately 1% of adults over the age of 60. Patients are usually diagnosed with the development of one or more of the core motor features of the disease, including tremor, slowing of movement (bradykinesia), and rigidity. However, there are numerous other disease manifestations, including motor and nonmotor features. Many PD symptoms are the direct result of neurodegeneration in selected brain regions; others appear to be driven by aberrant activity patterns in surviving neurons. This latter phenomenon, PD circuit dysfunction, is an area of intense study, as it likely underlies our ability to treat many disease symptoms in the face of (currently) irreversible neurodegeneration. This review will discuss key clinical features of PD and their basis in neural circuit dysfunction. We will first review important disease symptoms and some of the responsible neuropathology. We will then describe the basal ganglia-thalamocortical circuit, the major locus of PD-related circuit dysfunction, and some of the models that have influenced its study. We will review PD-related changes in network activity, subdividing findings into those that touch on the rate, rhythm, or synchronization of neurons. Finally, we suggest some critical remaining questions for the field, and areas for new developments.

2.2 Results

2.2.1 Clinical Features of Parkinson's Disease

Motor Features

Though the core, or classic, motor features of PD include tremor, bradykinesia, and rigidity, there are many other motor features, including alterations in gait and balance, eye movement control, speech and swallowing, and bladder control. In PD patients, bradykinesia manifests as reductions in movement amplitude, movement velocity, and difficulty in initiating movement. It can impact voluntary control of many muscle groups, including eye muscles (resulting in slowed initiation of saccades), muscles of speech (resulting in softer and sometimes slurred speech), and limb muscles (resulting in reduced dexterity). Patients describe difficulties in fine motor tasks like buttoning, writing, and using utensils.

Tremor is variable: most, but not all, patients have a tremor, typically present in one or both hands, but also can affect the legs or head. Hand tremor is usually present at rest, and consists of rhythmic movement, about 5 Hz in frequency, about the wrist. Tremor is greatly diminished during voluntary movement. Many core motor symptoms respond to dopamine replacement therapy with the dopamine precursor levodopa or dopamine agonists.

As the disease progresses, abnormalities outside the core motor features develop, and drive disability. These include impaired gait and balance. Initially gait slows, then later develops a shuffling quality with reduced stride length. Postural reflexes diminish, and instability becomes apparent, and increasingly likelihood of falls. These gait and balance symptoms are only partially responsive to dopamine replacement therapy. Speech and swallowing are typically impacted later in the disease course. Speech often becomes soft and sometimes difficult to understand, and the slowing of swallowing can cause both choking episodes and drooling. Indeed, swallowing impairment can lead to aspiration pneumonia. These symptoms rarely respond to dopaminergic medications. While these motor symptoms are very useful in current clinical diagnosis, there is

increasing awareness of the numerous nonmotor features of PD, many of which do not respond to standard pharmacological treatment. Nonmotor features of PD arise both before and after the onset of the classic motor symptoms, increase disability and reduce quality of life. They can be grouped into behavioral, cognitive, and autonomic categories.

Behavioral symptoms

Behavioral symptoms such as mood disorders and sleep disturbances arise throughout the course of PD, and may also represent a major complication of current treatments. PD patients often describe the development of anxiety or depression several years before the onset of typical motor symptoms (Abbott et al., 2001; Iranzo et al., 2009; Doty, 2012; Bezard and Fernagut, 2014), suggesting these symptoms are driven by the underlying disease process, rather than coping with the disease. Anxiety is present in approximately 40% of patients (Pontone et al., 2009), while depression affects approximately 40-50% of PD patients, depending on how depression is defined (Reijnders et al., 2008). Fortunately, these symptoms are often amenable to the same antidepressant therapies used in patients without PD.

PD is also characterized by multiple changes in sleep. Earliest to develop is REM sleep behavior disorder, a phenomenon in which patients physically enact their dreams, thrashing about during sleep, grabbing their bedpartner, or falling out of bed. In healthy individuals, brainstem circuitry produces paralysis during REM sleep (sleep atonia). This process goes awry in many patients with PD or other synucleinopathies (Louis et al., 2017), and is often present many years before the onset of motor symptoms (Postuma et al., 2009; Galbiati et al., 2018). Aside from REM sleep behavior, PD patients experience a number of sleep disruptions, including insomnia and alterations in sleep and wake cycles.

Dopamine replacement therapy can alleviate some behavioral symptoms, such as apathy or anhedonia, but may also create new behavioral symptoms in susceptible individuals. Two well-described behavioral phenomena associated with dopamine replacement therapy are impulse

control disorder (ICD) and the dopamine dysregulation syndrome (DDS). ICD is associated most commonly with dopamine agonist therapy, but can occur during levodopa treatment, as well. In this condition, patients impulsively or compulsively engage in reward-seeking behaviors, such as gambling, video-gaming, shopping, eating, and pornography or other sexual activities (Weintraub et al., 2010). DDS is a related condition in which patients develop addictive behaviors toward their dopaminergic medication (dopamine agonists or levodopa), taking larger amounts than prescribed, more frequently, and with dependence/withdrawal-type symptoms (Giovannoni et al., 2000).

Cognitive symptoms

Cognitive decline is one of the most disabling features of PD, and though some cognitive changes are evident even at the time of diagnosis (Williams-Gray et al., 2007; Aarsland et al., 2009), clinically significant cognitive impairment typically manifests some years later, and progresses steadily over time. Though initially PD was considered a movement disorder, without significant cognitive components, longitudinal studies have shown that essentially all PD patients eventually develop dementia (Hely et al., 2008). Historically, diagnostic distinctions were drawn between PD and the related synucleinopathy, Lewy body dementia. This distinction was based on the timing and severity of cognitive deficits (late and milder in PD versus early and marked in Lewy body dementia). However, with increased study of the entire range of symptoms and postmortem brain pathology, it appears these disorders may be part of a single spectrum (Jellinger, 2018). Thus many consider it appropriate to discuss the cognitive features of both conditions together.

Symptoms and measurable declines in nearly every cognitive domain have been reported in PD, but deficits can be subdivided into those that are dopamine-dependent (alleviated or exacerbated by dopamine replacement therapy) and those that are not (Sethi, 2008). Dopamine-dependent cognitive symptoms tend to emerge earlier, and include deficits in attention,

processing speed, set-switching, and verbal fluency (Lange et al., 1992; Marié et al., 1999; Dadgar et al., 2013). Dopamine-independent cognitive impairments tend to accumulate later, and include deficits in episodic memory and visuospatial function. In later stage disease, visual phenomena such as illusions and hallucinations frequently develop, which can unfortunately be worsened by dopamine replacement therapy (Sethi, 2008). Cognitive deficits in PD are commonly treated with cholinesterase inhibitors (Pagano et al., 2015), which may help compensate for decreased cholinergic input to the cortex from cholinergic basal forebrain neurons (Müller and Bohnen, 2013).

Autonomic symptoms

PD patients also experience symptoms related to dysfunction of the autonomic nervous system, including constipation, sexual dysfunction, urinary symptoms and incontinence, orthostatic hypotension, and changes in thermoregulation. Some symptoms, like constipation, frequently predate the onset of motor symptoms, while others, like orthostatic hypotension and incontinence, tend to become clinically significant in middle and later stages of the disease. These symptoms tend not to respond to dopamine replacement therapy or to be worsened by it (e.g. orthostatic hypotension). These key PD symptoms are rooted in the functional anatomy of the disease. Understanding some of the neuropathological features of PD, including the areas affected by neurodegeneration, informs our knowledge of which symptoms can be explained directly by cell loss, versus those that may arise from circuit dysfunction.

2.2.2 Patterns of Neurodegeneration in Parkinson's Disease

Though PD is a neurodegenerative disease, some disease symptoms can be directly linked to neuronal loss, while others appear to be caused by aberrant activity or connectivity in surviving neurons. Here we will briefly discuss the neurodegenerative features of PD. Functional components will be discussed subsequently at length.

As with the clinical features, the neuropathology of PD is highly heterogeneous, but there are some shared features across patients. The pathological hallmark of PD is the Lewy body, which contains the protein alpha synuclein. Lewy bodies are found in different regions of the postmortem brain, often but not always accompanied by neurodegenerative cell loss (Surmeier et al., 2017) corresponding to symptom burden. The most well-known site of Lewy body deposition and neurodegeneration is the midbrain, in the dopaminergic neurons of the substantia nigra pars compacta (SNc), and to a lesser degree the adjacent ventral tegmental area (VTA). The loss of dopamine neurons and their projections to the striatum is believed to produce the core motor symptoms of PD and contribute to some of the cognitive and behavioral features, including depression (Frisina et al., 2009). The chronic loss of dopaminergic signaling is believed to trigger many changes at the cellular and circuit levels, which will be detailed in the next sections.

Neurodegeneration is also extensive in brainstem nuclei, including both autonomic areas like the dorsal motor nucleus of the vagus, motor nuclei like the pedunculopontine nucleus, and neuromodulatory nuclei like the locus coeruleus and raphe (Seidel et al., 2015). Changes in noradrenergic and serotonergic projections may have different timing than loss of dopaminergic projections (Espay et al., 2014). In fact, in a postmortem immunohistochemical study of PD patients, it appeared that serotonin signaling might be enhanced in the striatum (perhaps as a compensatory mechanism or response to chronic treatment) (Bedard et al., 2011). These observations are consistent with serotonergic sprouting seen in a study of levodopa-treated parkinsonian patients, monkeys, and rats (Rylander et al., 2010). Loss of serotonergic and noraderenergic neurons might produce secondary effects on synaptic connectivity and function in its projection targets, much like the loss of dopaminergic projections profoundly alters striatal and frontal cortical connectivity and function. Less is known about clinical-pathological correlates in these areas, but positron emission tomography (PET) studies in PD patients show correlations between loss of serotonergic neurons and depression in PD (Pagano et al., 2017) or loss of serotonergic and noradrenergic signaling with sleep disturbances, mood disorders, and cognitive

deficits in PD (Espay et al., 2014; Politis and Niccolini, 2015). Neurodegeneration in limbic and neocortical areas is common in PD, and correlates strongly with cognitive decline (Horvath et al., 2013), though many older patients have concomitant Alzheimer's Disease pathology (Irwin et al., 2017).

Though the pattern of neurodegeneration seen in PD patients explains many aspects of the disease, some of the key clinical features, including the core motor symptoms (tremor, bradykinesia, and rigidity) are suspected to arise from aberrant patterns of activity within surviving neurons.

2.2.3 Anatomy and Circuit Models of the Basal Ganglia

Understanding the circuit mechanisms that drive motor symptoms of PD requires knowledge of the affected circuit components and their functions. Here, we review the anatomy and several prominent circuit models of the basal ganglia, a group of interconnected subcortical nuclei whose dysfunction following dopamine loss plays a critical role in the motor symptoms of PD. These models greatly simplify the underlying anatomy. Each model emphasizes different aspects of basal ganglia function, and may be complementary in some ways. Later sections addressing measures of activity in the basal ganglia such as firing rate, firing pattern, and synchrony that change following dopamine loss will be presented in the context of these models.

Parallel Circuit Model

The parallel circuit model (Figure 2.1) provides an anatomical basis for how different channels of information progress through the basal ganglia and for the prominent motor disruptions associated with PD. The primary input nucleus of the basal ganglia, the striatum, integrates glutamatergic input from the cortex and thalamus (centromedian and parafascicular, CM-PF) with dopaminergic input from midbrain regions including the VTA and SNc (Moore and Bloom, 1978). Early anatomical studies of the basal ganglia found that gross subdivisions of the

striatum receive glutamatergic and dopaminergic innervation from different input regions, and that output from these subdivisions to downstream basal ganglia nuclei tends to remain separated. Such findings helped lead to the development of the parallel circuit model (Alexander et al., 1986), which proposed that different types of information, such as limbic and motor, flow in parallel streams through the basal ganglia thalamo-cortical loop. At the simplest level, this model divides the striatum into three broadly defined regions: the ventral striatum, the caudate and pre-commissural putamen, and the post-commissural putamen (Figure 2.1, Galvan et al., 2015). The ventral striatum, comprised of the nucleus accumbens and olfactory tubercle, receives glutamatergic input from limbic regions, and is predominantly innervated by dopamine neurons in the VTA. The caudate and pre-commissural putamen receive dopaminergic input from the SNc and glutamatergic input from associative regions. Similarly, the post-commissural putamen receives dopaminergic input from the SNc, but receives greater input from sensorimotor regions of the cortex. Notably, in rodents, the dorsal striatum is contiguous, with the dorsomedial portion receiving greater associative input and the dorsolateral greater receiving sensorimotor input.

From these different striatal subdivisions, GABAergic output neurons, termed medium spiny neurons (MSNs, also known as spiny projection neurons or SPNs), project either directly or via several synapses (indirectly) to basal ganglia output nuclei, the globus pallidus pars interna (GPi, referred to as the entopeduncular nucleus in rodents) and substantia nigra pars reticulata (SNr). Indirect projections are relayed through GABAergic connections in the globus pallidus pars externa (GPe) and glutamatergic neurons in the subthalamic nucleus (STN), which in turn project to the GPi and SNr. GPi and SNr projections inhibit the brainstem motor centers or to the ventral anterior (VA) and ventral lateral (VL) thalamus (Parent and Parent, 2004). The distinct channels carrying limbic, associative, and sensorimotor information arise at the level of striatal input, but are preserved—in part—through downstream basal ganglia structures. Channel-specific information at the level of the cortex may cross-talk with other channels as it re-enters the basal ganglia loop (Calzavara et al., 2007; Frank, 2011). Thus, while many brain regions and functions

are affected by PD, the preferential loss of SNc dopamine neurons that innervate motor regions of the striatum (Bernheimer et al., 1973) may partially account for the early prominence of motor deficits. How nonmotor basal ganglia channels are affected in PD, and whether these changes are causal in the cognitive and behavioral symptoms, remains a crucial area for further investigation.

The Classical Model

The classical model of basal ganglia function has critically shaped understanding of how dopamine contributes to motor output and how loss of midbrain dopamine neurons leads to circuit-level changes underlying the motor symptoms of PD. Developed in the late 1980s and early 1990s (Albin et al., 1989; Alexander and Crutcher, 1990; DeLong, 1990), the classical model divides striatal MSNs into two populations, direct and indirect pathway MSNs, based on their projection targets (Figure 2.2). Direct pathway MSNs (dMSNs) project directly to basal ganglia output (GPi/SNr) and express $G_{\alpha olf}$-coupled D1-like dopamine receptors (Gerfen et al., 1990; Hervé et al., 1995; Deng et al., 2006). Thus, activation of the direct pathway is thought to decrease basal ganglia output, disinhibiting the thalamus and promoting movement. In contrast, indirect pathway MSNs (iMSNs) project to basal ganglia output indirectly via the GPe and STN, and express G_i-coupled D2-like dopamine receptors (Gerfen et al., 1990; Deng et al., 2006). Activation of this pathway is thought to increase basal ganglia output, inhibiting the thalamus and suppressing movement. Importantly, dopamine is hypothesized to have opposing effects on these two populations, increasing dMSN activity and decreasing iMSN activity. The net effect of dopaminergic signaling, according to this model, is to promote movement by suppressing basal ganglia output form the GPi. In PD, loss of dopamine would be predicted to cause an imbalance of activity between the two pathways at the level of the striatum. Excessive indirect pathway activity is hypothesized to suppress GPe firing, increasing STN activity and driving an increase in GPi-mediated thalamic inhibition. Concurrently, diminished direct pathway firing would be

predicted to disinhibit GPi neurons, increasing GPi firing further and adding to suppression of the thalamus and cortex. The classical model generated testable predictions on firing directionality of firing rate alterations throughout the basal ganglia following changes and served as a foundation for subsequent models of basal ganglia function.

Center-Surround Model

Accumulating evidence indicates an essential role for the basal ganglia not only in action initiation, but action selection. We use the term "center-surround model" to refer to ideas first proposed by Mink (Mink and Thach, 1993; Mink, 1996), but which have been developed in several directions by subsequent investigators. The center-surround model provides a conceptual framework for how basal output might control selection of actions and shape motor deficits (Nambu, 2005). The underlying concept of this model is that to execute an action, other similar or competing actions must be simultaneously suppressed. In this model, activation of direct cortical-STN projections–the hyperdirect pathway (Monakow et al., 1978)–produces widespread increases in GPi firing, which in turn inhibits thalamus and cortex and ultimately suppresses competing actions (Figure 2.3). Simultaneously, activation of dMSNs in the striatum leads to focal inhibition within GPi, releasing downstream inhibition and permitting execution of a selected action (Figure 2.3). Excitation of the STN is further shaped by release of GPe-mediated inhibition by the iMSNs in the striatum. Evidence for such interactions between the hyperdirect pathway and striatal output in guiding action selection was found in rodents trained in a cued stopping task (Schmidt et al., 2013). Similar to the classical model, the center-surround model predicts that in parkinsonism, there will be excessive STN and GPi activity, as well as decreased activity in some dMSNs and the GPe. However, while the classical model emphasized opposing responses of direct and indirect pathway MSNs to dopamine, the center-surround model highlights the complementary function of these two pathways in selecting action. The center-surround concept may also be recapitulated at different levels of the basal ganglia circuit, not only by the divergence

and convergence present in between nodes, but also by lateral connections and resultant patterns of activity within nodes. These connections may also be a potent substrate for PD-related circuit dysfunction.

2.2.4 Rate-Based Models of Parkinson's Disease Pathophysiology

While neuronal activity can be characterized in numerous ways, an underlying assumption in many models of basal ganglia function is that information is encoded in the firing *rate* of individual neurons. In this section, we explore evidence linking changes in basal ganglia firing rates with the motor deficits of PD. We review observational and interventional evidence obtained from parkinsonian non-human primate and rodent models. Notably, while these studies are highlighted for their findings relating to parkinsonism-associated alterations in firing rate, many also consider changes in firing *patterns* and *synchrony*, which are addressed in a later section.

Observations in Humans and Non-human Primates

Significant evidence for rate-based models of basal ganglia function was obtained from studies using non-human primate models of disease (Figure 2.4). The discovery that injection of 1-methyl-4-phenyl-1,2,3,6-tetrahydropyridine (MPTP) induced chronic parkinsonism in humans (Langston et al., 1983) and dopaminergic degeneration in macaques and squirrel monkeys (Burns et al., 1983; Langston et al., 1984) provided a key tool to explore how loss of dopamine changes neural activity. Initial studies examining 2-deoxyglucose uptake, a proxy for afferent terminal activity, indicated changes throughout the basal ganglia of parkinsonian primates, including increased uptake in the GPe, GPi, and thalamus (Crossman et al., 1985; Mitchell et al., 1986) and decreased uptake in caudate, STN, and cortex (Schwartzman and Alexander, 1985). Later, studies using extracellular single-unit recordings in parkinsonian primates and humans demonstrated increased baseline firing of GPi neurons, suggesting that parkinsonian motor deficits may be due to excessive basal ganglia output (Filion and Tremblay, 1991; Hutchison et

al., 1994; Boraud et al., 1996, 1998; Heimer et al., 2002), though similar changes were not observed within the SNr (Wichmann et al., 1999). Consistent with elevated GPi firing, increased baseline firing was also observed in the STN (Bergman et al., 1994; Benazzouz et al., 2002). Furthermore, both firing of GPe neurons and tonic GABA in the STN were reduced in parkinsonian primates compared to healthy animals (Boraud et al., 1998; Filion and Tremblay, 1991; Heimer et al., 2002; Soares et al., 2004). Together, findings such as these supported the classical model of basal ganglia function.

Notably, while multiple studies using parkinsonian non-human primates have recorded activity in downstream basal ganglia nuclei, for the most part, changes in striatal activity have been inferred. Classical models predict increased iMSN and decreased dMSN activity. However, evidence from humans and non-human primates is conflicting, either showing marked increases in the firing rate of MSNs (Liang et al., 2008; Singh et al., 2016) or no overall change (Deffains et al., 2016). Recent studies in rodents may provide a clearer picture of how parkinsonism changes the activity of dMSNs and iMSNs (see below).

The classical model predicts that increased basal ganglia output induces excessive inhibition of thalamus and cortex, leading to a paucity of movement. Consistent with these predictions, single-unit recordings showed reduced firing of in primary motor cortex of parkinsonian primates (Pasquereau and Turner, 2011; Pasquereau et al., 2016). At the level of the VA and VL thalamus, however, baseline firing was reportedly unchanged in parkinsonian primates (Pessiglione et al., 2005), while decreased rates have been reported in parkinsonian cats (Schneider and Rothblat, 1996), as well as PD patients compared to those with essential tremor and chronic pain (Molnar et al., 2005). Thus, firing rate changes observed throughout the basal ganglia, thalamus, and cortex of non-human primates and PD patients largely support rate predictions of the classical models. However, as discussed in the next section, manipulations of basal ganglia activity in parkinsonian and healthy animals suggest that other measures of activity likely play a critical role in PD motor deficits.

Manipulations in Humans and Non-human Primates

To support causal relationships between firing rates in basal ganglia circuit nodes and parkinsonian motor symptoms like bradykinesia, investigators have taken two broad approaches: (1) measuring physiological parameters before and after a therapeutic manipulation, such as administration of a dopamine agonist or levodopa, or DBS, and (2) pharmacological inactivation or electrolytic/chemical lesions of circuit nodes. Prior to the development of the MPTP primate models, surgical lesions of individual basal ganglia nuclei were known to alleviate motor deficits in PD patients. Aligning with the classical model, GPi lesions reduce rigidity in PD patients (Narabayashi et al., 1956; Cooper and Bravo, 1958), a result later replicated in parkinsonian primates (Baron et al., 2002). Studies using dopamine agonists, including levodopa, also observe decreased GPi firing (though notably no change in the STN or GPe) (Boraud et al., 1998; Filion et al., 1991; Levy et al., 2001). The advent of levodopa therapy for the treatment of PD diminished the use of surgical lesions, but interest climbed again in the early 1990s when lesions of the STN were found to alleviate motor symptoms in MPTP-treated primates (Bergman et al., 1990; Wichmann et al., 1994), leading to the development of STN and GPi electrical DBS (Aziz et al., 1991; Benazzouz et al., 1993; Limousin et al., 1995). These findings support classical model predictions that STN hyperactivity contributes to PD motor symptoms (Bergman et al., 1990; Wichmann et al., 1994), but also support alternative models that postulate lesions disrupt propagation of abnormal activity. While electrical stimulation may induce complex effects on activity in target structures, high frequency DBS was initially hypothesized to decrease output of target structures, functionally acting as a reversible lesion (Chiken and Nambu, 2016). However, while some studies indicate that DBS inhibits cell-bodies near the stimulation site (Meissner et al., 2005; Moran et al., 2011), others find evidence of increased target structure output, including increased GPi firing during STN DBS (Reese et al., 2011; McConnell et al., 2012) and decreased thalamic and cortical firing following GPi DBS (Anderson et al., 2003; Johnson et al., 2009) or no net change (Kammermeier et al., 2016). Furthermore, many studies, in both nonhuman primates

and PD patients, call into question whether abnormal firing rates, as predicted by the classical model, are a causal mechanism of PD motor symptoms. For example, motor output is either unaffected or reduced by GPe and GPi lesions in healthy animals (Horak and Anderson, 1984; Inase et al., 1996; Mink, 1996; Wenger et al., 1999; Desmurget and Turner, 2008; Soares et al., 2004), suggesting that rate changes in these regions is insufficient to drive PD motor deficits. Thus, while firing rate changes consistent with classical rate models have been observed, manipulations of the basal ganglia in parkinsonian and healthy animals suggest that other measures of activity such as pattern and synchrony play a role in driving PD motor symptoms.

Observations in Rodents

Electrophysiological recordings in healthy and parkinsonian rodents largely support those made in parkinsonian primates, demonstrating that dopamine depletion is followed by firing rate changes in multiple basal ganglia nuclei. Advancements in genetics, large-scale electrophysiology, and optical methods have enabled (1) cell-type specific and (2) large ensemble recordings, which reveal heterogeneous responses within individual regions. As in nonhuman primates, most investigators have used toxin-based models that target midbrain dopamine neurons, such as 6-hydroxydopamine (6-OHDA). While increased firing rates have been observed in the motor thalamus of parkinsonian rats compared to healthy controls (Bosch-Bouju et al., 2014), multiple studies have demonstrated increased SNr firing in parkinsonian rodents (Breit et al., 2007; Burbaud et al., 1995; Wang et al., 2010). As in primates, evidence in parkinsonian rodents is variable for increased STN firing, as predicted by the classical model. While some studies utilizing single-unit recordings have observed increased firing rates (Kreiss et al., 1997; Vila et al., 2000; Aristieta et al., 2012; Park et al., 2018) others have observed no change (Ni et al., 2008; Lindemann et al., 2013; Delaville et al., 2015). In the STN, changes in activity *pattern* appear more consistent (see next section). Cell-type specific manipulations of STN

neurons to alleviate parkinsonian motor symptoms also point toward a central role of patterned activity.

GPe unit recordings in awake parkinsonian rats demonstrated overall decreases in baseline firing (Pan and Walters, 1988) comparable to that observed in primates (Filion and Tremblay, 1991; Boraud et al., 1996). In anesthetized rats, GPe firing was decreased during active phases of slow wave activity and following toe pinches compared to healthy animals (Mallet et al., 2008). This and a subsequent study further distinguished two populations of GPe neurons, whose firing rate and synchrony to cortical oscillations differed in the parkinsonian state: prototypical neurons that project to the STN and arkypallidal neurons that send inhibitory projections back to the striatum (Mallet et al., 2008, 2012). Activation of both prototypical and arkypallidal neurons has been associated with movement cessation (Mallet et al., 2016) in healthy animals, and though the contribution of these populations to PD motor symptoms is unknown, recent work in parkinsonian rodents indicates that subpopulations within the GPe may play distinct roles (see below).

Whereas studies of striatal activity have produced conflicting results in parkinsonian non-human primates, evidence in rodents supports bidirectional changes in iMSN and dMSN activity consistent with classical models. In anesthetized parkinsionian rats, antidromically identified dMSNs showed decreased firing as compared to healthy animals, while presumed iMSNs showed elevated firing (Mallet et al., 2006; Kita and Kita, 2011). Recent single-unit recordings of optically and antidromically identified iMSNs and dMSNs in freely moving parkinsonian mice confirmed these bidirectional changes in firing (Ryan et al., 2018; Sagot et al., 2018). Notably, Ryan and colleagues also found that the firing of both iMSNs and dMSNs loses its normal correlation to locomotion, and that iMSN firing was specifically enhanced during periods of immobility. Another recent study in parkinsonian mice using two-photon calcium imaging to measure the activity of thousands of MSNs made similar observations: bidirectional changes in iMSN and dMSN activity and loss of locomotion correlations (Parker et al., 2018). Together, results like these highlight the

utility of parkinsonian rodents, which can extend findings from humans and primates by linking activity changes to discrete populations with potentially distinct contributions to parkinsonian motor symptoms.

Manipulations in Rodents

Rodent models of PD have provided a genetic platform for linking circuit level and cell-type specific changes in firing to motor output. Basal ganglia nuclei that have recently been targeted for study using optogenetics or chemogenetics include the STN, GPe, and striatum. While we consider how manipulations of these regions relate to firing rate changes, it is important to keep in mind that other measures of neuronal activity are inevitably perturbed as well.

Manipulations in rodent models of PD have provided key insights into the contribution of STN firing to motor deficits and the therapeutic mechanisms underlying DBS. As described above, lesions and inactivation of the STN ameliorate motor deficits in parkinsonian primates, consistent with rate model predictions. Similar results have been observed with lesions and pharmacological blockade of the STN in rodent models (Klockgether and Turski, 1990; Piallat et al., 1996; Blandini et al., 1997; Henderson et al., 1999; Luo et al., 2002). The discovery that high-frequency STN DBS results in comparable behavioral effects led to the hypothesis that DBS works through functional inactivation. Testing this hypothesis directly, Gradinaru and others optogenetically inhibited excitatory STN neurons in parkinsonian rats (Gradinaru et al., 2009). Surprisingly, while electrical stimulation reversed parkinsonian symptoms, direct inhibition of excitatory STN neurons cell bodies had no effect. Similarly, high-frequency stimulation of the same population also failed to change behavior. However, activation of terminals from layer 5 pyramidal neurons innervating the STN, which are also likely activated during electrical stimulation (Li et al., 2012), robustly reversed parkinsonian deficits (Gradinaru et al., 2009). This finding was later replicated using ultra-fast opsins (Sanders and Jaeger, 2016). These findings have led to the hypothesis that STN

DBS may alleviate motor deficits by altering cortical activity directly through anterograde activation, rather than by altering basal ganglia and thalamic output.

The classical model predicts that loss of SNc dopamine neurons leads to decreased firing of GPe neurons and that manipulations enhancing GPe firing should alleviate parkinsonian motor symptoms. While unit recordings generally support the first prediction, a recent study using optogenetic stimulation of subpopulations within the GPe paints a more complicated picture (Mastro et al., 2017). Global optical activation of GPe neurons in severely parkinsonian mice failed to rescue motor deficits. However, optogenetic manipulations that enhanced activity of parvalbumin (PV)-expressing GPe neurons, as compared to those expressing Lim homeobox 6 (Lhx-6), either by activation of the former or inhibition of the latter, produced long-lasting motor improvements. Together, these findings suggest that relative changes of output within the GPe play a greater role than total output.

Optogenetic and chemogenetic manipulations of dMSNs and iMSNs have been used to determine their effect on motor output and downstream brain region activity in both healthy and parkinsonian rodents. In line with predictions from the classical model, optogenetic and chemogenetic activation of dMSNs increased locomotion in healthy mice, and was sufficient to rescue parkinsonian motor deficits (Kravitz et al., 2010; Alcacer et al., 2017). Conversely, iMSN activation reduced measures of locomotion and promoted freezing (Kravitz et al., 2010; Alcacer et al., 2017). These results are consistent with classical rate model predictions, and supported by studies in healthy rodents showing increases and decreases in motor thalamic and motor cortical activity following stimulation of the direct activation of direct and indirect pathway, respectively (Oldenburg and Sabatini, 2015; Lee et al., 2016). Notably, while experiments in healthy rodents indicate that activation of the direct and indirect pathway can produce complex patterns of activity in downstream nuclei (Freeze et al., 2013; Lee et al., 2016), chemogenetic stimulation of the GPe, or inhibition of the GPi/SNr, has been shown to be sufficient to improve motor output in parkinsonian rodents (Assaf and Schiller). Taken together, manipulations in rodents highlight an

important distinction between activity changes that cause PD motor deficits and those sufficient to alleviate them. Multiple manipulations appear sufficient to reverse parkinsonian motor deficits, however, future work using manipulations in rodents will likely aim to identify the activity changes that are sufficient to cause such deficits.

2.2.5 Patterned Neural Activity in Parkinson's Disease

While there are changes in firing rates across many nodes in the basal ganglia-thalamocortical loop in both PD patients and animal models of PD, there is extensive evidence suggesting that PD is characterized by significant alterations in both the pattern of single-cell firing and in synchronization between circuit nodes. In fact, many investigators have challenged the idea that static changes in rate are the key causal mechanism of PD motor symptoms, and postulate changes in pattern are the most critical change in neural activity associated with PD. Despite accumulating evidence for these types of changes in activity, investigators are now trying to determine if patterned activity actually *causes* different symptoms of PD. Many experiments are consistent with the idea that pattern is a key causal mechanism, but there is some data suggesting that these markers of patterned activity do not consistently correlate with motor impairments, in both rodent and nonhuman primate models (Leblois et al., 2007; Muralidharan et al., 2016).

Bursting and Synchronization

Bursting of individual neurons, and synchronization between neurons, are two phenomena commonly associated with PD and animal models of PD (Bevan et al., 2002). Some of these changes are schematized in Figure 2.4. The bursting pattern of neuronal activity may reflect changes in the intrinsic properties or synaptic input of neurons, and together with PD-related changes in local and long-range connectivity, may be a key contributor to changes in the local field potential in basal ganglia circuit structures. Though changes in these measures have been

reported across many nuclei in the basal ganglia circuit, their functional contribution to PD symptoms remains unclear. At the level of basal ganglia output, several groups have found altered bursting activity in GPi neurons in human PD patients (Hutchison et al., 1994; Starr et al., 2005), as well as parkinsonian nonhuman primates (Miller and DeLong, 1988; Boraud et al., 1998; Muralidharan et al., 2016) . Bursting has also been observed in the GPe and STN of both PD patients and parkinsonian nonhuman primates (Bergman et al., 1994; Soares et al., 2004). The motor cortex has also been identified as a site of abnormal patterned activity in parkinsonian monkeys (McCairn and Turner, 2015). Though bursting patterns of activity are found in some thalamic neurons under normal conditions, there is also evidence for increased numbers of bursting neurons in the motor thalamus of PD patients (Magnin et al., 2000). The same group observed bursting neurons in the centromedial/parafascicular (CM-PF) thalamus, whose activity corresponded to patients' tremor. Though far less studied, one group found that about half of striatal projection neurons had irregular and bursty firing in parkinsonian nonhuman primates, identified as predominantly putative dMSNs (Singh et al., 2015).

As with studies of firing rate in basal ganglia nuclei, it has been challenging to causally link bursting activity specifically with parkinsonian motor deficits. Measuring bursting in the context of pharmacological treatment or DBS for parkinsonism is one approach. However, changes in bursting may occur in the context of changes in rate, synchronization, and oscillations (see below), making it hard to definitively say which change was responsible for the relief of bradykinesia. Consistent with the idea that bursting is pathological, dopamine replacement therapy in parkinsonian nonhuman primates reduces bursting in striatum (Singh et al., 2015), GPi and GPe (Filion et al., 1991) in parallel with therapeutic changes in motor function. Similar observations have been made in the GPi patients in response to levodopa (Boraud et al., 1998). In other experiments in parkinsonian nonhuman primates, it appears synchronization, rather than bursting, is reduced by therapeutic DBS, at the level of basal ganglia output and motor cortex (McCairn and Turner, 2009, 2015).

Synchronized activity between cells is another key alteration in single-unit activity. Synchronization amongst neurons has several potential neural substrates, including alterations in local connectivity and shared synaptic input. In PD patients and animal models, synchronization has been measured with multiple simultaneous single-unit recordings or between single-unit activity and the local field potential (LFP) (Shimamoto et al., 2013), and has been both widely observed and closely correlated with symptom severity (reviewed in (Hammond et al., 2007)). Synchronized firing was seen in the STN of PD patients undergoing DBS (Levy et al., 2000) and in parkinsonian rats (Lintas et al., 2012). Additionally, investigators observed enhanced synchronization between individual neurons at the level of the motor cortex (Goldberg et al., 2002). A key caveat of such studies, however, is that motor output and/or sensory experience can provide an external trigger to synchronize activity. An extreme example is tremor, which is present in many PD patients. While abnormal rhythmic and synchronized activity may generate tremor, it is also possible that tremor produces rhythmic activity in the brain. In one study using dual microelectrodes in PD patients undergoing stereotactic surgery for DBS or lesioning of basal ganglia nuclei, the authors found synchronization between GPe, GPi, and SNr neurons only in patients with tremor (in fact, oscillating at the tremor frequency); it was absent in patients without tremor (Levy et al., 2002). This observation points to another key issue in interpreting human and animal model data: most, but not all, PD patients have tremor, while few animal models do (e.g. MPTP-treated African green monkeys). This phenotypic difference may potently influence the neural signals recorded in each species, due to differences in the pathophysiology, or in responses to the tremor itself.

The functional role of bursting and synchronization between individual neurons remains unclear, but recent work is beginning to test how these features of neural activity might contribute to PD symptoms. One of the key manipulations used to investigate the causal role of bursting in both PD patients and nonhuman primates is therapeutic DBS of the STN or GPi. At the appropriate settings, DBS greatly reduces bradykinesia. Thus, the particular component of neural

activity that changes in response to therapeutic DBS may contribute to motor symptoms such as bradykinesia. Some such studies have found that GPi DBS does not markedly change the firing rate or burstiness of GPi neurons, but does reduce synchronization between single units (McCairn and Turner, 2009), suggesting that changes in synchronization (or oscillations) may be more critical than rate or bursting for the therapeutic effects of DBS. In contrast, in a rat model of PD, STN electrical stimulation relieved bradykinesia when calibrated to reduce burst firing, but not when a similar protocol was used that increased burst firing (Tai et al., 2012). The same group explicitly tested whether STN neuronal burst firing versus oscillations produce bradykinesia, and found that bursting was the critical component (Pan et al., 2016).

Beta Oscillations

Convergent evidence from both human patients and animal models suggests that parkinsonism is accompanied by changes in the LFP across multiple basal ganglia circuit nodes, which has been reviewed extensively elsewhere (Hammond et al., 2007; Brittain et al., 2014). Most evidence supporting a role for such changes in LFP in PD symptoms are correlative, but over the past few years there has been increasing interest in determining whether these changes are an epiphenomenon versus a causal mechanism of parkinsonism.

In human patients, the advent of DBS surgery permitted invasive microelectrode recordings of the STN and GPi during awake implantation surgery. The LFP from such recordings can be measured intraoperatively, both in the parkinsonian state and after administration of dopamine replacement therapy. In addition, the DBS device itself can be used to obtain LFP recordings, which has permitted similar LFP measurements postoperatively. Finally, more recent DBS devices have chronic recording functionality (Quinn et al., 2015; Swann et al., 2018), such that LFP signals can be measured in patients outside the operating room, either at home or in the clinic during directed tasks. Some of these devices, designed for closed-loop stimulation using

electrophysiological signals in the cortex to trigger STN stimulation, permit LFP measurements in two locations, such as the motor cortex (via electrocorticography) and STN (via the DBS device).

Measurements using various methodologies have shown that in PD patients, there is consistently higher LFP power in the beta frequency range (8-35 Hz, but typically around 20 Hz), as compared to non-PD comparators, as measured in the STN (Brown et al., 2001). Indeed, STN LFP beta power seems to correlate well with parkinsonian symptoms such as bradykinesia and rigidity (Kuhn et al., 2009), and is reduced in response to the two major types of PD therapy: dopamine replacement therapy (Giannicola et al., 2013) and basal ganglia DBS (Quinn et al., 2015). Not only are such LFP signals seen at individual circuit nodes, but there is some predictable synchronization of these rhythms across brain regions. Nevertheless, beta oscillations also occur in many regions during normal movement in healthy individuals (Engel and Fries, 2010), so there is nothing intrinsically pathological about beta-range LFP power. Recent work indicates that the duration of beta bouts is more specific to parkinsonism, however (Deffains et al., 2018). Similar beta oscillatory activity has been seen in the LFP at multiple nodes in parkinsonian nonhuman primates. In rodent models, evidence regarding beta oscillations has been somewhat more inconsistent. In awake-behaving parkinsonian rats, enhanced beta-range power is at a somewhat higher frequency (approx. 35 Hz) than is seen in humans, but has been found in the STN (Delaville et al., 2015), SNr (Avila et al., 2010; Brazhnik et al., 2014), thalamus (Brazhnik et al., 2016), and motor cortex (Brazhnik et al., 2012). In anesthetized parkinsonian rats, cortical activation led to increased beta-range LFP power in the GPe, and individual GPe units frequently entrained to this rhythm (Mallet et al., 2008). There are many fewer instances of beta oscillations seen in mice, however, and most oscillatory activity has been seen in anesthetized animals. Interestingly, one group observed that patterned activity in parkinsonian mice is greatly attenuated in the awake-restrained versus the anesthetized state (Lobb and Jaeger, 2015). To our knowledge, there are no reported instances of beta oscillations in the striatum of parkinsonian mice, though modeling suggests it could be generated there (McCarthy

et al., 2011). As better tools now exist for recording in awake-behaving parkinsonian mice, investigators may or may not find evidence of strong oscillatory activity in the LFP. The discrepancies between primate, rat, and mouse recordings may be due to differences in the recording configurations (anesthetized, head-fixed, freely moving), differences in symptoms seen in the PD models, or perhaps differences in the complexity or density of connections between circuit nodes, likely a critical ingredient in producing strong oscillatory activity. However, as all models display bradykinesia, the lack of demonstrated beta in awake-behaving parkinsonian mice is puzzling, and may call into question the causal relationship between this physiological phenomenon and bradykinesia.

It is challenging to directly test if altered LFP power in different frequency ranges causally contributes to parkinsonism. Part of the difficulty is that LFP changes are most robust in human patients and parkinsonian monkeys, where fewer specific interventional techniques are available. In addition, efforts to modulate LFP beta power often entail changing the overall spiking activity and/or synchronization of a group of neurons, such that multiple mechanisms may be responsible for behavioral changes. However, investigators have taken several approaches to get at the question of whether changes in beta oscillatory activity causes parkinsonian motor impairments. First, investigators have used therapeutic interventions, such as DBS, in conjunction with neural recordings, to see which features of neural activity change with therapeutic stimulation. As mentioned above, DBS studies in nonhuman primates have yielded a variety of results, but in some studies changes in rate appear relatively minor, whereas synchronization and beta oscillations are potently reduced (McCairn and Turner, 2009). In rodents, treatments also reduced beta-range LFP power in parallel with therapeutic effects (Brazhnik et al., 2014). Second, some have tried to induce beta oscillations in healthy human subjects to test whether such a manipulation can provoke bradykinesia, using transcranial current stimulation (Krause et al., 2013; Pogosyan et al., 2009). Additionally, there is evidence that STN DBS at low frequencies (which might be hypothesized to enhance beta oscillatory activity in the STN or connected

structures) may worsen bradykinesia (Timmermann et al., 2004), and that more specific stimulation of hyperdirect pathway neurons at low frequencies in rodents can worsen bradykinesia (Gradinaru et al., 2009). Another way to examine the causal role of different firing patterns and/or LFP oscillations is to look at alternative models of PD. One group compared SNr activity in an alpha-synuclein overexpression model, which recapitulates many of the motor and nonmotor features of PD, but does not show the same dopaminergic cell loss seen in toxin-based models. They found much more subtle changes in firing rate in the overexpression model, and if anything, beta oscillations were reduced, rather than enhanced, in this model of PD (Lobb et al., 2013). Together, this work begins to address the question of whether increased beta oscillations are part of causal network changes in PD.

Loss of Functional Segregation in Parkinsonian Basal Ganglia Circuits

As discussed above, separate lines of information such as limbic, associative, and sensorimotor are thought to progress through the basal ganglia in parallel (Figure 2.1). Another level of segregation, best understood within the sensorimotor channel, is by specific somatosensory or motor maps in each circuit node of the basal ganglia. Though less well-studied than the simpler rate or pattern-based changes in parkinsonian subjects, the aberrant mapping of sensory responses or specific actions is likely a major type of PD circuit dysfunction, the importance of which we have yet to fully explore. The advent of chronic recordings in patients and high-density recordings in awake behaving parkinsonian nonhuman primates or calcium imaging in freely moving parkinsonian rodents (Barbera et al., 2016; Klaus et al., 2017; Markowitz et al., 2018) makes possible the more detailed investigation of these maps across multiple neurons in a given circuit node.

While there is evidence for somatotopy and motor mapping at several levels of the basal ganglia circuit, the exact cellular and synaptic structure supporting these maps (and action selection) is as yet unclear. However, several studies have examined the sensory receptive fields

of basal ganglia neurons during single-unit recordings, and have observed changes in parkinsonian animals. In the striatum of rats and cats, clusters of units responsive to somatosensory stimulation shrank in size and showed diminished spatial specificity (Rothblat and Schneider, 1995; Cho et al., 2002). Similarly, while most GPi neurons in healthy primates responded to one type of passive joint movement, in parkinsonian animals the majority of neurons responded to multiple joint movements (Boraud et al., 2000). Results looking at the motor thalamus have proven more variable, with some studies showing increases in the number of responsive units and their receptive fields (Pessiglione et al., 2005), others reporting a decrease in the number of responsive units (Schneider and Rothblat, 1996), and other finding no change (Kiss et al., 2003). Changes in receptive fields suggest the possibility that dopamine-related changes in synaptic connectivity may lead to deficits in action selection. The underlying cellular and synaptic substrate of these changes may include lateral connections within individual basal ganglia nuclei. Interestingly, lateral connections in healthy mice are potently regulated by dopamine (Dobbs et al., 2016), and in parkinsonian mice, the likelihood of lateral connections between iMSN-iMSN or dMSN-dMSN pairs was significantly decreased, while connections from iMSNs to dMSNs were largely spared (Taverna et al., 2008). Such changes may help explain differences in striatal information processing observed in vivo. Still, how somatosensory and motor mapping evolve during PD and how such changes may causally contribute to activity patterns and motor symptoms remains to be explored.

Basal Ganglia Mechanisms of Cognitive Parkinson's Disease Symptoms

As mentioned above, some PD cognitive symptoms correlate well with primary neurodegenerative processes in the cortex and other higher cognitive regions. However, given the fact that some cognitive features of PD (1) are modulated by dopamine replacement therapy, and (2) can be observed in toxin-based animal models (where cortical neurodegeneration is not present), these features may be mediated by aberrant neural activity, much like the classic motor

features of PD. Aberrant neural activity may be present in the cognitive/associative or behavioral/limbic streams that course through the basal ganglia loops, which could in turn contribute to impaired action selection-like phenomena in cognitive (poor set-switching and reward-based learning) and behavioral (depression, apathy) domains. Though this theory has not been investigated extensively, there are indications that some of the same impairments seen in the dorsolateral, motor portions of basal ganglia nuclei and motor cortex are also seen in the more medial and ventral portions of the same basal ganglia nuclei (Kish et al., 1988; Carriere et al., 2014) and cognitive portions of frontal cortex (Wang et al., 2017; Chung et al., 2018). However, in parkinsonian rats, the high beta-range oscillatory activity seen in the primary motor cortex is far less prominent in prefrontal cortical areas important for cognitive function (Delaville et al., 2015). Some studies have directly measured circuit activity during more cognitive tasks in patients. In one such study, investigators correlated changes in STN LFP oscillations with performance on a speeded cognitive task (Siegert et al., 2014). Another recent study measured STN LFP during chronic recordings in PD patients during a response inhibition task, and showed correlations between STN oscillatory activity and task performance (Hell et al., 2018). These type of studies are relatively rare, but may yield important information about how circuit changes contribute to cognitive deficits. To date it remains unclear whether the same neural signatures contribute to cognitive and behavioral dysfunction, or whether distinct physiological phenomena mediate these symptoms.

There are very few studies attempting to link parkinsonian cognitive deficits with circuit dysfunction in rodents or nonhuman primate models. A major limitation is that toxin-based models produce fairly profound motor dysfunction, and most cognitive assays have a motor-dependent outcome measure (in rodents, swimming to a hidden platform in the water maze, nosepoking or pushing a lever to indicate choice; in monkeys reaching for a reward or pushing a button). However, other models show potential for such studies. In nonhuman primates, several groups have characterized a PD-like frontal pattern of cognitive deficits in lower dose MPTP-treated

primates that have minimal or no motor deficits (Schneider and Kovelowski, 1990; Schneider and Roeltgen, 1993). Interestingly, in this type of model (as in many patients), doses of levodopa that greatly ameliorate motor symptoms do not improve (and can even worsen) cognitive performance (Schneider et al., 2013). In rodents, non-toxin based models may also be useful. One example is the Mito-Park model, which replicates several motor, nonmotor, and pathological features of human PD. At early time points (before marked motor impairment develops) Mito-Park mice show deficits on the Barnes maze and novel object recognition (tests of visuospatial learning and memory) (Li et al., 2013). There is also evidence for a relationship between non-dopaminergic circuit changes and cognitive dysfunction in PD animal models. In mouse α-synuclein overexpression models, there are multiple cognitive deficits observed, some of which can be linked to cortical cholinergic deficits (as are seen in PD patients). In an extensive behavioral study, investigators found many cognitive deficits that mirror those of PD patients: reversal learning, habit learning, and visuospatial memory (Magen et al., 2012). These models that allow focused study of PD-related cognitive deficits may be a good platform upon which to build more circuit-level analyses, in order to more directly link circuit changes to cognitive deficits.

2.3 Future Directions

The recent advances in neural monitoring technology, both in humans and animal models, represents a major opportunity for gathering additional, and more representative, data about the patterns of neural activity that accompany symptoms in PD. In patients, there are opportunities to probe neural activity in multiple brain regions. For example, an investigational DBS system developed for future use in closed-sloop stimulation has also been used to monitor the activity of both the motor cortex and STN, both intraoperatively and chronically, in patients with PD (Swann et al., 2018). This approach permits chronic recordings of the relationship between neural activity in these two nodes in patients with different movement disorders, but perhaps most interestingly, in relation to specific disease symptoms (Swann et al., 2016). In animal models, tools now allow simultaneous electrical recordings of hundreds of neurons in a given brain region, but also across multiple brain areas, during behavior. The development of genetically-encoded calcium indicators and voltage sensors permits gathering of even larger numbers of single-cell data, though thus far the temporal characteristics of these indicators cannot match traditional electrophysiology for determining tight synchronization between single cells. In rodents, and now nonhuman primates (Galvan et al., 2017), the use of optogenetic and chemogenetic tools permit more direct tests of whether specific patterns of activity (changes in rate, pattern, or synchronization).

Despite the accumulation of extensive supportive evidence for different circuit mechanisms in driving the symptoms of PD, a number of major questions remain. We have listed some of the questions that we think are particularly critical to address:

1. *How do low-level changes in synaptic connectivity and firing rate or pattern contribute to higher-level phenomena such as synchronization between neurons or brain regions, and local-field potential oscillations at particular frequencies?* Connecting cellular and synaptic

observations to the disease-related changes in the local field potential at different nodes in the basal ganglia thalamo-cortical loop is an important basic science question, but will also help bridge extensive work at these two levels of analysis in the PD field.

2. *Do changes in firing rate, pattern, or synchronization <u>cause</u> disease symptoms*? It will likely require both more sophisticated observational studies (a more detailed look at the timing of neural activity and behavioral changes) and causal manipulation studies to fully address this question. Observational studies will be greatly facilitated by new technology permitting high channel-count electrophysiology, as well as deep imaging methods that permit physiological measurement from tens to hundreds of neurons at the same time. Though tools like optogenetics will no doubt be useful in this quest, we should be careful to use them to mimic healthy or disease-related activity (informed by the decades of work in this area), rather than imposing yet new rates or patterns of activity on neural circuits. Otherwise, results may be difficult to interpret.

3. *How do our major therapies for PD work*? Ongoing studies involving current therapies, such as oral medications (levodopa, dopamine agonists) or DBS, in both patients and animal models, may also give us insights into which circuit changes cause, vs correlate with, disease symptoms. In the course of these studies, investigators may identify multiple therapeutic mechanisms, which could guide development of new treatments.

4. *Do motor and nonmotor aspects of PD have shared or distinct circuit mechanisms?* Mechanistic studies of the nonmotor aspects of PD have been limited to date, largely because of the challenges in identifying and quantifying these symptoms. However, the advent of chronic ambulatory recordings in PD patients now allows recordings of neural activity in conjunction with cognitive task performance, or alignment with patient-identified symptoms that arise at home. In addition, improvements in high-throughput testing of higher cognitive function in rodents will allow more invasive testing of the hypotheses generated by observational studies in both patients and nonhuman primates.

5. *Are changes in circuit function, at the level of connectivity and neural activity not just a feature of pathophysiology, but also a contributor to ongoing pathogenesis?* Historically, most PD research has been separated into two branches: pathogenesis (focused on cellular and molecular mechanisms of neurodegeneration) and pathophysiology (focused on circuit mechanisms in the circuit). However, it may be that these two processes are intertwined. Activity may be a key contributor to neurodegeneration (Surmeier, 2018), and synaptic connectivity may be a mechanism of disease spread (Braak et al., 2003).

Key to progress is communication and collaboration between investigators studying human patients, nonhuman primate, rodent, and even cellular models of PD. Those of us who work with animal models need to identify which questions can be answered with our current tools (including the animal models themselves), and which should be set aside until the tools improve, or would be best answered by our colleagues working with patients. In addition, as each group of scientists makes progress in unraveling the circuit mechanisms of PD, it will be important to check findings against those in other models, and ultimately, in the disease itself.
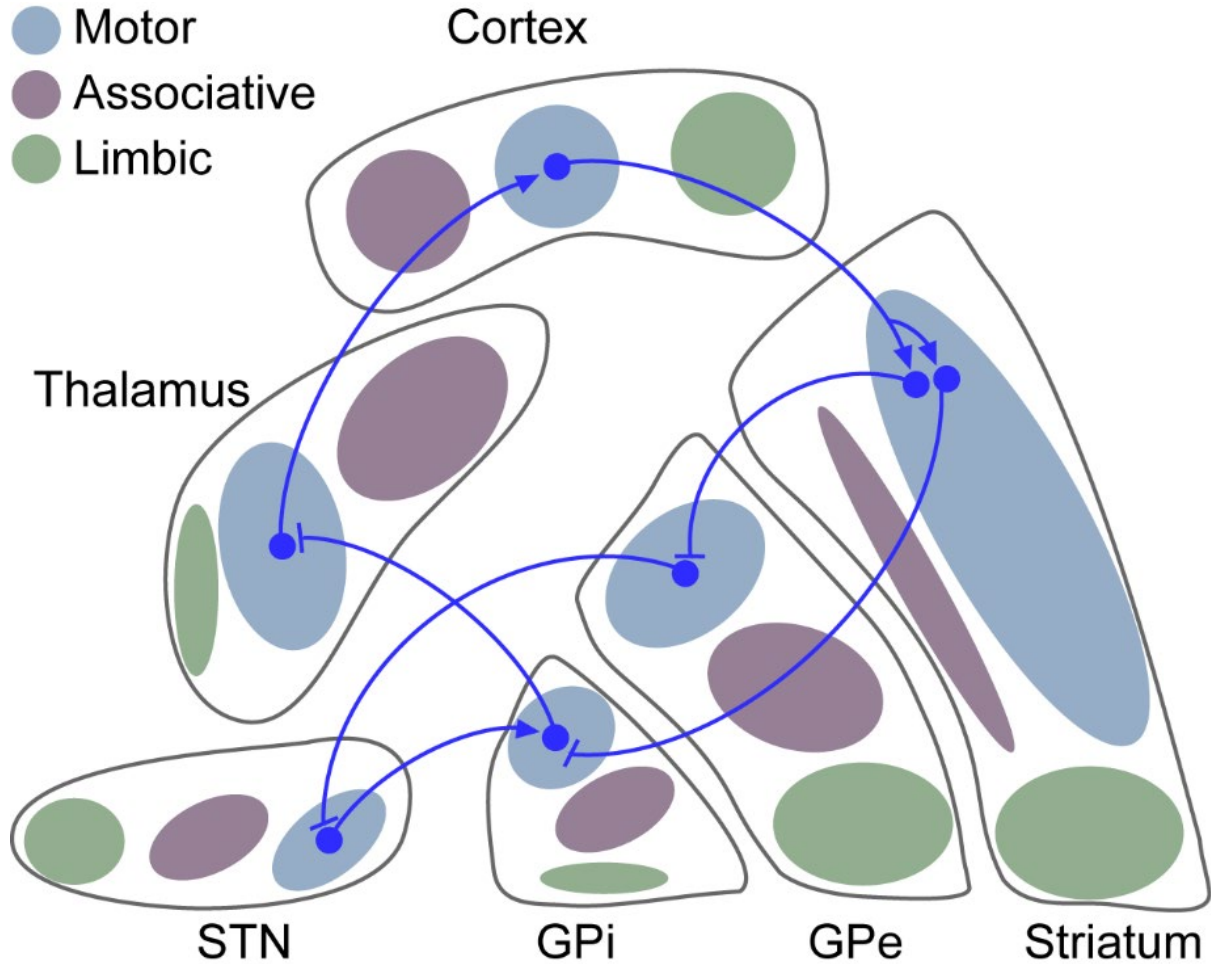
Figure 2.1: Parallel circuit model of basal ganglia. Limbic (green), associative (purple), and sensorimotor (blue) information from excitatory (arrows) cortical afferents is distributed in parallel to regions of the striatum. Anatomical separation of these channels is preserved in downstream basal ganglia nuclei. As an example, inhibitory projections (flat arrows) from sensorimotor striatum send innervate sensorimotor regions GPi, either directly or intermediately through the GPe and STN. Projections from sensorimotor regions of GPi then innervate the motor thalamus, which projects back to sensorimotor regions of the cortex.
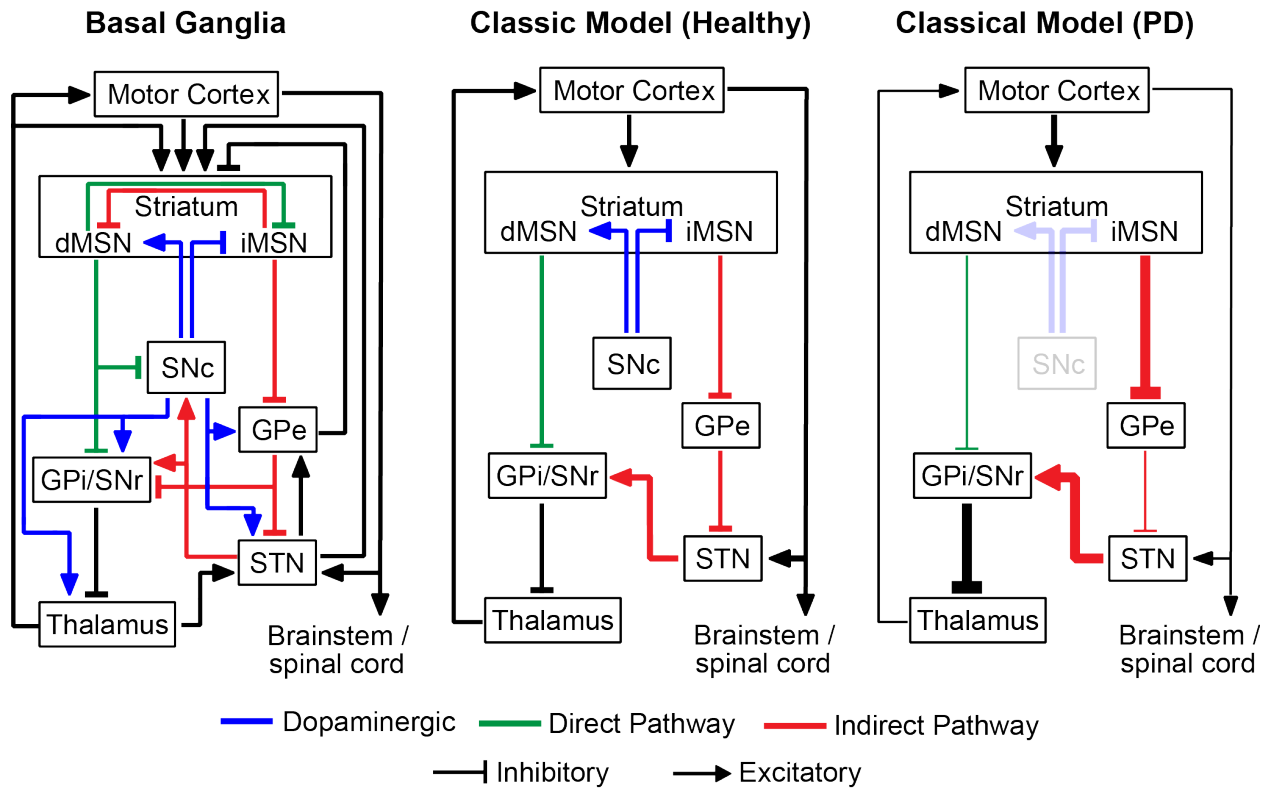
Figure 2.2: Classical model of the basal ganglia. (Left) A fuller representations of the connectivity within the basal ganglia demonstrates the simplification present in the classical model. In the healthy condition (middle), dopamine (blue) from the SNc to the striatum activates direct pathway (green) MSNs and inhibits indirect pathway (red) MSNs. This effect decreases GPi output, releasing inhibition on the thalamus and cortex and promoting movement. In the parkinsonian condition (right), loss of SNc dopamine causes hypoactivity of the direct pathway and hyperactivity of the indirect pathway that leads to excessive GPi output. As a result, over inhibition of the thalamus and cortex leads to a suppression of movement. (Adapted from DeLong, 1990)
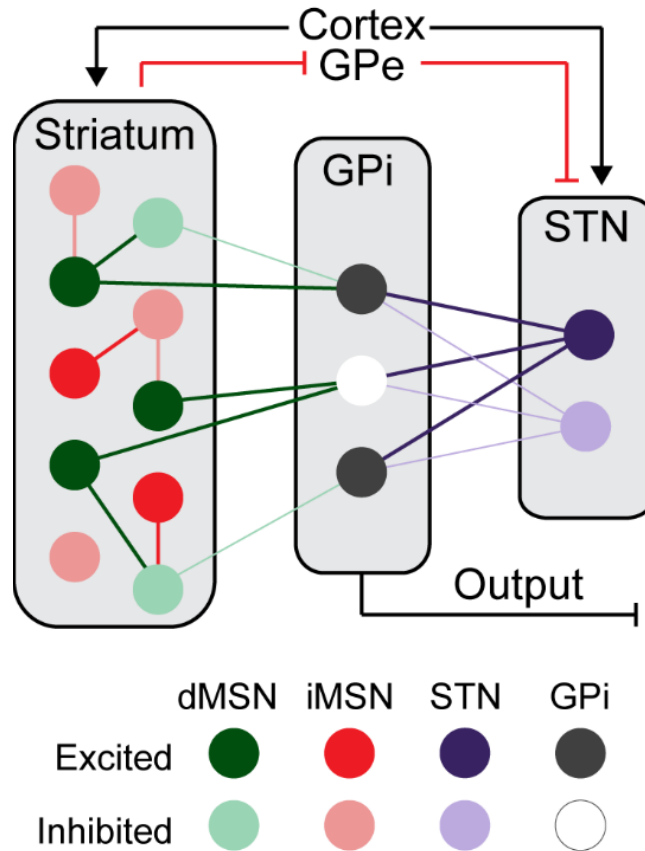
Figure 2.3: Center-surround model of the basal ganglia. Cortical input activates STN neurons (purple) that broadly excite GPi neurons (black), suppressing actions. Concurrently, cortical input to the striatum activates iMSNs that shape STN activity through the GPe, as well as dMSNs (green) that converge and inhibit a subset of GPi neurons to permit selective execution of movement. At the striatal level, inhibitory connections between MSNs may contribute to conceptually similar center-surround patterns.

	Healthy	Parkinsonian	Citations
Striatum			
dMSNs			(Kita & Kita 2011; Mallet 2012; Parker
iMSNs			2018; Ryan 2018; Sagot 2018)
GPe			
Proto			(Filion 1991; Boraud 1998; Pan 1998;
Arky			Heimer 2002; Soares 2004; Mallet 2008, 2012, 2015)
STN			(Bergman 1994; Hassini 1996)
GPi			(Miller 1988; Fillion 1991; Hutchinson 1994; Boraud 1996,1998; Heimer 2002; Muralidharan 2016)
SNr			(Wichmann 1999)
Thalamus		?	(Schneider 1996; Pessiglione 2005; Molanar 2005)
M1 Cortex			(Doudet 1990; Pasquereau 2011, 2016; McCairn 2015)

Figure 2.4: Changes in firing between healthy and parkinsonian conditions. Schematic depiction of pattern and rate changes observed across healthy and parkinsonian animals in basal ganglia, thalamus and cortex (Arky, arkypallidal; proto, prototypical; M1, primary motor cortex).

2.5 References

Aarsland, D., Brønnick, K., Larsen, J.P., Tysnes, O.B., Alves, G., and Norwegian ParkWest Study Group (2009). Cognitive impairment in incident, untreated Parkinson disease: the Norwegian ParkWest study. Neurology *72*, 1121–1126.

Abbott, R.D., Petrovitch, H., White, L.R., Masaki, K.H., Tanner, C.M., Curb, J.D., Grandinetti, A., Blanchette, P.L., Popper, J.S., and Ross, G.W. (2001). Frequency of bowel movements and the future risk of Parkinson's disease. Neurology *57*, 456–462.

Albin, R.L., Young, A.B., and Penney, J.B. (1989). The functional anatomy of basal ganglia disorders. Trends Neurosci. *12*, 366–375.

Alcacer, C., Andreoli, L., Sebastianutto, I., Jakobsson, J., Fieblinger, T., and Cenci, M.A. (2017). Chemogenetic stimulation of striatal projection neurons modulates responses to Parkinson's disease therapy. J. Clin. Invest. *127*, 720–734.

Alexander, G.E., and Crutcher, M.D. (1990). Functional architecture of basal ganglia circuits: neural substrates of parallel processing. Trends Neurosci. *13*, 266–271.

Alexander, G.E., DeLong, M.R., and Strick, P.L. (1986). Parallel organization of functionally segregated circuits linking basal ganglia and cortex. Annu. Rev. Neurosci. *9*, 357–381.

Anderson, M.E., Postupna, N., and Ruffo, M. (2003). Effects of High-Frequency Stimulation in the Internal Globus Pallidus on the Activity of Thalamic Neurons in the Awake Monkey. J. Neurophysiol. *89*, 1150–1160.

Aristieta, A., Azkona, G., Sagarduy, A., Miguelez, C., Ruiz-Ortega, J.Á., Sanchez-Pernaute, R., and Ugedo, L. (2012). The Role of the Subthalamic Nucleus in L-DOPA Induced Dyskinesia in 6-Hydroxydopamine Lesioned Rats. PLOS ONE *7*, e42652.

Assaf, F., and Schiller, Y. A chemogenetic approach for treating experimental Parkinson's disease. Mov. Disord. *0*.

Avila, I., Parr-Brownlie, L.C., Brazhnik, E., Castañeda, E., Bergstrom, D.A., and Walters, J.R.

(2010). Beta frequency synchronization in basal ganglia output during rest and walk in a hemiparkinsonian rat. Exp. Neurol. *221*, 307–319.

Aziz, T.Z., Peggs, D., Sambrook, M.A., and Crossman, A.R. (1991). Lesion of the subthalamic nucleus for the alleviation of 1-methyl-4-phenyl-1,2,3,6-tetrahydropyridine (MPTP)-induced parkinsonism in the primate. Mov. Disord. Off. J. Mov. Disord. Soc. *6*, 288–292.

Barbera, G., Liang, B., Zhang, L., Gerfen, C.R., Culurciello, E., Chen, R., Li, Y., and Lin, D.T. (2016). Spatially Compact Neural Clusters in the Dorsal Striatum Encode Locomotion Relevant Information. Neuron *92*, 202–213.

Baron, M.S., Wichmann, T., Ma, D., and DeLong, M.R. (2002). Effects of Transient Focal Inactivation of the Basal Ganglia in Parkinsonian Primates. J. Neurosci. *22*, 592–599.

Bedard, C., Wallman, M.J., Pourcher, E., Gould, P.V., Parent, A., and Parent, M. (2011). Serotonin and dopamine striatal innervation in Parkinson's disease and Huntington's chorea. Park. Relat Disord *17*, 593–598.

Benazzouz, A., Gross, C., Féger, J., Boraud, T., and Bioulac, B. (1993). Reversal of Rigidity and Improvement in Motor Performance by Subthalamic High-frequency Stimulation in MPTP-treated Monkeys. Eur. J. Neurosci. *5*, 382–389.

Benazzouz, A., Breit, S., Koudsie, A., Pollak, P., Krack, P., and Benabid, A.-L. (2002). Intraoperative microrecordings of the subthalamic nucleus in Parkinson's disease. Mov. Disord. Off. J. Mov. Disord. Soc. *17 Suppl 3*, S145-149.

Bergman, H., Wichmann, T., and DeLong, M.R. (1990). Reversal of experimental parkinsonism by lesions of the subthalamic nucleus. Science *249*, 1436–1438.

Bergman, H., Wichmann, T., Karmon, B., and DeLong, M.R. (1994). The primate subthalamic nucleus. II. Neuronal activity in the MPTP model of parkinsonism. J. Neurophysiol. *72*, 507–520.

Bernheimer, H., Birkmayer, W., Hornykiewicz, O., Jellinger, K., and Seitelberger, F. (1973). Brain

dopamine and the syndromes of Parkinson and Huntington Clinical, morphological and neurochemical correlations. J. Neurol. Sci. *20*, 415–455.

Bevan, M.D., Magill, P.J., Terman, D., Bolam, J.P., and Wilson, C.J. (2002). Move to the rhythm: oscillations in the subthalamic nucleus-external globus pallidus network. Trends Neurosci *25*, 525–531.

Bezard, E., and Fernagut, P.-O. (2014). Premotor parkinsonism models. Parkinsonism Relat. Disord. *20*, S17–S19.

Blandini, F., Garcia-Osuna, M., and Greenamyre, J.T. (1997). Subthalamic Ablation Reverses Changes in Basal Ganglia Oxidative Metabolism and Motor Response to Apomorphine Induced by Nigrostriatal Lesion in Rats. Eur. J. Neurosci. *9*, 1407–1413.

Boraud, T., Bezard, E., Bioulac, B., and Gross, C. (1996). High frequency stimulation of the internal Globus Pallidus (GPi) simultaneously improves parkinsonian symptoms and reduces the firing frequency of GPi neurons in the MPTP-treated monkey. Neurosci. Lett. *215*, 17–20.

Boraud, T., Bezard, E., Guehl, D., Bioulac, B., and Gross, C. (1998). Effects of l-DOPA on neuronal activity of the globus pallidus externalis (GPe) and globus pallidus internalis (GPi) in the MPTP-treated monkey. Brain Res. *787*, 157–160.

Boraud, T., Bezard, E., Bioulac, B., and Gross, C.E. (2000). Ratio of Inhibited-to-Activated Pallidal Neurons Decreases Dramatically During Passive Limb Movement in the MPTP-Treated Monkey. J. Neurophysiol. *83*, 1760–1763.

Bosch-Bouju, C., Smither, R.A., Hyland, B.I., and Parr-Brownlie, L.C. (2014). Reduced Reach-Related Modulation of Motor Thalamus Neural Activity in a Rat Model of Parkinson's Disease. J. Neurosci. *34*, 15836–15850.

Braak, H., Tredici, K.D., Rüb, U., de Vos, R.A.I., Jansen Steur, E.N.H., and Braak, E. (2003). Staging of brain pathology related to sporadic Parkinson's disease. Neurobiol. Aging *24*, 197–211.

Brazhnik, E., Cruz, A.V., Avila, I., Wahba, M.I., Novikov, N., Ilieva, N.M., McCoy, A.J., Gerber, C., and Walters, J.R. (2012). State-dependent spike and local field synchronization between motor cortex and substantia nigra in hemiparkinsonian rats. J. Neurosci. Off. J. Soc. Neurosci. *32*, 7869–7880.

Brazhnik, E., Novikov, N., McCoy, A.J., Cruz, A.V., and Walters, J.R. (2014). Functional correlates of exaggerated oscillatory activity in basal ganglia output in hemiparkinsonian rats. Exp. Neurol. *261*, 563–577.

Brazhnik, E., McCoy, A.J., Novikov, N., Hatch, C.E., and Walters, J.R. (2016). Ventral Medial Thalamic Nucleus Promotes Synchronization of Increased High Beta Oscillatory Activity in the Basal Ganglia-Thalamocortical Network of the Hemiparkinsonian Rat. J. Neurosci. Off. J. Soc. Neurosci. *36*, 4196–4208.

Breit, S., Bouali-Benazzouz, R., Popa, R.C., Gasser, T., Benabid, A.L., and Benazzouz, A. (2007). Effects of 6-hydroxydopamine-induced severe or partial lesion of the nigrostriatal pathway on the neuronal activity of pallido-subthalamic network in the rat. Exp. Neurol. *205*, 36–47.

Brittain, J.-S., Sharott, A., and Brown, P. (2014). The highs and lows of beta activity in cortico-basal ganglia loops. Eur. J. Neurosci. *39*, 1951–1959.

Brown, P., Oliviero, A., Mazzone, P., Insola, A., Tonali, P., and Di Lazzaro, V. (2001). Dopamine dependency of oscillations between subthalamic nucleus and pallidum in Parkinson's disease. J Neurosci *21*, 1033–1038.

Burbaud, P., Gross, C., Benazzouz, A., Coussemacq, M., and Bioulac, B. (1995). Reduction of apomorphine-induced rotational behaviour by subthalamic lesion in 6-OHDA lesioned rats is associated with a normalization of firing rate and discharge pattern of pars reticulata neurons. Exp. Brain Res. *105*, 48–58.

Burns, R.S., Chiueh, C.C., Markey, S.P., Ebert, M.H., Jacobowitz, D.M., and Kopin, I.J. (1983). A

primate model of parkinsonism: selective destruction of dopaminergic neurons in the pars compacta of the substantia nigra by N-methyl-4-phenyl-1,2,3,6-tetrahydropyridine. Proc. Natl. Acad. Sci. *80*, 4546–4550.

Calzavara, R., Mailly, P., and Haber, S.N. (2007). Relationship between the corticostriatal terminals from areas 9 and 46, and those from area 8A, dorsal and rostral premotor cortex and area 24c: an anatomical substrate for cognition to action. Eur. J. Neurosci. *26*, 2005–2024.

Carriere, N., Besson, P., Dujardin, K., Duhamel, A., Defebvre, L., Delmaire, C., and Devos, D. (2014). Apathy in Parkinson's disease is associated with nucleus accumbens atrophy: a magnetic resonance imaging shape analysis. Mov. Disord. Off. J. Mov. Disord. Soc. *29*, 897–903.

Chiken, S., and Nambu, A. (2016). Mechanism of Deep Brain Stimulation: Inhibition, Excitation, or Disruption? The Neuroscientist *22*, 313–322.

Cho, J., Duke, D., Manzino, L., Sonsalla, P.K., and West, M.O. (2002). Dopamine depletion causes fragmented clustering of neurons in the sensorimotor striatum: Evidence of lasting reorganization of corticostriatal input. J. Comp. Neurol. *452*, 24–37.

Chung, J.W., Burciu, R.G., Ofori, E., Coombes, S.A., Christou, E.A., Okun, M.S., Hess, C.W., and Vaillancourt, D.E. (2018). Beta-band oscillations in the supplementary motor cortex are modulated by levodopa and associated with functional activity in the basal ganglia. NeuroImage Clin. *19*, 559–571.

Cooper, I.S., and Bravo, G. (1958). Chemopallidectomy and Chemothalamectomy. J. Neurosurg. *15*, 244–250.

Crossman, A.R., Mitchell, I.J., and Sambrook, M.A. (1985). Regional brain uptake of 2-deoxyglucose in N-methyl-4-phenyl-1,2,3,6-tetrahydropyridine (MPTP)—induced parkinsonism in the macaque monkey. Neuropharmacology *24*, 587–591.

Dadgar, H., Khatoonabadi, A.R., and Bakhtiyari, J. (2013). Verbal Fluency Performance in

Patients with Non-demented Parkinson's Disease. Iran. J. Psychiatry *8*, 55–58.

Deffains, M., Iskhakova, L., Katabi, S., Haber, S.N., Israel, Z., and Bergman, H. (2016). Subthalamic, not striatal, activity correlates with basal ganglia downstream activity in normal and parkinsonian monkeys. ELife *5*, e16443.

Deffains, M., Iskhakova, L., Katabi, S., Israel, Z., and Bergman, H. (2018). Longer beta oscillatory episodes reliably identify pathological subthalamic activity in Parkinsonism. Mov Disord *33*, 1609–1618.

Delaville, C., McCoy, A.J., Gerber, C.M., Cruz, A.V., and Walters, J.R. (2015). Subthalamic Nucleus Activity in the Awake Hemiparkinsonian Rat: Relationships with Motor and Cognitive Networks. J. Neurosci. *35*, 6918–6930.

DeLong, M.R. (1990). Primate models of movement disorders of basal ganglia origin. Trends Neurosci. *13*, 281–285.

Deng, Y.-P., Lei, W.-L., and Reiner, A. (2006). Differential perikaryal localization in rats of D1 and D2 dopamine receptors on striatal projection neuron types identified by retrograde labeling. J. Chem. Neuroanat. *32*, 101–116.

Desmurget, M., and Turner, R.S. (2008). Testing Basal Ganglia Motor Functions Through Reversible Inactivations in the Posterior Internal Globus Pallidus. J. Neurophysiol. *99*, 1057–1076.

Dobbs, L.K., Kaplan, A.R., Lemos, J.C., Matsui, A., Rubinstein, M., and Alvarez, V.A. (2016). Dopamine Regulation of Lateral Inhibition between Striatal Neurons Gates the Stimulant Actions of Cocaine. Neuron *90*, 1100–1113.

Doty, R.L. (2012). Olfactory dysfunction in Parkinson disease. Nat. Rev. Neurol. *8*, 329–339.

Engel, A.K., and Fries, P. (2010). Beta-band oscillations—signaling the status quo? Curr. Opin. Neurobiol. *20*, 156–165.

Espay, A.J., LeWitt, P.A., and Kaufmann, H. (2014). Norepinephrine deficiency in Parkinson's disease: the case for noradrenergic enhancement. Mov Disord *29*, 1710–1719.

Filion, M., and Tremblay, L. (1991). Abnormal spontaneous activity of globus pallidus neurons in monkeys with MPTP-induced parkinsonism. Brain Res. *547*, 140–144.

Filion, M., Tremblay, L., and Bedard, P.J. (1991). Effects of dopamine agonists on the spontaneous activity of globus pallidus neurons in monkeys with MPTP-induced parkinsonism. Brain Res *547*, 152–161.

Frank, M.J. (2011). Computational models of motivated action selection in corticostriatal circuits. Curr. Opin. Neurobiol. *21*, 381–386.

Freeze, B.S., Kravitz, A.V., Hammack, N., Berke, J.D., and Kreitzer, A.C. (2013). Control of Basal Ganglia Output by Direct and Indirect Pathway Projection Neurons. J. Neurosci. *33*, 18531–18539.

Frisina, P.G., Haroutunian, V., and Libow, L.S. (2009). The neuropathological basis for depression in Parkinson's disease. Park. Relat Disord *15*, 144–148.

Galbiati, A., Verga, L., Giora, E., Zucconi, M., and Ferini-Strambi, L. (2018). The risk of neurodegeneration in REM sleep behavior disorder: A systematic review and meta-analysis of longitudinal studies. Sleep Med. Rev. *43*, 37–46.

Galvan, A., Devergnas, A., and Wichmann, T. (2015). Alterations in neuronal activity in basal ganglia-thalamocortical circuits in the parkinsonian state. Front. Neuroanat. *9*.

Galvan, A., Stauffer, W.R., Acker, L., El-Shamayleh, Y., Inoue, K., Ohayon, S., and Schmid, M.C. (2017). Nonhuman Primate Optogenetics: Recent Advances and Future Directions. J. Neurosci. *37*, 10894–10903.

Gerfen, C.R., Engber, T.M., Mahan, L.C., Susel, Z., Chase, T.N., Monsma, F.J., and Sibley, D.R. (1990). D1 and D2 dopamine receptor-regulated gene expression of striatonigral and striatopallidal neurons. Science *250*, 1429–1432.

Giannicola, G., Rosa, M., Marceglia, S., Scelzo, E., Rossi, L., Servello, D., Menghetti, C., Pacchetti, C., Zangaglia, R., Locatelli, M., et al. (2013). The effects of levodopa and deep brain

stimulation on subthalamic local field low-frequency oscillations in Parkinson's disease. Neurosignals *21*, 89–98.

Giovannoni, G., O'Sullivan, J.D., Turner, K., Manson, A.J., and Lees, A.J.L. (2000). Hedonistic homeostatic dysregulation in patients with Parkinson's disease on dopamine replacement therapies. J. Neurol. Neurosurg. Psychiatry *68*, 423–428.

Goldberg, J.A., Boraud, T., Maraton, S., Haber, S.N., Vaadia, E., and Bergman, H. (2002). Enhanced synchrony among primary motor cortex neurons in the 1-methyl-4-phenyl-1,2,3,6-tetrahydropyridine primate model of Parkinson's disease. J. Neurosci. Off. J. Soc. Neurosci. *22*, 4639–4653.

Gradinaru, V., Mogri, M., Thompson, K.R., Henderson, J.M., and Deisseroth, K. (2009). Optical Deconstruction of Parkinsonian Neural Circuitry. Science *324*, 354–359.

Hammond, C., Bergman, H., and Brown, P. (2007). Pathological synchronization in Parkinson's disease: networks, models and treatments. Trends Neurosci. *30*, 357–364.

Heimer, G., Bar-Gad, I., Goldberg, J.A., and Bergman, H. (2002). Dopamine Replacement Therapy Reverses Abnormal Synchronization of Pallidal Neurons in the 1-Methyl-4-Phenyl-1,2,3,6-Tetrahydropyridine Primate Model of Parkinsonism. J. Neurosci. *22*, 7850–7855.

Hell, F., Taylor, P.C.J., Mehrkens, J.H., and Bötzel, K. (2018). Subthalamic stimulation, oscillatory activity and connectivity reveal functional role of STN and network mechanisms during decision making under conflict. NeuroImage *171*, 222–233.

Hely, M.A., Reid, W.G.J., Adena, M.A., Halliday, G.M., and Morris, J.G.L. (2008). The Sydney multicenter study of Parkinson's disease: The inevitability of dementia at 20 years. Mov. Disord. *23*, 837–844.

Henderson, J.M., Annett, L.E., Ryan, L.J., Chiang, W., Hidaka, S., Torres, E.M., and Dunnett, S.B. (1999). Subthalamic nucleus lesions induce deficits as well as benefits in the hemiparkinsonian rat. Eur. J. Neurosci. *11*, 2749–2757.

Herve´, D., Rogard, M., and Le´vi-Strauss, M. (1995). Molecular analysis of the multiple Golf α

    subunit mRNAs in the rat brain. Mol. Brain Res. *32*, 125–134.

Horak, F.B., and Anderson, M.E. (1984). Influence of globus pallidus on arm movements in

    monkeys. I. Effects of kainic acid-induced lesions. J. Neurophysiol. *52*, 290–304.

Horvath, J., Herrmann, F.R., Burkhard, P.R., Bouras, C., and Kovari, E. (2013). Neuropathology

    of dementia in a large cohort of patients with Parkinson's disease. Park. Relat Disord *19*,

    864–868; discussion 864.

Hutchison, W.D., Lozano, A.M., Davis, K.D., Saint-Cyr, J.A., Lang, A.E., and Dostrovsky, J.O.

    (1994). Differential neuronal activity in segments of globus pallidus in Parkinson's disease

    patients. Neuroreport *5*, 1533–1537.

Inase, M., Buford, J.A., and Anderson, M.E. (1996). Changes in the control of arm position,

    movement, and thalamic discharge during local inactivation in the globus pallidus of the

    monkey. J. Neurophysiol. *75*, 1087–1104.

Iranzo, A., Santamaria, J., and Tolosa, E. (2009). The clinical and pathophysiological relevance

    of REM sleep behavior disorder in neurodegenerative diseases. Sleep Med. Rev.

    13, 385–401.

Irwin, D.J., Grossman, M., Weintraub, D., Hurtig, H.I., Duda, J.E., Xie, S.X., Lee, E.B., Van

    Deerlin, V.M., Lopez, O.L., Kofler, J.K., et al. (2017). Neuropathological and genetic

    correlates of survival and dementia onset in synucleinopathies: a retrospective analysis.

    Lancet Neurol *16*, 55–65.

Jellinger, K.A. (2018). Dementia with Lewy bodies and Parkinson's disease-dementia: current

    concepts and controversies. J. Neural Transm. *125*, 615–650.

Johnson, M.D., Vitek, J.L., and McIntyre, C.C. (2009). Pallidal stimulation that improves

    parkinsonian motor symptoms also modulates neuronal firing patterns in primary motor

    cortex in the MPTP-treated monkey. Exp. Neurol. *219*, 359–362.

Kammermeier, S., Pittard, D., Hamada, I., and Wichmann, T. (2016). Effects of high-frequency

stimulation of the internal pallidal segment on neuronal activity in the thalamus in parkinsonian monkeys. J. Neurophysiol. *116*, 2869–2881.

Kish, S.J., Shannak, K., and Hornykiewicz, O. (1988). Uneven Pattern of Dopamine Loss in the Striatum of Patients with Idiopathic Parkinson's Disease. N. Engl. J. Med. *318*, 876–880.

Kiss, Z.H.T., Davis, K.D., Tasker, R.R., Lozano, A.M., Hu, B., and Dostrovsky, J.O. (2003). Kinaesthetic neurons in thalamus of humans with and without tremor. Exp. Brain Res. *150*, 85–94.

Kita, H., and Kita, T. (2011). Role of Striatum in the Pause and Burst Generation in the Globus Pallidus of 6-OHDA-Treated Rats. Front. Syst. Neurosci. *5*.

Klaus, A., Martins, G.J., Paixao, V.B., Zhou, P., Paninski, L., and Costa, R.M. (2017). The Spatiotemporal Organization of the Striatum Encodes Action Space. Neuron *96*, 949.

Klockgether, T., and Turski, L. (1990). NMDA antagonists potentiate antiparkinsonian actions of L-dopa in monoamine-depleted rats. Ann. Neurol. *28*, 539–546.

Krause, V., Wach, C., Sudmeyer, M., Ferrea, S., Schnitzler, A., and Pollok, B. (2013). Cortico-muscular coupling and motor performance are modulated by 20 Hz transcranial alternating current stimulation (tACS) in Parkinson's disease. Front Hum Neurosci *7*, 928.

Kravitz, A.V., Freeze, B.S., Parker, P.R.L., Kay, K., Thwin, M.T., Deisseroth, K., and Kreitzer, A.C. (2010). Regulation of parkinsonian motor behaviours by optogenetic control of basal ganglia circuitry. Nature *466*, 622–626.

Kreiss, D.S., Mastropietro, C.W., Rawji, S.S., and Walters, J.R. (1997). The Response of Subthalamic Nucleus Neurons to Dopamine Receptor Stimulation in a Rodent Model of Parkinson's Disease. J. Neurosci. *17*, 6807–6819.

Kuhn, A.A., Tsui, A., Aziz, T., Ray, N., Brucke, C., Kupsch, A., Schneider, G.H., and Brown, P. (2009). Pathological synchronisation in the subthalamic nucleus of patients with Parkinson's disease relates to both bradykinesia and rigidity. Exp Neurol *215*, 380–387.

Lange, K.W., Robbins, T.W., Marsden, C.D., James, M., Owen, A.M., and Paul, G.M. (1992). l-

Dopa withdrawal in Parkinson's disease selectively impairs cognitive performance in tests sensitive to frontal lobe dysfunction. Psychopharmacology (Berl.) *107*, 394–404.

Langston, J.W., Ballard, P., Tetrud, J.W., and Irwin, I. (1983). Chronic Parkinsonism in humans due to a product of meperidine-analog synthesis. Science *219*, 979–980.

Langston, J.W., Forno, L.S., Rebert, C.S., and Irwin, I. (1984). Selective nigral toxicity after systemic administration of 1-methyl-4-phenyl-1,2,5,6-tetrahydropyrine (MPTP) in the squirrel monkey. Brain Res. *292*, 390–394.

Leblois, A., Meissner, W., Bioulac, B., Gross, C.E., Hansel, D., and Boraud, T. (2007). Late emergence of synchronized oscillatory activity in the pallidum during progressive Parkinsonism. Eur J Neurosci *26*, 1701–1713.

Lee, H.J., Weitz, A.J., Bernal-Casas, D., Duffy, B.A., Choy, M., Kravitz, A.V., Kreitzer, A.C., and Lee, J.H. (2016). Activation of Direct and Indirect Pathway Medium Spiny Neurons Drives Distinct Brain-wide Responses. Neuron *91*, 412–424.

Levy, R., Hutchison, W.D., Lozano, A.M., and Dostrovsky, J.O. (2000). High-frequency synchronization of neuronal activity in the subthalamic nucleus of parkinsonian patients with limb tremor. J. Neurosci. Off. J. Soc. Neurosci. *20*, 7766–7775.

Levy, R., Dostrovsky, J.O., Lang, A.E., Sime, E., Hutchison, W.D., and Lozano, A.M. (2001). Effects of apomorphine on subthalamic nucleus and globus pallidus internus neurons in patients with Parkinson's disease. J Neurophysiol *86*, 249–260.

Levy, R., Hutchison, W.D., Lozano, A.M., and Dostrovsky, J.O. (2002). Synchronized neuronal discharge in the basal ganglia of parkinsonian patients is limited to oscillatory activity. J Neurosci *22*, 2855–2861.

Li, Q., Ke, Y., Chan, D.C.W., Qian, Z.-M., Yung, K.K.L., Ko, H., Arbuthnott, G.W., and Yung, W.-H. (2012). Therapeutic Deep Brain Stimulation in Parkinsonian Rats Directly Influences Motor Cortex. Neuron *76*, 1030–1041.

Li, X., Redus, L., Chen, C., Martinez, P.A., Strong, R., Li, S., and O'Connor, J.C. (2013). Cognitive

dysfunction precedes the onset of motor symptoms in the MitoPark mouse model of Parkinson's disease. PloS One *8*, e71341.

Liang, L., DeLong, M.R., and Papa, S.M. (2008). Inversion of Dopamine Responses in Striatal Medium Spiny Neurons and Involuntary Movements. J. Neurosci. *28*, 7537–7547.

Limousin, P., Pollak, P., Benazzouz, A., Hoffmann, D., Broussolle, E., Perret, J.E., and Benabid, A.-L. (1995). Bilateral subthalamic nucleus stimulation for severe Parkinson's disease. Mov. Disord. *10*, 672–674.

Lindemann, C., Alam, M., Krauss, J.K., and Schwabe, K. (2013). Neuronal activity in the medial associative-limbic and lateral motor part of the rat subthalamic nucleus and the effect of 6-hydroxydopamine-induced lesions of the dorsolateral striatum. J. Comp. Neurol. *521*, 3226–3240.

Lintas, A., Silkis, I.G., Albéri, L., and Villa, A.E.P. (2012). Dopamine deficiency increases synchronized activity in the rat subthalamic nucleus. Brain Res. *1434*, 142–151.

Lobb, C.J., and Jaeger, D. (2015). Bursting activity of substantia nigra pars reticulata neurons in mouse parkinsonism in awake and anesthetized states. Neurobiol. Dis. *75*, 177–185.

Lobb, C.J., Zaheer, A.K., Smith, Y., and Jaeger, D. (2013). In vivo electrophysiology of nigral and thalamic neurons in alpha-synuclein-overexpressing mice highlights differences from toxin-based models of parkinsonism. J. Neurophysiol. *110*, 2792–2805.

Louis, E.K.S., Boeve, A.R., and Boeve, B.F. (2017). REM Sleep Behavior Disorder in Parkinson's Disease and Other Synucleinopathies. Mov. Disord. *32*, 645–658.

Luo, J., Kaplitt, M.G., Fitzsimons, H.L., Zuzga, D.S., Liu, Y., Oshinsky, M.L., and During, M.J. (2002). Subthalamic GAD gene therapy in a Parkinson's disease rat model. Science *298*, 425–429.

Magen, I., Fleming, S.M., Zhu, C., Garcia, E.C., Cardiff, K.M., Dinh, D., De La Rosa, K., Sanchez, M., Torres, E.R., Masliah, E., et al. (2012). Cognitive deficits in a mouse model of pre-manifest Parkinson's disease. Eur. J. Neurosci. *35*, 870–882.

Magnin, M., Morel, A., and Jeanmonod, D. (2000). Single-unit analysis of the pallidum, thalamus and subthalamic nucleus in parkinsonian patients. Neuroscience *96*, 549–564.

Mallet, N., Ballion, B., Moine, C.L., and Gonon, F. (2006). Cortical Inputs and GABA Interneurons Imbalance Projection Neurons in the Striatum of Parkinsonian Rats. J. Neurosci. *26*, 3875–3884.

Mallet, N., Pogosyan, A., Márton, L.F., Bolam, J.P., Brown, P., and Magill, P.J. (2008). Parkinsonian Beta Oscillations in the External Globus Pallidus and Their Relationship with Subthalamic Nucleus Activity. J. Neurosci. *28*, 14245–14258.

Mallet, N., Micklem, B.R., Henny, P., Brown, M.T., Williams, C., Bolam, J.P., Nakamura, K.C., and Magill, P.J. (2012). Dichotomous Organization of the External Globus Pallidus. Neuron *74*, 1075–1086.

Mallet, N., Schmidt, R., Leventhal, D., Chen, F., Amer, N., Boraud, T., and Berke, J.D. (2016). Arkypallidal Cells Send a Stop Signal to Striatum. Neuron *89*, 308–316.

Marié, R.M., Barré, L., Dupuy, B., Viader, F., Defer, G., and Baron, J.C. (1999). Relationships between striatal dopamine denervation and frontal executive tests in Parkinson's disease. Neurosci. Lett. *260*, 77–80.

Markowitz, J.E., Gillis, W.F., Beron, C.C., Neufeld, S.Q., Robertson, K., Bhagat, N.D., Peterson, R.E., Peterson, E., Hyun, M., Linderman, S.W., et al. (2018). The Striatum Organizes 3D Behavior via Moment-to-Moment Action Selection. Cell *174*, 44-58 e17.

Mastro, K.J., Zitelli, K.T., Willard, A.M., Leblanc, K.H., Kravitz, A.V., and Gittis, A.H. (2017). Cell-specific pallidal intervention induces long-lasting motor recovery in dopamine-depleted mice. Nat. Neurosci. *20*, 815–823.

McCairn, K.W., and Turner, R.S. (2009). Deep brain stimulation of the globus pallidus internus in the parkinsonian primate: local entrainment and suppression of low-frequency oscillations. J. Neurophysiol. *101*, 1941–1960.

McCairn, K.W., and Turner, R.S. (2015). Pallidal stimulation suppresses pathological dysrhythmia

in the parkinsonian motor cortex. J. Neurophysiol. *113*, 2537–2548.

McCarthy, M.M., Moore-Kochlacs, C., Gu, X., Boyden, E.S., Han, X., and Kopell, N. (2011). Striatal origin of the pathologic beta oscillations in Parkinson's disease. Proc. Natl. Acad. Sci. U. S. A. *108*, 11620–11625.

McConnell, G.C., So, R.Q., Hilliard, J.D., Lopomo, P., and Grill, W.M. (2012). Effective Deep Brain Stimulation Suppresses Low-Frequency Network Oscillations in the Basal Ganglia by Regularizing Neural Firing Patterns. J. Neurosci. *32*, 15657–15668.

Meissner, W., Leblois, A., Hansel, D., Bioulac, B., Gross, C.E., Benazzouz, A., and Boraud, T. (2005). Subthalamic high frequency stimulation resets subthalamic firing and reduces abnormal oscillations. Brain J. Neurol. *128*, 2372–2382.

Miller, W.C., and DeLong, M.R. (1988). Parkinsonian symptomatology. An anatomical and physiological analysis. Ann N Acad Sci *515*, 287–302.

Mink, J.W. (1996). THE BASAL GANGLIA: FOCUSED SELECTION AND INHIBITION OF COMPETING MOTOR PROGRAMS. Prog. Neurobiol. *50*, 381–425.

Mink, J.W., and Thach, W.T. (1993). Basal ganglia intrinsic circuits and their role in behavior. Curr. Opin. Neurobiol. *3*, 950–957.

Mitchell, I.J., Cross, A.J., Sambrook, M.A., and Crossman, A.R. (1986). Neural mechanisms mediating 1-methyl-4-phenyl-1,2,3,6-tetrahydropyridine-induced parkinsonism in the monkey: Relative contributions of the striatopallidal and striatonigral pathways as suggested by 2-deoxyglucose uptake. Neurosci. Lett. *63*, 61–65.

Molnar, G.F., Pilliar, A., Lozano, A.M., and Dostrovsky, J.O. (2005). Differences in Neuronal Firing Rates in Pallidal and Cerebellar Receiving Areas of Thalamus in Patients With Parkinson's Disease, Essential Tremor, and Pain. J. Neurophysiol. *93*, 3094–3101.

Monakow, K.H., Akert, K., and Künzle, H. (1978). Projections of the precentral motor cortex and other cortical areas of the frontal lobe to the subthalamic nucleus in the monkey. Exp. Brain Res. *33*, 395–403.

Moore, R.Y., and Bloom, F.E. (1978). Central Catecholamine Neuron Systems: Anatomy and Physiology of the Dopamine Systems. Annu. Rev. Neurosci. *1*, 129–169.

Moran, A., Stein, E., Tischler, H., Belelovsky, K., and Bar-Gad, I. (2011). Dynamic stereotypic responses of Basal Ganglia neurons to subthalamic nucleus high-frequency stimulation in the parkinsonian primate. Front. Syst. Neurosci. *5*, 21.

Müller, M.L.T.M., and Bohnen, N.I. (2013). Cholinergic Dysfunction in Parkinson's Disease. Curr. Neurol. Neurosci. Rep. *13*, 377.

Muralidharan, A., Jensen, A.L., Connolly, A., Hendrix, C.M., Johnson, M.D., Baker, K.B., and Vitek, J.L. (2016). Physiological changes in the pallidum in a progressive model of Parkinson's disease: Are oscillations enough? Exp Neurol *279*, 187–196.

Nambu, A. (2005). A new approach to understand the pathophysiology of Parkinson's disease. J. Neurol. *252*, iv1–iv4.

Narabayashi, H., Okuma, T., and Shikiba, S. (1956). Procaine Oil Blocking of the Globus Pattidus. AMA Arch. Neurol. Psychiatry *75*, 36–48.

Ni, Z., Bouali-Benazzouz, R., Gao, D., Benabid, A.-L., and Benazzouz, A. (2000). Changes in the firing pattern of globus pallidus neurons after the degeneration of nigrostriatal pathway are mediated by the subthalamic nucleus in the rat. Eur. J. Neurosci. *12*, 4338–4344.

Oldenburg, I.A., and Sabatini, B.L. (2015). Antagonistic but Not Symmetric Regulation of Primary Motor Cortex by Basal Ganglia Direct and Indirect Pathways. Neuron *86*, 1174–1181.

Pagano, G., Rengo, G., Pasqualetti, G., Femminella, G.D., Monzani, F., Ferrara, N., and Tagliati, M. (2015). Cholinesterase inhibitors for Parkinson's disease: a systematic review and meta-analysis. J Neurol Neurosurg Psychiatry *86*, 767–773.

Pagano, G., Niccolini, F., Fusar-Poli, P., and Politis, M. (2017). Serotonin transporter in Parkinson's disease: A meta-analysis of positron emission tomography studies. Ann Neurol *81*, 171–180.

Pan, H.S., and Walters, J.R. (1988). Unilateral lesion of the nigrostriatal pathway decreases the

firing rate and alters the firing pattern of globus pallidus neurons in the rat. Synapse *2*, 650–656.

Pan, M.-K., Kuo, S.-H., Tai, C.-H., Liou, J.-Y., Pei, J.-C., Chang, C.-Y., Wang, Y.-M., Liu, W.-C., Wang, T.-R., Lai, W.-S., et al. (2016). Neuronal firing patterns outweigh circuitry oscillations in parkinsonian motor control. J. Clin. Invest. *126*, 4516–4526.

Parent, M., and Parent, A. (2004). The pallidofugal motor fiber system in primates. Parkinsonism Relat. Disord. *10*, 203–211.

Park, S.E., Song, K.-I., Kim, H., Chung, S., and Youn, I. (2018). Graded 6-OHDA-induced dopamine depletion in the nigrostriatal pathway evokes progressive pathological neuronal activities in the subthalamic nucleus of a hemi-parkinsonian mouse. Behav. Brain Res. *344*, 42–47.

Parker, J.G., Marshall, J.D., Ahanonu, B., Wu, Y.-W., Kim, T.H., Grewe, B.F., Zhang, Y., Li, J.Z., Ding, J.B., Ehlers, M.D., et al. (2018). Diametric neural ensemble dynamics in parkinsonian and dyskinetic states. Nature *557*, 177–182.

Pasquereau, B., and Turner, R.S. (2011). Primary Motor Cortex of the Parkinsonian Monkey: Differential Effects on the Spontaneous Activity of Pyramidal Tract-Type Neurons. Cereb. Cortex *21*, 1362–1378.

Pasquereau, B., DeLong, M.R., and Turner, R.S. (2016). Primary motor cortex of the parkinsonian monkey: altered encoding of active movement. Brain *139*, 127–143.

Pessiglione, M., Guehl, D., Rolland, A.-S., François, C., Hirsch, E.C., Féger, J., and Tremblay, L. (2005). Thalamic Neuronal Activity in Dopamine-Depleted Primates: Evidence for a Loss of Functional Segregation within Basal Ganglia Circuits. J. Neurosci. *25*, 1523–1531.

Piallat, B., Benazzouz, A., and Benabid, A.L. (1996). Subthalamic Nucleus Lesion in Rats Prevents Dopaminergic Nigral Neuron Degeneration After Striatal 6-OHDA Injection: Behavioural and Immunohistochemical Studies. Eur. J. Neurosci. *8*, 1408–1414.

Pogosyan, A., Gaynor, L.D., Eusebio, A., and Brown, P. (2009). Boosting cortical activity at Beta-

band frequencies slows movement in humans. Curr Biol *19*, 1637–1641.

Politis, M., and Niccolini, F. (2015). Serotonin in Parkinson's disease. Behav. Brain Res. *277*, 136–145.

Pontone, G.M., Williams, J.R., Anderson, K., Chase, G., Goldstein, S., Grill, S., Hirsch, E.S., Lehmann, S., Little, J.T., Margolis, R.L., et al. (2009). Prevalence of Anxiety Disorders and Anxiety Subtypes in Patients With Parkinson's Disease. Mov. Disord. Off. J. Mov. Disord. Soc. *24*, 1333–1338.

Postuma, R.B., Gagnon, J.-F., Vendette, M., and Montplaisir, J.Y. (2009). Idiopathic REM sleep behavior disorder in the transition to degenerative disease. Mov. Disord. Off. J. Mov. Disord. Soc. *24*, 2225–2232.

Quinn, E.J., Blumenfeld, Z., Velisar, A., Koop, M.M., Shreve, L.A., Trager, M.H., Hill, B.C., Kilbane, C., Henderson, J.M., and Bronte-Stewart, H. (2015). Beta oscillations in freely moving Parkinson's subjects are attenuated during deep brain stimulation. Mov Disord *30*, 1750–1758.

Reese, R., Leblois, A., Steigerwald, F., Pötter-Nerger, M., Herzog, J., Mehdorn, H.M., Deuschl, G., Meissner, W.G., and Volkmann, J. (2011). Subthalamic deep brain stimulation increases pallidal firing rate and regularity. Exp. Neurol. *229*, 517–521.

Reijnders, J.S.A.M., Ehrt, U., Weber, W.E.J., Aarsland, D., and Leentjens, A.F.G. (2008). A systematic review of prevalence studies of depression in Parkinson's disease. Mov. Disord. Off. J. Mov. Disord. Soc. *23*, 183–189; quiz 313.

Rothblat, D.S., and Schneider, J.S. (1995). Alterations in pallidal neuronal responses to peripheral sensory and striatal stimulation in symptomatic and recovered Parkinsonian cats. Brain Res. *705*, 1–14.

Ryan, M.B., Bair-Marshall, C., and Nelson, A.B. (2018). Aberrant Striatal Activity in Parkinsonism and Levodopa-Induced Dyskinesia. Cell Rep. *23*, 3438-3446.e5.

Rylander, D., Parent, M., O'Sullivan, S.S., Dovero, S., Lees, A.J., Bezard, E., Descarries, L., and

Cenci, M.A. (2010). Maladaptive plasticity of serotonin axon terminals in levodopa-induced dyskinesia. Ann Neurol *68*, 619–628.

Sagot, B., Li, L., and Zhou, F.-M. (2018). Hyperactive Response of Direct Pathway Striatal Projection Neurons to L-dopa and D1 Agonism in Freely Moving Parkinsonian Mice. Front. Neural Circuits *12*.

Sanders, T.H., and Jaeger, D. (2016). Optogenetic stimulation of cortico-subthalamic projections is sufficient to ameliorate bradykinesia in 6-ohda lesioned mice. Neurobiol. Dis. *95*, 225–237.

Schmidt, R., Leventhal, D.K., Mallet, N., Chen, F., and Berke, J.D. (2013). Canceling actions involves a race between basal ganglia pathways. Nat. Neurosci. *16*, 1118–1124.

Schneider, J.S., and Kovelowski, C.J. (1990). Chronic exposure to low doses of MPTP. I. Cognitive deficits in motor asymptomatic monkeys. Brain Res. *519*, 122–128.

Schneider, J.S., and Roeltgen, D.P. (1993). Delayed matching-to-sample, object retrieval, and discrimination reversal deficits in chronic low dose MPTP-treated monkeys. Brain Res. *615*, 351–354.

Schneider, J.S., and Rothblat, D.S. (1996). Alterations in intralaminar and motor thalamic physiology following nigrostriatal dopamine depletion. Brain Res. *742*, 25–33.

Schneider, J.S., Pioli, E.Y., Jianzhong, Y., Li, Q., and Bezard, E. (2013). Levodopa improves motor deficits but can further disrupt cognition in a macaque Parkinson model. Mov. Disord. Off. J. Mov. Disord. Soc. *28*, 663–667.

Schwartzman, R.J., and Alexander, G.M. (1985). Changes in the local cerebral metabolic rate for glucose in the 1-methyl-4-phenyl-1,2,3,6-tetrahydropyridine (MPTP) primate model of Parkinson's disease. Brain Res. *358*, 137–143.

Seidel, K., Mahlke, J., Siswanto, S., Kruger, R., Heinsen, H., Auburger, G., Bouzrou, M., Grinberg, L.T., Wicht, H., Korf, H.W., et al. (2015). The brainstem pathologies of Parkinson's disease and dementia with Lewy bodies. Brain Pathol *25*, 121–135.

Sethi, K. (2008). Levodopa unresponsive symptoms in Parkinson disease. Mov. Disord. *23*, S521–S533.

Shimamoto, S.A., Ryapolova-Webb, E.S., Ostrem, J.L., Galifianakis, N.B., Miller, K.J., and Starr, P.A. (2013). Subthalamic nucleus neurons are synchronized to primary motor cortex local field potentials in Parkinson's disease. J Neurosci *33*, 7220–7233.

Siegert, S., Herrojo Ruiz, M., Brücke, C., Huebl, J., Schneider, G.-H., Ullsperger, M., and Kühn, A.A. (2014). Error signals in the subthalamic nucleus are related to post-error slowing in patients with Parkinson's disease. Cortex J. Devoted Study Nerv. Syst. Behav. *60*, 103–120.

Singh, A., Liang, L., Kaneoke, Y., Cao, X., and Papa, S.M. (2015). Dopamine regulates distinctively the activity patterns of striatal output neurons in advanced parkinsonian primates. J Neurophysiol *113*, 1533–1544.

Singh, A., Mewes, K., Gross, R.E., DeLong, M.R., Obeso, J.A., and Papa, S.M. (2016). Human striatal recordings reveal abnormal discharge of projection neurons in Parkinson's disease. Proc Natl Acad Sci U A *113*, 9629–9634.

Soares, J., Kliem, M.A., Betarbet, R., Greenamyre, J.T., Yamamoto, B., and Wichmann, T. (2004). Role of External Pallidal Segment in Primate Parkinsonism: Comparison of the Effects of 1-Methyl-4-Phenyl-1,2,3,6-Tetrahydropyridine-Induced Parkinsonism and Lesions of the External Pallidal Segment. J. Neurosci. *24*, 6417–6426.

Starr, P.A., Rau, G.M., Davis, V., Marks, W.J., Jr., Ostrem, J.L., Simmons, D., Lindsey, N., and Turner, R.S. (2005). Spontaneous pallidal neuronal activity in human dystonia: comparison with Parkinson's disease and normal macaque. J Neurophysiol *93*, 3165–3176.

Surmeier, D.J. (2018). Determinants of dopaminergic neuron loss in Parkinson's disease. FEBS J. *285*, 3657–3668.

Surmeier, D.J., Obeso, J.A., and Halliday, G.M. (2017). Selective neuronal vulnerability in Parkinson disease. Nat. Rev. Neurosci. *18*, 101–113.

Swann, N.C., de Hemptinne, C., Miocinovic, S., Qasim, S., Wang, S.S., Ziman, N., Ostrem, J.L., San Luciano, M., Galifianakis, N.B., and Starr, P.A. (2016). Gamma Oscillations in the Hyperkinetic State Detected with Chronic Human Brain Recordings in Parkinson's Disease. J Neurosci *36*, 6445–6458.

Swann, N.C., de Hemptinne, C., Miocinovic, S., Qasim, S., Ostrem, J.L., Galifianakis, N.B., Luciano, M.S., Wang, S.S., Ziman, N., Taylor, R., et al. (2018). Chronic multisite brain recordings from a totally implantable bidirectional neural interface: experience in 5 patients with Parkinson's disease. J Neurosurg *128*, 605–616.

Tai, C.H., Pan, M.K., Lin, J.J., Huang, C.S., Yang, Y.C., and Kuo, C.C. (2012). Subthalamic discharges as a causal determinant of parkinsonian motor deficits. Ann Neurol *72*, 464–476.

Taverna, S., Ilijic, E., and Surmeier, D.J. (2008). Recurrent collateral connections of striatal medium spiny neurons are disrupted in models of Parkinson's disease. J. Neurosci. Off. J. Soc. Neurosci. *28*, 5504–5512.

Timmermann, L., Wojtecki, L., Gross, J., Lehrke, R., Voges, J., Maarouf, M., Treuer, H., Sturm, V., and Schnitzler, A. (2004). Ten-Hertz stimulation of subthalamic nucleus deteriorates motor symptoms in Parkinson's disease. Mov. Disord. *19*, 1328–1333.

Vila, M., Périer, C., Féger, J., Yelnik, J., Faucheux, B., Ruberg, M., Raisman-Vozari, R., Agid, Y., and Hirsch, E.C. (2000). Evolution of changes in neuronal activity in the subthalamic nucleus of rats with unilateral lesion of the substantia nigra assessed by metabolic and electrophysiological measurements. Eur. J. Neurosci. *12*, 337–344.

Wang, Y., Zhang, Q.J., Liu, J., Ali, U., Gui, Z.H., Hui, Y.P., Chen, L., and Wang, T. (2010). Changes in firing rate and pattern of GABAergic neurons in subregions of the substantia nigra pars reticulata in rat models of Parkinson's disease. Brain Res. *1324*, 54–63.

Wang, Z., Liang, S., Yu, S., Xie, T., Wang, B., Wang, J., Li, Y., Shan, B., and Cui, C. (2017).

Distinct Roles of Dopamine Receptors in the Lateral Thalamus in a Rat Model of Decisional Impulsivity. Neurosci. Bull. *33*, 413–422.

Weintraub, D., Koester, J., Potenza, M.N., Siderowf, A.D., Stacy, M., Voon, V., Whetteckey, J., Wunderlich, G.R., and Lang, A.E. (2010). Impulse Control Disorders in Parkinson Disease: A Cross-Sectional Study of 3090 Patients. Arch. Neurol. *67*, 589–595.

Wenger, K.K., Musch, K.L., and Mink, J.W. (1999). Impaired Reaching and Grasping After Focal Inactivation of Globus Pallidus Pars Interna in the Monkey. J. Neurophysiol. *82*, 2049–2060.

Wichmann, T., Bergman, H., and DeLong, M.R. (1994). The primate subthalamic nucleus. III. Changes in motor behavior and neuronal activity in the internal pallidum induced by subthalamic inactivation in the MPTP model of parkinsonism. J. Neurophysiol. *72*, 521–530.

Wichmann, T., Bergman, H., Starr, P.A., DeLong, M.R., Watts, R.L., and Subramanian, T. (1999). Comparison of MPTP-induced changes in spontaneous neuronal discharge in the internal pallidal segment and in the substantia nigra pars reticulata in primates. Exp. Brain Res. *125*, 397–409.

Williams-Gray, C.H., Foltynie, T., Brayne, C.E.G., Robbins, T.W., and Barker, R.A. (2007). Evolution of cognitive dysfunction in an incident Parkinson's disease cohort. Brain J. Neurol. *130*, 1787–1798.

CHAPTER 3

Functionally Distinct Connectivity of Developmentally Targeted Striosome Neurons

---

3.1 Abstract

One longstanding model of striatal function divides the striatum into compartments called striosome and matrix. While some anatomical evidence suggests that these populations represent distinct striatal pathways with differing inputs and outputs, functional investigation has been limited by the methods for identifying and manipulating these populations. Here, we utilize *hs599*^{CreER} mice as a new tool for targeting striosome projection neurons and testing their functional connectivity. Extending anatomical work, we demonstrate that striosome neurons receive greater synaptic input from prelimbic cortex, whereas matrix neurons receive greater input from primary motor cortex. We also identify functional differences in how striosome and matrix neurons process excitatory input, providing the first electrophysiological method for delineating striatal output neuron subtypes. Lastly, we provide the first functional demonstration that striosome neurons are the predominant striatal output to substantia nigra pars compacta dopamine neurons. These results identify striosome and matrix as functionally distinct striatal pathways.

3.2 Introduction

The striatum is the primary input nucleus of the basal ganglia and plays a critical role in a wide range of behaviors. Classical models of striatal function divide the output neurons, medium spiny neurons (MSNs), into two groups: direct and indirect pathway cells. These populations have proven useful for understanding striatal functions such as movement control (Kravitz and Kreitzer, 2012; Cui et al., 2013) and are differentiated by their connectivity to downstream basal ganglia nuclei. An alternative model that may help explain other striatal functions, including certain forms of learning and decision making (Brown et al., 1999; Friedman et al., 2015), divides striatal output neurons into populations called striosome and matrix. Like the direct-indirect pathway model, striosome and matrix neurons are hypothesized to mediate distinct functions, based in large part on proposed differences in their upstream and downstream connectivity.

Historically, striosome and matrix neurons have been distinguished by their localization within neurochemically distinct compartments. Striosome compartments, which appear as irregularly distributed islands within the surrounding matrix, show enriched expression of markers such as μ-opioid receptors (MORs) and diminished expression of markers such as calbindin (Pert et al., 1976; Gerfen, 1985). Early and recent anatomical tracing studies found that terminals from limbic and sensorimotor regions show preferential localization in striosome and matrix compartments, respectively (Ragsdale and Graybiel, 1988; Sadikot et al., 1992; Eblen and Graybiel, 1995; Kincaid and Wilson, 1996; Lévesque and Parent, 1998; Friedman et al., 2015). Additionally, while MSNs in both compartments project to canonical downstream basal ganglia targets such as the substantia nigra pars reticulata (SNr), tracing studies suggest that striosome MSNs in the dorsal striatum send additional output to dopamine neurons in the substantia nigra pars compacta (SNc), while those in the ventral striatum project to dopamine neurons in the ventral tegmental area (VTA) (Gerfen, 1985; Jiménez-Castellanos and Graybiel, 1989; Fujiyama et al., 2011; Watabe-Uchida et al., 2012). These anatomical findings led to the hypothesis that

striosomes comprise a distinct striatal pathway that integrates limbic information and regulates activity of SNc dopamine neurons.

Neurochemically-defined striosome and matrix compartments have been recognized for decades, but without tools to identify and manipulate these neurons *in vivo*, studies of how potential structural differences in connectivity translate functionally have been limited. Much of our current knowledge is derived from postmortem neuroanatomical studies, with methods to facilitate functional study of striosome and matrix MSNs in living tissue only recently becoming available (Davis and Iii, 2011; Gerfen et al., 2013; Banghart et al., 2015; Lopez-Huerta et al., 2016; Smith et al., 2016; Crittenden et al., 2017). Such approaches have enabled novel insights into differences between striosome and matrix, but also raised debate over whether striosome and matrix MSNs indeed differ in their inputs and outputs. Here, we use Cre-mediated recombination from the hs599[CreER] mouse line to target developing striosome MSNs. We find that striosome and matrix MSNs receive biased input from limbic and sensorimotor regions at the synaptic level. We also show that striosome and matrix MSNs have divergent intrinsic properties. Finally, we demonstrate that striosome and matrix MSNs have functionally distinct inhibitory output to SNc dopamine neurons. Together, our data establish the *hs599*[CreER] mouse line as a highly specific tool for studying striosomes and confirm that striosome and matrix represent functionally distinct striatal pathways.

3.3 Results

3.3.1 Enhancer hs599 drives gene expression in postmitotic neurons of the developing striatum

hs599 is a 1678 bp DNA fragment from the human genome that was discovered to drive *LacZ* expression in the E11.5 mouse striatum using a mouse transgenic screen of candidate regulatory elements (Visel et al., 2013). hs599 was then cloned upstream of *CreERT2-IRES-eGFP,* and used to generate a stable mouse transgenic line (*hs599*^{CreERT2-eGFP}, referred to here as *hs599*^{CreER}) which confirmed its activity in the E11.5 striatum (Silberberg et al., 2016). Here we investigated *hs599*^{CreER} as a tool for labelling components of the developing striatum.

To explore its ability to label striosomes, we examined hs599-driven CreER-eGFP expression and CreER-mediated recombination during development following a single administration of tamoxifen. Previous studies demonstrate that striosome and matrix cells are derived from the lateral ganglionic eminence (LGE) starting at E10.5 (van der Kooy and Fishell, 1987), with striosome neurons born prior to matrix neurons. Because the hs599 is active in the LGE during this time (Silberberg et al., 2016), we hypothesized that tamoxifen administration at E10.5 would label early-born neurons that give rise to striosomes (Figure 3.1A). Therefore, we administered tamoxifen at E10.5 to *hs599*^{CreER};Ai14 mice and observed CreER-eGFP expression (eGFP) and Cre-mediated recombination (tdTomato) in the striatum of embryos and pups (E12.5, E15.5, E18.5; Figure 3.1B, 3S1A-C). In the LGE at E12.5, recombination appeared restricted to the neuronal zone (mantle zone), suggesting hs599 was not active in progenitor cells (Figure 3.1B). To confirm that recombination was restricted to post-mitotic cells, we stained E12.5 sections for either Ki67 or phospho-histone H3, markers of proliferating cells. Neither eGFP nor Cre-driven tdTomato expression overlapped with either marker within the LGE, except for a small domain at the pallial/subpallial boundary (Figure 3.1C-D, asterisks in Figure 3S1A). This region produces interneurons of the olfactory bulb and pyramidal neurons of the piriform cortex; both of these structures had low levels of recombination (Figure 3.1E). No recombination was observed

in the progenitor domains of the medial ganglionic eminence (Figure 3.1B). While we did observe

recombined cells in the external globus pallidus (GPe), they were NKX2-1-negative, and therefore

unlikely to be derived from the MGE (Figure 3S2A) (Flandin et al., 2010; Nóbrega-Pereira et al.,

2010; Hernández et al., 2015; Dodson et al., 2015). In line with hs599 enhancer embryonic

activity, fate-mapping of tdTomato$^+$ cells in adult animals (P30) revealed labeling in the

GABAergic regions of the telencephalon (striatum, olfactory bulb, olfactory tubercle, septal nuclei,

bed nucleus of the stria terminalis (BNST), amygdala (central and intercalated nucleus), and

diencephalon (reticular thalamus, zona incerta) (Figure 3.1E). Notably, tdTomato$^+$ cell bodies

were not observed in the substantia nigra (Figure 3.1E, 3S2B). These data show that *hs599^{CreER}*

mice can be used to label a subset of striatal neurons born during specific developmental time

points.

3.3.2 *hs599^{CreER}* Mice Enable Genetic Targeting of Striosome MSNs

hs599^{CreER};Ai14 mice given tamoxifen at E10.5 lead to patchy striatal tdTomato expression by

adulthood, suggesting the possibility of striosome labeling (Figure 3.1B, right). To test this

hypothesis, we double-labeled striatal sections from *hs599*^{CreER};Ai14 mice for μ-opioid receptors

(MORs) and calbindin, markers of striosome and matrix compartments, respectively (Pert et al.,

1976; Gerfen et al., 1985). tdTomato$^+$ cells were found in regions enriched for MOR and poor in

calbindin expression (Figures 3.2A-B), consistent with striosome labeling. Previous studies

targeting striosomes developmentally indicate a tradeoff between penetrance and specificity

across different developmental time points (Kelly et al., 2018; van der Kooy and Fishell, 1987;

Mason et al., 2005). Therefore, we estimated the penetrance and specificity of striosome labeling

in the dorsal striatum of *hs599^{CreER}*;Ai14 mice (tamoxifen administration at E10.5) by quantifying

the density of tdTomato$^+$ cells in striosome and matrix compartments (Figure 3.2C-D). We

observed an approximately 12-fold higher density of labelling in striosome compared to matrix

compartments (12,211 ± 820 vs. 1,058 ± 79 cells/mm, N=3, Figure 3.2I). Notably, tamoxifen

administration at E15.5 led to increased striatal labeling, but in a broader and more nonspecific pattern (data not shown). Next, to confirm whether labeling was restricted to striatal projection neurons (medium spiny neurons, MSNs), we stained for markers of striatal interneurons: choline acetyltransferase (ChAT), parvalbumin (PV), and neuropeptide Y (NPY) (Figure 3.2E-G). We observed almost no overlap of tdTomato with ChAT, PV, or NPY (Figure 3.2J). These findings indicate that *hs599*^{CreER} mice enable highly enriched labeling of striosome MSNs.

Striosome and matrix compartments each contain direct and indirect pathway MSNs. To determine if *hs599*^{CreER} mice preferentially label either pathway, we first measured the endogenous proportion of indirect pathway MSNs in each compartment. Striatal slices from an indirect pathway reporter mouse line (D2-GFP, Gong et al., 2003) were stained for MORs and the neuronal marker NeuN, enabling quantification of the proportion of GFP$^+$ neurons in striosomes and matrix (Figure 3.2H). While approximately half of identified matrix neurons were GFP$^+$ (45.8 ± 0.6%, N=4), striosomes showed a small but consistent reduction in this proportion (38.7 ± 1.2%, N=4), suggesting a slight enrichment for direct pathway MSNs (Figure 3.2K). Using *hs599*^{CreER};Ai14;D2-GFP mice, we next quantified the proportion of tdTomato$^+$ neurons that were D2-GFP$^+$. We observed minimal overlap between GFP$^+$ and tdTomato$^+$ neurons (Figure 3.2H,K, 9.8 ± 0.9%, N=3), indicating that labeled neurons in *hs599*^{CreER} mice underrepresent indirect pathway MSNs within striosomes. Thus, our data indicate that striatal neurons labeled in *hs599*^{CreER} mice are primarily direct pathway striosome MSNs.

3.3.3 Striosome and Matrix Receive Differential Input from Prelimbic and Primary Motor Cortex

The advent of novel tools for studying striosome and matrix MSNs has raised questions over whether these populations receive differing levels of input from limbic and sensorimotor neocortical regions. With the *hs599*^{CreER} mouse line as a tool to identify and manipulate striosome MSNs, we next tested the hypothesis that striosome MSNs receive differential inputs from

upstream brain regions, as compared to neighboring matrix MSNs. While terminals from prelimbic cortex (PL) and primary motor cortex (M1) have been found to preferentially distribute onto striosome and matrix compartments, respectively (Eblen and Graybiel, 1995; Kincaid and Wilson, 1996; Lévesque and Parent, 1998; Miyamoto et al., 2018), it is unknown how such anatomical differences translate at the functional level. To address this question, we expressed channelrhodopsin (ChR2-eYFP) in either prelimbic (PL) or primary motor cortex (M1) of $hs599^{CreER}$;Ai14 mice. Consistent with previous findings, ChR2-eYFP$^+$ fibers from the PL were enriched in tdTomato-labeled striosomes (Figure 3S3A-C), while those from M1 concentrated in the matrix (Figure 3S3D-F). Next, we targeted sequential pairs of neighboring striosome and matrix MSNs in *ex vivo* brain slices (Figure 3.3A) and measured optically evoked excitatory postsynaptic currents (oEPSCs) in whole-cell voltage-clamp configuration. Brief pulses of blue light induced short latency oEPSCs (< 5 ms) from PL and M1 inputs in both matrix and striosome MSNs (Figure 3.3A). The amplitude of PL-derived EPSCs was greater in striosome (776 ± 175 pA) than in matrix (483 ± 182 pA) MSNs (Figure 3.3B left, Wilcoxon sign-rank, p = 0.0099, n = 17 pairs, N = 4). Conversely, the amplitude of M1-derived EPSCs was significantly lower in striosome (202 ± 48 pA) compared to matrix (756 ± 201 pA) MSNs (Figure 3.3C left, Wilcoxon sign-rank, p =0.0072, n = 19 pairs, N = 4). To quantify the functional bias of PL and M1 inputs for striosome MSNs, we averaged the ratio of oEPSC amplitudes [striosome / (striosome + matrix)] for all recorded pairs, as well as for each animal. Values greater than 0.5 represent preference for striosome MSNs, while values less than 0.5 represent preference for matrix MSNs. PL and M1 showed opposing biases, with PL favoring striosome MSNs (Figure 3.3B right, 0.65) and M1 favoring matrix MSNs (Figure 3.3C right, 0.28). The directionality of this bias was consistent across all animals for both PL and M1. In combination, these results extend anatomical findings, showing that PL and M1 inputs onto individual striosome and matrix MSNs differ at the functional level.

3.3.4 Direct Pathway Striosome MSNs Have Increased Intrinsic Excitability Compared to Matrix MSNs

Though striosome and matrix MSNs may receive distinct synaptic input from PL and M1, how they transform synaptic input into spiking relies in part on their intrinsic properties. Using whole-cell current-clamp recordings in *ex vivo* brain slices to measure instantaneous firing rates in response to current injections, we compared the intrinsic excitability of striosome and matrix MSNs (Figure 3.3D-E). To control for potential differences in excitability between direct and indirect pathway MSNs (Gertler et al., 2008; Lieberman et al., 2018; Planert et al., 2013), we used *hs599^{CreER}*;Ai14;D2-GFP mice to compare labeled striosome MSNs to direct and indirect pathway MSNs in the matrix. As very few labeled striosome neurons were indirect pathway neurons (Figure 3.2K), only direct pathway MSNs within striosomes were examined (see Methods). Because direct pathway MSNs have lower intrinsic excitability than indirect pathway MSNs, we would expect to see lower excitability in tdTomato^+ striosome MSNs compared to matrix MSNs. However, we observed higher intrinsic excitability in labeled striosome MSNs (n = 34, N = 5) compared to matrix MSNs (Figure 3.3F, n = 25, N = 5). In fact, intrinsic excitability of presumed direct pathway striosome MSNs (n = 34, N=5) was increased over both direct (Figure 3.3G, n=12, N = 5) and indirect (Figure 3.3H, n=13, N=5) pathway MSNs in the matrix. Histologically confirmed direct pathway striosome MSNs showed similar excitability to that of the overall striosome population (Figure 3S3G). No difference was observed in the maximal firing rate (Figure 3S3H, striosome = 50 ± 3.0 spikes/sec, matrix D1 = 55 ± 4.4 spikes/sec, matrix D2 = 51 ± 5.4 spikes/sec Kruskal-Wallis, p = 0.595) or resting membrane potential (Figure 3S3I, striosome = -89 ± 0.9 mV, matrix D1 = -93 ± 1.5 mV, matrix D2 = -87 ± 1.4 mV, Kruskal-Wallis, p = 0.032) of any group. However, direct pathway striosome MSNs had higher input resistance at rest (Figure 3S3J, striosome = 236 ± 14 MΩ, matrix D1 = 151 ± 16 MΩ, matrix D2 = 162 ± 25 MΩ, Kruskal-Wallis, p=0.00052, Dunn post-hoc, striosome vs. D1 matrix, p = 0.0018, D2 matrix, p = 0.0023) and showed a substantial shift in rheobase (Figure 3S3K, striosome = 207±17 pA, matrix D1 = 404 ± 47 pA, matrix D2 =

325 ± 32 pA, Kruskal-Wallis, p < 0.0001, Dunn post-hoc, striosome vs. D1 matrix p < 0.0001, D2 matrix p=0.0008). Given the marked difference in excitability between striosome and matrix MSNs, we wondered if this electrophysiological property could be used as a surrogate marker for compartmental identity. Striosome and matrix direct pathway MSNs showed minimal overlap in their rheobase distribution (Figure 3S3K). Therefore, we quantified the positive and negative predictive value (PPV and NPV) of various rheobase cutoffs for identifying direct pathway MSNs in striosomes from those in the matrix (Figure 3S3L-N). Notably, a rheobase cutoff of 200 pA or less had a PPV of 100% for labeled striosome neurons, while a rheobase cutoff of 250 pA or more had a NPV of 92.7% (Figure 3S3L,M). Repeating this measure without a priori knowledge of direct or indirect pathway identity produced similar results (Figure 3S3N, PPV = 76.9%, NPV = 92.0%) Together, these data indicate striosome MSNs have greater intrinsic excitability compared to matrix MSNs of either pathway, and provide a potential non-transgenic approach for electrophysiological identification of direct pathway striosome MSNs in slice recordings.

3.3.5 Striosome MSNs Are a Predominant Source of Striatal Input to SNc Dopamine

We next asked if striosome MSNs send outputs to distinct downstream targets. Previous anatomical studies suggest that direct pathway striosome MSNs, unlike those in the matrix, project monosynaptically to substantia nigra pars compacta (SNc) dopamine neurons, in addition to canonical target regions such as the substantia nigra pars reticulata (SNr) (Gerfen, 1985; Jiménez-Castellanos and Graybiel, 1989; Fujiyama et al., 2011; Watabe-Uchida et al., 2012; Yang et al., 2018). However, this anatomical connection from striosome MSNs to SNc dopamine neurons, and its specificity, have not been explored at the physiological level. Furthermore, recent evidence suggested that striosome output may not differ from that of matrix (Smith et al., 2016). To address if striosome MSN synaptic output is distinct from that of direct pathway MSNs as a whole, we expressed ChR2-eYFP in direct pathway MSNs (both striosome and matrix; D1-Cre;Ai32) or selectively within striosome MSNs (*hs599*^{CreER};Ai32), and recorded light-evoked

currents in SNc dopamine neurons. To control for differences in ChR2 expression across lines, we also recorded light-evoked currents in SNr neurons, allowing for normalization of synaptic output as a ratio between the two target regions (SNc/SNr; Figure 3.4A). In both D1-Cre;Ai32 (D1) and $hs599^{CreER}$;Ai32 (599) mice, we observed ChR2-eYFP$^+$ terminals within the SNc as identified by staining for tyrosine hydroxylase, a marker of dopaminergic neurons (Figures 3S4A-B). Brief pulses of blue light induced optically evoked inhibitory postsynaptic currents (oIPSCs) with short latency (<5 ms), which were unaffected by application of glutamatergic antagonists (NBQX + APV) and abolished by application of the GABA$_A$ antagonist picrotoxin (Figures 3.4B-C). In SNc dopamine neurons identified by biocytin fill (Figure 3S4C) or cell-attached spike waveform (Figure 3S4D-E), we observed no difference in the oIPSC amplitude between 599 and D1 mice (Figure 3.4D, 599 = 428 ± 145 pA, n = 9, N=5; D1 = 281 ± 109 pA, n=7, N=5; p =0.70). If we assume that D1-Cre captures all direct pathway neurons, these results indicate that the majority of striatal input to SNc dopamine neurons is derived from striosome neurons. Consistent with this assumption, oIPSC amplitude in SNr neurons was significantly less in 599 compared to D1 mice (Figure 3.4E, 599 = 1603 ± 505 pA, n=14, N=5; D1 = 4417 ± 392 pA, n=14, N =5; p = 0.0012). The normalized ratio oIPSC amplitude (SNc:SNr) averaged 0.25 in 599 mice and 0.06 in D1 mice, suggesting that striosome output shows increased bias towards SNc dopamine neurons compared to D1 MSNs as a whole. To compare these ratios statistically, we bootstrapped data acquired from D1 and 599 mice to obtain a probability distribution of outcomes, which were significantly different (Figure 3.4F, Kolmogorov–Smirnov test, p <0.001). Next, to show that striosome MSNs can regulate SNc dopamine neuron firing, we recorded spontaneous activity of dopamine neurons in a cell-attached configuration and activated striosome terminals using $hs599^{CreER}$;Ai32 mice and brief trains of blue light (5 pulses, 10 Hz; Figure 3.4G). Activation of striosome MSNs was sufficient to inhibit firing in SNc dopamine neurons (Figure 3.4H, n=7, N=4). Thus, these results demonstrate that striosome MSNs are the major source of striatal output to SNc dopamine neurons.

3.4 Discussion

As a new tool for studying striosome and matrix MSNs, it is important to consider how the *hs599*^{CreER} mouse line compares to existing methods. Our data indicate that by targeting early-born, post-mitotic neurons of the LGE, *hs599*^{CreER} mice label striosomes with higher specificity compared to non-inducible Cre lines, such as the Sepw1NP67-Cre line (Smith et al., 2016), though with reduced penetrance. Labeling of more ventral striosomes was especially variable, being present in some mice, but appearing largely absent in others. As with other mouse lines for targeting striosomes (Kelly et al., 2018; Smith et al., 2016), labeling in *hs599*^{CreER} mice was present in MSNs but not major interneuron populations. Furthermore, labeling within MSNs was strongly biased towards those of the direct pathway, a feature of other methods for targeting striosomes (Davis and Iii, 2011; Banghart et al., 2015; Smith et al., 2016). Although our data support a slightly greater proportion of direct pathway MSNs in striosomes compared to matrix, labeling with these lines and *hs599*^{CreER} mice underrepresents the numbers of indirect pathway MSNs in striosomes. The presence of this bias across different methods for isolating striosomes may suggest that molecular differences between striosome and matrix are more marked across direct pathway than indirect pathway MSNs. It is important to note though that other developmental strategies have produced more even labelling of indirect and direct pathway MSNs in striosomes, suggesting that the bias observed in *hs599*^{CreER} mice results from regulation of CreER expression, rather than developmental timing (Kelly et al., 2018). Thus, *hs599*^{CreER} mice may be particularly useful when high specificity of striosome labeling is required, or for studying dorsal direct pathway striosome MSNs in particular.

Using the *hs599*^{CreER} mouse line, we found that at the functional level, PL inputs preferentially target striosome MSNs, whereas M1 inputs preferentially target matrix MSNs. These results are consistent with previous anterograde tracing studies using traditional neurochemically defined striosomes. However, it is important to integrate these local differences in innervation across striosome and matrix with the differences present across anatomical axes, such as

dorsoventral and mediolateral. Inputs to striosome and matrix are highly heterogeneous across these axes, meaning that inputs to MSNs in neighboring compartments may be more similar than when compared to distant MSNs in the corresponding compartment. It is likely then that, like matrix MSNs, striosome MSNs in different striatal regions serve distinct functions. Recent work has highlighted the molecular heterogeneity of striosomes throughout the striatum (Miyamoto et al., 2018); future studies should aim to extend such analysis to the level of *in vivo* activity and behavior.

We also found higher intrinsic excitability in direct pathway striosome MSNs compared to those in the matrix, which may amplify differences in excitatory inputs. In fact, the nearly non-overlapping rheobases of striosome and matrix MSNs may provide a new means of studying striosome MSNs in slice preparations, without transgenic labeling. However, additional validation across genetic backgrounds and ages will be necessary. Critically important is how these differences in both excitatory inputs and intrinsic properties affect activity patterns *in vivo*. Calcium imaging in awake mice indicates that reward-predictive stimuli elicit stronger responses in striosomes than matrix (Bloem et al., 2017; Yoshizawa et al., 2018). This difference might be explained by differences in intrinsic excitability, though contributions from glutamatergic and dopaminergic input remain to be examined.

 Lastly, we provide evidence that striosome MSNs account for the majority of striatal inhibitory input onto SNc dopamine neurons. With the differences in cortical inputs described here, and the segregation of lateral connectivity between striosome and matrix populations shown previously (Kawaguchi et al., 1989; Banghart et al., 2015), these data support the longstanding hypothesis that striosome and matrix neurons constitute functionally distinct striatal pathways. However, how the activity of striosome neurons, or their inhibition of dopamine neurons, shapes behavior remains an open question. Recent calcium-imaging studies indicate that genetically-defined striosome and matrix MSNs are activated by reward (Bloem et al., 2017; Yoshizawa et al., 2018), but striosome output to SNc dopamine neurons suggests that the response of striosome neurons

may have distinct effects compared to matrix MSNs. This hypothesis is supported by recent studies showing that manipulations targeting striosome or matrix-biased cortical inputs bias decision-making in different ways (Friedman et al., 2015, 2017). Based on basal ganglia actor-critic models, striosome input may suppress reward-driven responses when rewards are expected (Brown et al., 1999).

Our finding that striosome activation is sufficient to alter spontaneous firing of SNc dopamine neurons suggests that striosome MSNs could fill such a role. Understanding how striosome inputs shape dopamine neuron activity *in vivo* may clarify the true functional role of striosome MSNs. Together, our results re-establish striosome and matrix as functionally distinct striatal pathways and provide a new tool for investigating the role of striosomes in behavior.

3.5 Experimental Procedures

Animals

Prenatal and adult mice of either sex (age >6 weeks) from six different transgenic lines were used in this study. For histological experiments and identification of striosomes in slice, hemizygous *hs599*[CreER] females (CD-1 IGS, Silberberg et al., 2016) were crossed to homozygous Ai14 (C57BL/6, Madisen et al., 2010) male breeders, to yield experimental animals hemizygous for both Ai14 and *hs599*[CreER]. To identify indirect and direct pathway neurons within striosome and matrix compartments, homozygous Ai14 (C57Bl/6) and hemizygous D2-GFP mice (C57Bl/6; Gong et al., 2003) were crossed, with male hemizygous offspring subsequently bred to *hs599*[CreER] (CD1) females. Experimental animals from this cross were hemizygous for D2-GFP, Ai14, and *hs599*[CreER]. Finally, expression of ChR2-eYFP in striosome or direct pathway neurons was produced by crossing homozygous Ai32 (C57/BL6, Madisen et al., 2012) males to either hemizygous *hs599*[CreER] or D1-Cre (C57BL/6, Gerfen et al., 2013) females, respectively, yielding mice hemizygous for Ai32 and D1-Cre or *hs599*[CreER]. All animals were housed 1-5 per cage and maintained on 12 hr light/dark cycle with food and water provided *ad libitum*. Experimental procedures were carried out with approval of the Institutional Animal Care and Use Committee at University of California, San Francisco and complied with local and national ethical and legal regulations regarding research using mice.

Genotyping of *hs599*[CreER] mice

For *hs599*[CreER] mice, tail biopsies were digested overnight at 55°C in 200 µL of buffer containing 50 mM KCl, 10 mM Tris-HCl (pH 8.3), 2.5 mM MgCl2-6H2O, 0.1 mg/mL gelatin, 0.45% IGEPAL CA-630 (by volume), 0.45% Tween 20 (by volume), and 0.25 mg/mL proteinase K. Tails were then boiled for 10 min and spun down for 5 min at 2400 rpms. Next, supernatant (1 µL) was added to a mixture of dNTPs (2.5 µL), 10X LA PCR Buffer II (Mg^{2+} plus) (2.5 µL), dH20 (17.75 µL), forward primer (1 µL, CACTACTGTTTCTAAGTGTTTCC), and reverse primer (1 µL,

CAGCACAGGCTCAAAGTTGCC). PCR conditions were as follows: 93°C for 3 min, then hold at 82°C and 0.25 µL TaKaRa LA Taq added. Then, 35 cycles of 93°C for 30s, 58°C for 30s, 65°C for 30s. Products were held at 4°C, then run on a 1% agarose gel with SYBR Safe for 40 min at 110 V. Gels were imaged with UV light and presence of the transgene was indicated by a 398bp band.

Tamoxifen Administration

Activation of transgene expression in striosome neurons was achieved by orally gavaging female hs599^{CreER} breeders with tamoxifen (125 mg/kg) dissolved in corn oil (20 mg/mL) on developmental day E10.5. Developmental time points were determined by checking mice each morning for vaginal plugs, with 12:00 pm set as E0.5 following plug detection.

Virus Injections

Anesthesia was induced with intraperitoneal injection of ketamine-xylazine (15-30 mg), after which mice were placed in a stereotaxic frame (Kopf Instruments). Anesthesia was maintained with 1% isoflurane (inhaled) for the duration of the procedure. After opening the scalp, a mounted drill was used to make bilateral burr holes above either prelimbic (PL) or primary motor (M1) cortex. Next, 250 µL of AAV5-hSyn-hChR2(H134R)-eYFP (UNC Vector Core) was delivered using a 33 gauge blunt needle and Micro4 pump (WPI) at 50 nL/min at the following coordinates relative to bregma and surface of the dura (in mm): PL, AP: +2.5 ML: ±0.3 DV -1.0; M1, AP: +1.2 ML: ±1.6 DV: -0.8. Ten minutes after completion of the injection, the needle was removed, the scalp sutured, and animals kept on a heating pad until awakening. Virus was allowed to express for a minimum of 6 weeks prior to experimentation. Injection sites were confirmed following recordings using a Nikon 6D conventional wide-field microscope. Notably, in one animal injected with virus in M1, we observed a small amount of ChR2 expression in the most dorsal portion of striatum. Data from this animal was included, as all recorded cells were distant from the area of

labeling, no intrinsic light responses were observed using 500 ms light pulses, and all GABAergic transmission was blocked using picrotoxin.

Histology

For histological characterization of striosome labeling in *hs599*^{CreER} mice, animals were deeply anesthetized with ketamine-xylazine (100-200 mg, IP) and transcardially perfused with 4% paraformaldehyde in PBS. Following perfusion, brains were dissected, post-fixed for 3-12 hr, and stored in 30% sucrose at 4°C. Embryonic brains were embedded in OCT (Tissue TEK) and sectioned onto slides using a cryostat at 20uM thickness. For immunostaining, embryonic tissue was washed 3 times in PBS with 0.2% TritonX-100 and blocked with with 10% normal goat serum, 0.2% gelatin and 2% non-fat milk in PBS with 0.2% TritonX-100. Postnatal brains were sliced into 35 μm coronal sections using a freezing microtome and kept in PBS. For staining of calbindin, NPY, and PV, sections were blocked in 3% normal donkey serum (NDS) and permeabilized using 0.1% Triton X-100 for 2 hr on a shaker at 4°C. Primary antibody in 3% NDS was then added and sections incubated overnight at 4°C. Following 5 washes (10 min) with PBS, sections were incubated in 3% NDS with appropriate secondary antibody. Lastly, sections were washed 5 times with PBS and mounted in Vectashield Mounting Medium on glass slides for imaging. Immunohistochemistry for ChAT and MOR was performed with minor variations. Blocking serum for ChAT and MOR stains contained 5% NDS with 1.0% or 0.3% Triton-X, respectively. Additionally, primary antibody for MOR was incubated for 48 hr and washes were done using PBS with 0.3% Triton-X.

Primary and secondary antibodies used included: Rabbit anti-Calbindin (Swant, 1:2000), Rabbit anti-PV (Swant, 1:2000), Rabbit anti-NPY (Cell Signaling Technologies, 1:1000), Goat-anti ChAT (Millipore, 1:500), Mouse anti-NeuN (Millipore, 1:1000), Chicken anti-GFP (Aves, 1:500), Chicken anti-GFP (Abcam 1:500), Rabbit anti-RFP (Living Colors 1:1000), Rabbit anti-Ki67 (Abcam 1:300), Rabbit anti-PH3 (Millipore 1:300), Rabbit anti-Nkx2.1 (Santa Cruz Biotechnology

1:500), Rabbit anti-MOR (Immunostar, 1:2000), Rabbit anti-TH (Pel-Freez, 1:1000), Alexa Fluor 568 donkey anti-rabbit (Life Technologies, 1:500), Alexa Fluor 647 donkey anti-mouse (Jackson ImmunoResearch, 1:500), Alexa Fluor 488 donkey-anti rabbit (Jackson ImmunoResearch, 1:500), Alexa Fluor 647 donkey anti-rabbit (Jackson ImmunoResearch, 1:300), Alexa Fluor 488 goat anti-chicken (Molecular Probes 1:300) and Alexa Fluor goat anti-rabbit Cy3 (Molecular Probes 1:300).

A Nikon 6D conventional wide-field microscope was used to take stitched multi-channel fluorescence images at 4-10x when imaging whole brain sections. To colocalize tdTomato expression with other neuronal markers, multi-channel Z-stacks were taken at 40x using a Nikon Spinning Disk confocal microscope. Exposure times and laser intensity were matched between all images of the same type.

Slice Electrophysiology

Mice were deeply anesthetized with ketamine-xylazine (100-200 mg, IP) and perfused with a carbogenated, ice-cold glycerol-based artificial cereberospinal fluid (ACSF) solution containing (in mM): 250 glycerol, 2.5 KCl, 1.2 NaH_2PO_4, 10 HEPES, 21 $NaHCO_3$, 5 D-glucose, 2 $MgCl_2$, 2 $CaCl_2$. Following decapitation, brains were dissected, mounted on a chuck, and submerged in ice-cold glycerol solution. A vibrating microtome (Leica) was used to cut sequential 275 µm coronal slices containing either the striatum or the midbrain, which were immediately transferred to warm (34°C), carbogenated ACSF containing (in mM): 125 NaCl, 26 $NaHCO_3$, 2.5 KCl, 1.25 NaH_2PO_4, 12.5 D-glucose, 1 $MgCl_2$, 2 $CaCl_2$. Slices were incubated for 30-60 min, then kept at room temperature (~23°C) until use.

During all recordings, slices were superfused with carbogenated ACSF at 31-33°C. Differential interference contrast (DIC) optics on an Olympus BX 51 WIF microscope were used to target MSNs and midbrain neurons, which were patched in a whole-cell configuration using borosilicate glass electrodes (2-5 MΩ). To record excitatory synaptic currents from PL and M1

onto MSNs, we used a cesium methanesulfonate-based internal containing (in mM): 120 CsMeSO$_3$, 15 CsCl, 8 NaCl, 0.5 EGTA, 10 HEPES, pH=7.3. Striosome and matrix MSNs within neighboring fields of view (~200 μm) were patched serially in a randomized order. Excitatory currents were optically evoked using 2 ms pulses of 473 nm light ranging in power from 0.5-10 mW and delivered by a TTL-controlled LED (Olympus) passed through a GFP filter (Chroma). Differences in intrinsic excitability between MSNs were measured using a potassium methanesulfonate-based internal containing (in mM): 130 KMeSO3, 10 NaCl, 2 MgCl2, 0.16 CaCl2, 0.5 EGTA, 10 HEPES, pH=7.3. To control for age-related changes in intrinsic excitability (Lieberman et al., 2018), animals used for these experiments were all between 90-160 days old. Picrotoxin (50 μM, Sigma Aldrich) was included in the ACSF for all intrastriatal experiments to block GABA$_A$-mediated inhibition.

To record inhibitory synaptic currents in midbrain neurons, we used a cesium methanesulfonate-based internal with high chloride, which contained (in mM): 120 CsCl, 15 CsMESO3, 8 NaCl, 0.5 EGTA, 10 HEPES, pH=7.3. Inhibitory synaptic currents were evoked as described above. During a subset of whole-cell current clamp recordings, we examined if activation of striosome terminals was sufficient to inhibit spontaneous firing during cell-attached recordings. For these experiments, a potassium-based internal (described above) was used and 473 nm light delivered in 2 ms pulses at 20 Hz. Input resistance and holding current were measured continuously as proxies of recording stability.

All whole-cell recordings were conducted using a MultiClamp 700B amplifier (Molecular Devices) and digitized using an ITC-18 A/D board (HEKA). Igor Pro 6.0 software (Wavemetrics) and custom acquisition routines (mafPC, courtesy of M.A. Xu-Friedman). Both voltage clamp and current-clamp recordings were filtered at 5 kHz and digitized at 10 kHz.

Post-hoc Identification of Recorded Neurons

Biocytin (Sigma Aldrich) was included in internal recording solutions (5 mg/mL) for experiments

comparing intrinsic excitability of MSNs and synaptic input onto SNc dopamine neurons. In the first experiment, tdTomato fluorescence in the emission range of GFP confounded online identification of direct and indirect pathway neurons within striosomes in some cases, necessitating post-hoc confirmation. Three steps were taken to address this issue. First, we showed that 90.2% of tdTomato$^+$ MSNs belonged to the direct pathway, as described above (Figure 3.2K). Second, we used biocytin-fill, far-red staining for GFP, and confocal microscopy to identify recorded MSNs as direct or indirect pathway post-hoc. Of all the striosome MSNs recovered, 100% (9/9) were identified as direct pathway, supporting the hypothesis recorded striosome MSNs were predominantly from the direct pathway. Finally, we compared the intrinsic excitability of identified direct pathway striosome MSNs to that of all recorded striosome MSNs and found no difference (Figure 3S3G). Therefore, data for striosome MSNs appeared representative of direct pathway MSNs.

For recording synaptic input to SNc dopamine neurons, biocytin was used to confirm midbrain neurons with compatible physiology as being Tyrosine-hydroxylase (TH)-expressing SNc dopamine neurons. Recorded neurons were filled for a minimum of 15 minutes before carefully detaching the recording pipette. Slices were then fixed with 4% PFA for 3-12 hr at 4°C and transferred to 30% sucrose in PBS. A sliding microtome was used to cut 55 μm subsections, which were stored in PBS until use. To identify D2-GFP in tdTomato+ cells, sections were stained with chicken anti-GFP (Aves, 1:500) and Alexa Fluor 647 Donkey anti-chicken secondary antibody (1:500), as described for NPY, PV, and calbindin stains, with TritonX-100 replaced by 0.3% Tween20 (Chem-impex Inernational Inc.). Rabbit anti-TH (1:1000, Pel Freez) and Alexa Fluor 568 Donkey anti-rabbit secondary antibody (1:500) were used to identify dopamine neurons. Alexa Fluor 350 streptavidin (3:500) was included with the secondary antibody to visualize biocytin-filled neurons. Biocytin-filled cells were located using a Nikon 6D conventional wide-field microscope at 4-10x and colocalization of fluorophores imaged using a Nikon Spinning Disk confocal microscope at 40x.

In addition to identifying dopamine neurons by post-hoc staining for TH, a subset of SNc dopamine neurons were identified based on cell-attached waveforms, using criteria similar to that previously described (Chieng et al., 2011). Custom code in Matlab was used to extract on-cell spikes based on current thresholds, which were manually determined for individual neurons. All waveforms were then manually confirmed to prevent contamination from potential artifacts. Following normalization of the peak-to-trough amplitude, normalized waveforms were averaged across each recorded neuron and the time from the peak to trough calculated. A threshold of 1 ms for peak-trough duration was selected for positive identification of dopamine neurons, as this effectively segregated biocytin-confirmed SNc dopamine neurons from neighboring GABAergic neurons in the SNr.

QUANTIFICATION AND STATISTICAL ANALYSIS

Statistics

All data are presented as the mean ± SEM, with N referring to the number of animals and n to the number of cells.

Histology and Cell Counting

Specificity and penetrance of striosome labeling in hs599^{CreER};Ai14 mice was determined using coronal sections from three points along the AP-axis (+0.5, +1.0, and +1.5 mm relative to Bregma) from each animal. Striosomes and neighboring matrix regions in the dorsal half of the striatum were identified by MOR expression using a spinning disk confocal microscope, with the experimenter imaging blinded to tdTomato$^+$ labelling pattern. After imaging tdTomato expression, the number of tdTomato$^+$ cells were quantified manually with FIJI/ImageJ software by a rater blinded to compartmental origin. Density (Ai14$^+$ cells/mm) in striosome and matrix were used as a measure of penetrance and specificity, respectively. For both measures, cell bodies within the

subcallosal strip were excluded for analysis, though notably this region showed consistent MOR and tdTomato labeling across animals.

To quantify colocalization of tdTomato expression with interneuron markers (ChAT, PV, or NPY) or a marker of indirect pathway MSNs (D2-GFP), striosomes from three striatal sections along the AP-axis (+0.5, +1.0, and +1.5 relative to Bregma) were imaged in their entirety, and the number of GFP[+] and tdTomato[+] nuclei counted manually. The proportion of indirect pathway MSNs in histologically defined striosomes and matrix was quantified in D2-GFP mice using coronal striatal sections from five APs (+1.0, +0.5, 0, -0.5, and -1.0 relative to Bregma). Striosome and matrix were identified by MOR expression, and the proportion of NeuN^{+} cells positive for GFP quantified manually. The Mouse Brain Atlas in Stereotaxic Coordinates (hard copy, 4th edition, by George Paxinos and Keither B.J Franklin) was consulted for anatomical reference.

Slice Electrophysiology

To characterize intrinsic excitability, custom code in Igor Pro (Wavemetrics) was used to extract the instantaneous firing rate for each current step, rheobase, maximum firing rate, and resting membrane potential. Input resistance was manually calculated using Ohm's law ($V=I*R$) and the current transient induced by a -5 mV step from -70 mV holding in voltage clamp. For all measures, significance was determined using a Kruskal-Wallis test with a Bonferroni correction applied to control for multiple comparisons. A Dunn's post-hoc test was applied to test for significance between individual groups. The positive and negative predictive values of various rheobase thresholds to identify striosome from matrix MSNs were calculated using the following equations: [positive predictive value = true positives / (true positives + false positives)], [negative predictive value = true negatives / (true negatives + false negatives)].

Average amplitudes of oEPSCs and oIPSCs were quantified manually in Igor. A Wilcoxon sign-rank test was used to compare oEPSC amplitude from M1 or PL onto striosome and matrix MSNs. For comparison of oIPSC amplitude onto midbrain neurons, we used a Wilcoxon rank-

sum test. In all experiments involving optical stimulation, data was drawn from stimulations at ~3.5 mW light power.

To determine if the observed output of striosome and direct pathway matrix MSNs to SNr and SNc neurons differed statistically, 50% of oIPSC amplitudes from SNr and SNc neurons were randomly sampled with replacement 10,000 times for each genotype using custom Matlab code (Mathworks). For each trial, the ratio of output (SNr:SNc) was calculated using the average oIPSC amplitude sampled from each cell type. Ratios were binned in units of 1 and the probability density distributions obtained by dividing the total number of counts in each bin by the total number of trials. A Kolmogorov–Smirnov test was used to test for differences between the probability distribution obtained from $hs599^{CreER}$;Ai32 and D1-Cre;Ai32 mice.

DATA AND CODE AVAILABILITY

Any data or code supporting the current study are available from the corresponding author upon request.

3.6 Author Contributions

M.M.M, A.B.N, G.L.M., and J.L.R.R. designed experiments. Histological validation of *hs599^{CreER}* mice were performed by G.L.M., M.M.M, and C.J.B.M. M.M.M, A.E.G, and A.B.N carried out electrophysiological experiments. Manuscript was prepared by M.M.M and A.B.N, with input from G.L.M and J.L.R.R.

3.7 Figures
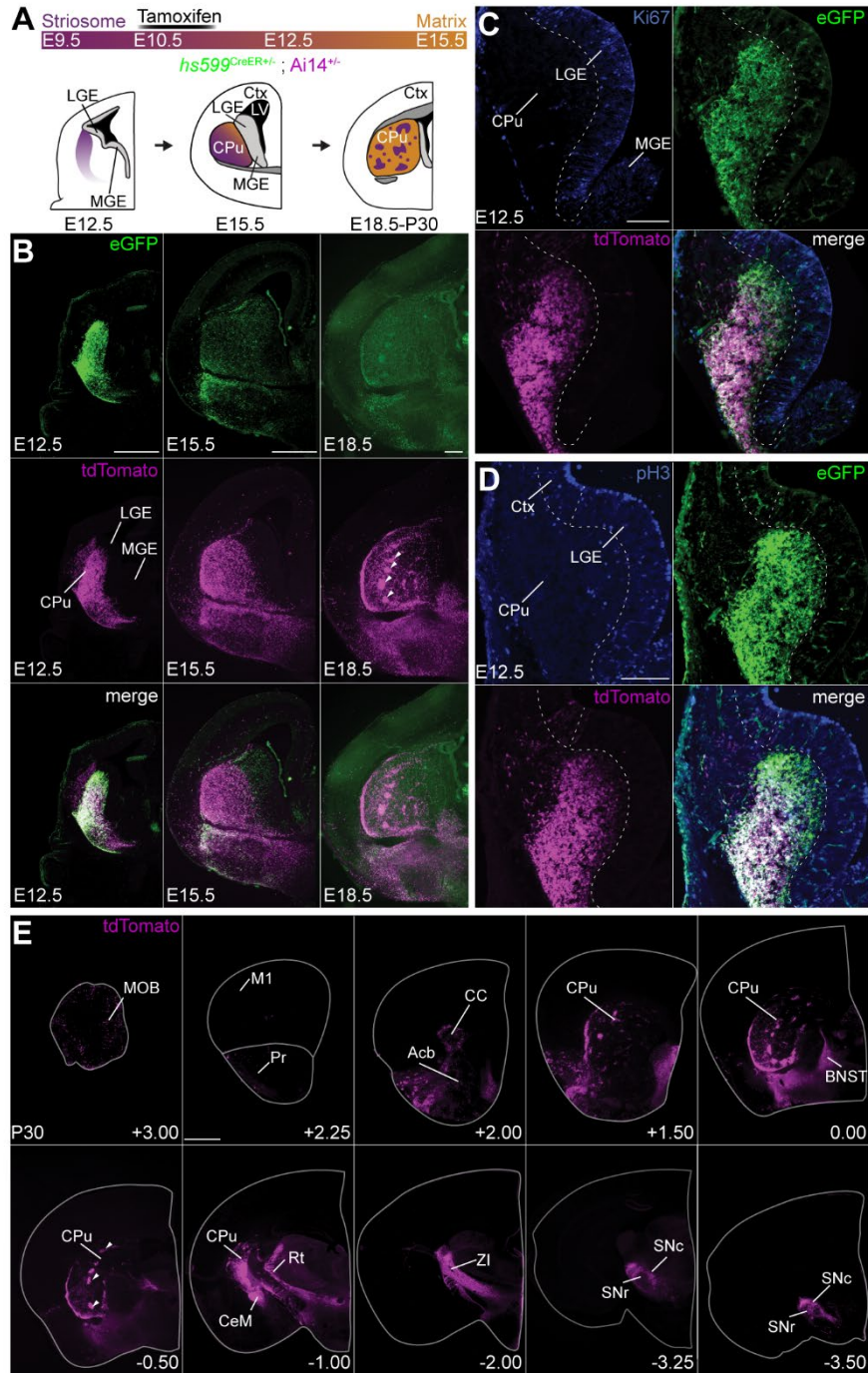
Figure 3.1: Targeting of early-born striatal neurons using *hs599^CreER* mice. (A) Schematic of striosome (purple) and matrix (orange) development and strategy for using tamoxifen to capture early born striatal neurons (CPu, caudoputamen (striatum); Ctx, cortex; LGE, lateral ganglionic eminence; LV, lateral ventrical; MGE, medial ganglionic eminence). **(B)** tdTomato⁺ (magenta) and CreER-eGFP⁺ (green) cells at E12.5 (left), E15.5 (middle), and E18.5 (right) following E10.5 tamoxifen administration. Arrows indicate potential striosomes. **(C-D)** Overlap of tdTomato⁺ and CreER-eGFP⁺ cells with progenitor cells marked by **(C)** Ki67 (blue) or **(D)** phospho-histone H3

(pH3, blue). **(E)** Sample coronal sections illustrating tdTomato-labeled structures in the adult brain (P30) following tamoxifen administration at E10.5. Abbreviations: MOB, main olfactory bulb; M1, primary motor cortex; Pr, piriform cortex; CC, corpus callosum; acb, nucleus accumbens; str, striatum BNST, bed nucleus of the stria terminalis; Rt, reticular thalamus, CeM, central amygdala; ZI, zona incerta; SNr, substantia nigra pars reticulata; SNc, substantia nigra pars compacta. Scale bars represents 0.5 mm (B, E) and 50 μm (C-D). See also Figure S1 and S2.
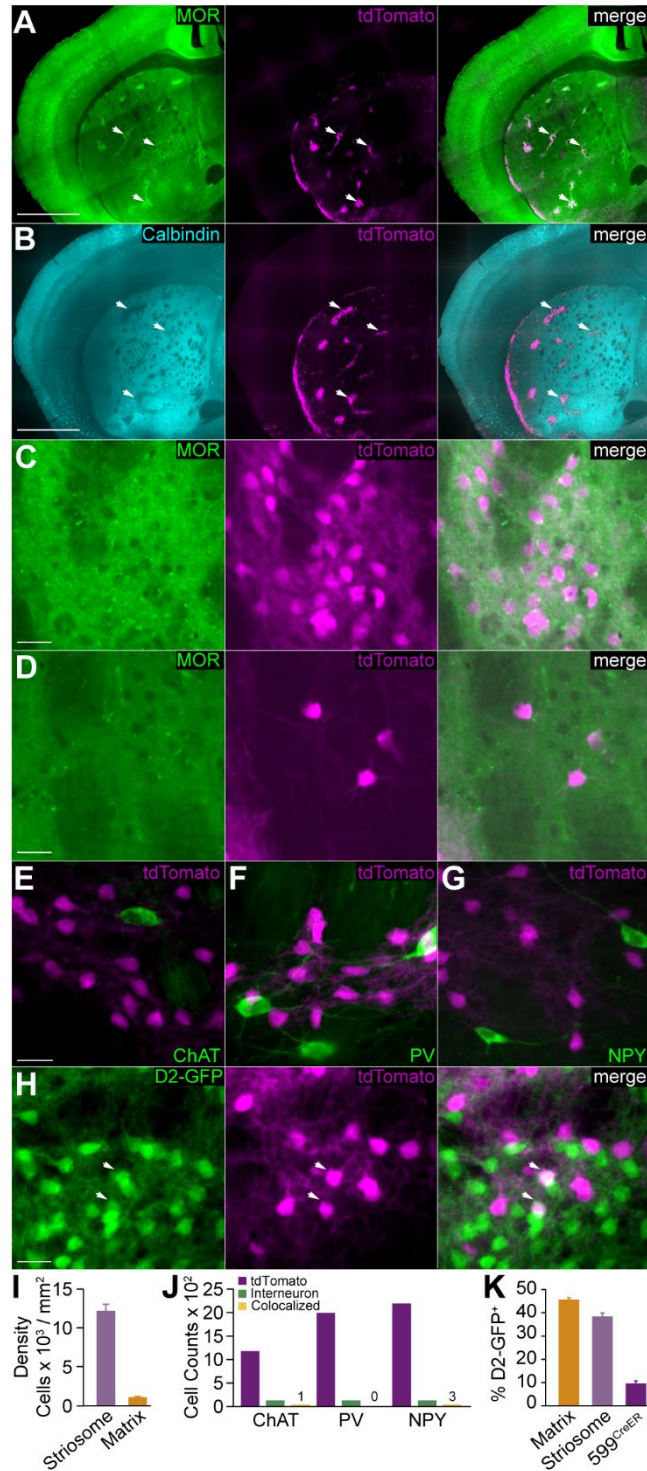
Figure 3.2: *hs599^{CreER}* **mice enable targeting of striosome MSNs. (A-B)** Overlap of tdTomato^+ cells (magenta) in striosomes (arrows) identified by **(A)** increased μ-opioid receptor (MOR, green) or **(B)** decreased calbindin (blue) staining. **(C-D)** Example of high-magnification image used to quantify the density tdTomato^+ cells in **(C)** striosome and **(D)** matrix compartments as identified by MOR staining. **(E-G)** Overlap of tdTomato^+ cells with interneurons (green), marked by staining for **(E)** choline acetyltransferase (ChAT), **(F)** parvalbumin (PV), and **(G)** neuropeptide Y (NPY) **(H)**

Example of overlap between tdTomato$^+$ and D2-GFP$^+$ cells. **(I)** Quantification of tdTomato$^+$ cell density in striosome and matrix. **(J)** Cell counts of tdTomato$^+$ cells, interneurons, and double-labeled cells for ChAT, PV, and NPY. **(K)** Percentage of matrix, striosome, and tdTomato$^+$ cells that are D2-GFP$^+$. Scale bars represents 1.0 mm (A-B) and 20 µm (C-H). Data are displayed as mean ± SEM.
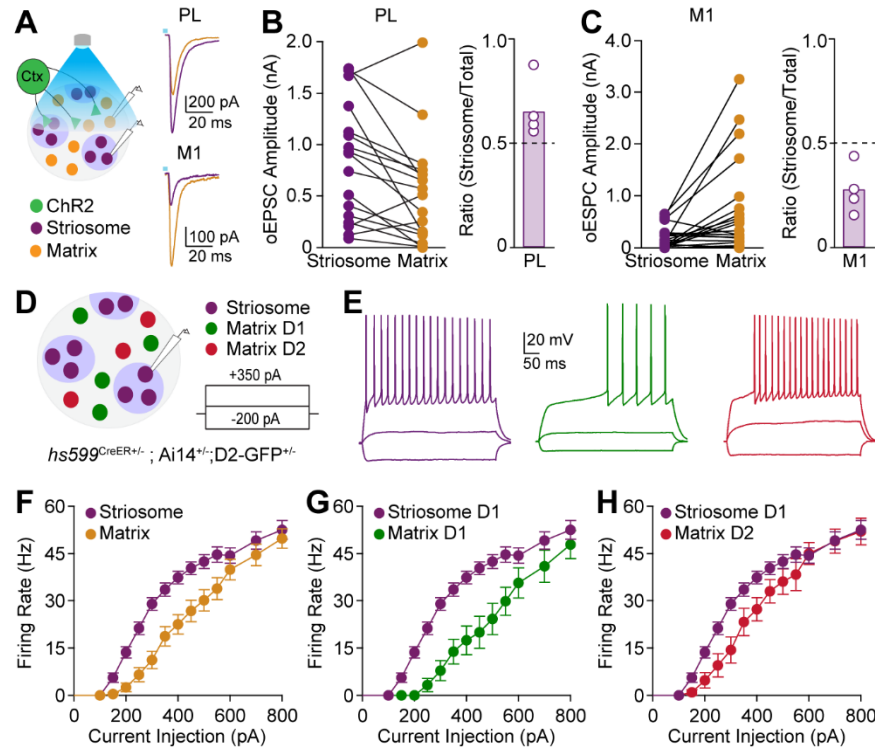
Figure 3.3: Cortical innervation and intrinsic excitability differs between striosome and matrix MSNs. (A) Schematic of recording configuration (left) and examples of optically-evoked excitatory post-synaptic currents (oEPSCs) from prelimbic (PL, top right) and primary motor (M1, bottom right) cortex in striosome (purple) and matrix neurons (orange). **(B)** Left: Amplitudes of oEPSCs from PL cortex in sequential pairs of striosome and matrix neurons. Right: Bias of PL for striosome based on oEPSC amplitudes. Bar represents the average for all recorded pairs, while individual points represent the average calculated for individual animals. A value of 1 represents input exclusively to striosome neurons, while a value of 0 represents input exclusively to matrix neurons. **(C)** Left: Amplitudes of oEPSCs from M1 cortex in sequential pairs of striosome and matrix neurons. Right: Bias of M1 input for matrix calculated as in B. **(D)** Schematic of excitability recording configuration. **(E)** Responses of a direct pathway striosome (purple), direct pathway matrix (green), and indirect pathway matrix (red) to three example current injections. **(F-H)** Current-frequency plot for **(F)** all striosome and matrix MSNs, **(G)** direct pathway striosome and matrix MSNs, and **(H)** direct pathway striosome and indirect pathway matrix MSNs. Data are displayed as mean ± SEM. See also Figure S3.
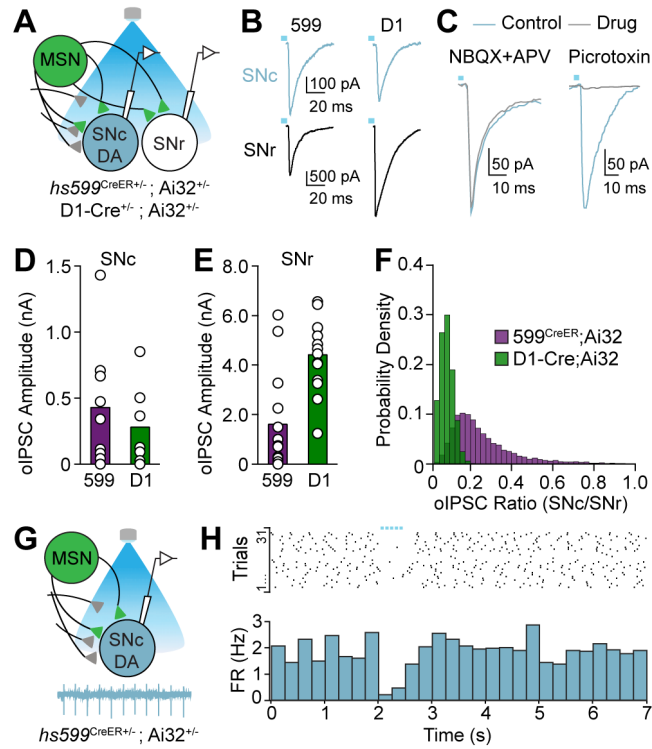
Figure 3.4: Striosome output to midbrain neurons is distinct from direct pathway MSNs.
(A) Schematic of recording configuration. **(B)** Example optically-evoked inhibitory currents (oIPSCs) in SNc dopamine (blue) and SNr (black) neurons from hs599[CreER];Ai32 (left) and D1-Cre;Ai32 (right) mice. **(C)** Effect of NBQX and APV or picrotoxin on oIPSCs in a SNc dopamine neuron from a *hs599[CreER]*;Ai32 mouse. **(D)** oIPSC amplitudes in SNr dopamine neurons for striosome and direct pathway terminal stimulation. **(E)** oIPSC amplitudes in SNc neurons for striosome and direct pathway terminal stimulation. **(F)** Probability density plot of oIPSC amplitude ratios (SNc:SNr) obtained by bootstrapping data from *hs599[CreER]* (green) and D1-Cre (purple) mice. **(G)** Configuration for cell-attached recording of SNc dopamine neurons with example trace. **(H)** Top: raster of spontaneous SNc DA neuron firing (31 trials across 7 cells) with suppression by striosome terminal stimulation (blue bars). Bottom: Firing rates over time (500 ms bins) for all dopamine neurons. Data are displayed as the mean. See also Figure S4.
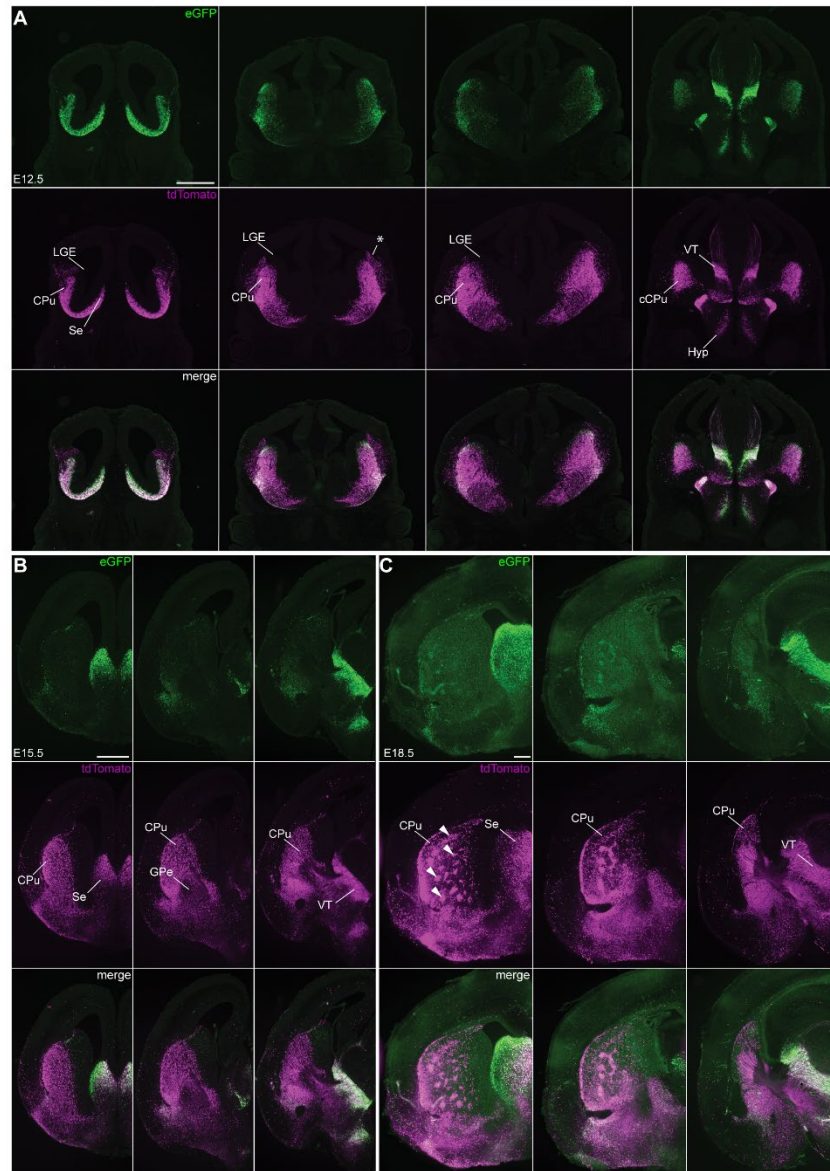
145

3.8 Supplemental Figures

Figure 3S1. CreER expression and recombination throughout the brain of prenatal *hs599^CreER*;**Ai14 mice. Related to Figure 1. (A-C)** CreER-eGFP (green) and tdTomato (magenta) expression in coronal sections across the anterior-posterior axis from **(A)** E12.5, **(B)** E15.5, or **(C)** E18.5 brains taken from a *hs599^CreER*;Ai14 mice administered tamoxifen at E10.5. Arrows indicate potential striosomes. Asterisk indicates pallial/subpallial boundary recombination. Abbreviations: CPu, caudoputamen; cCPu, caudual caudoputamen; LGE, lateral ganglionic eminence; Hyp, hypothalamus; SE, septum; VT, ventral thalamus. Scale bars represent 500 μm.
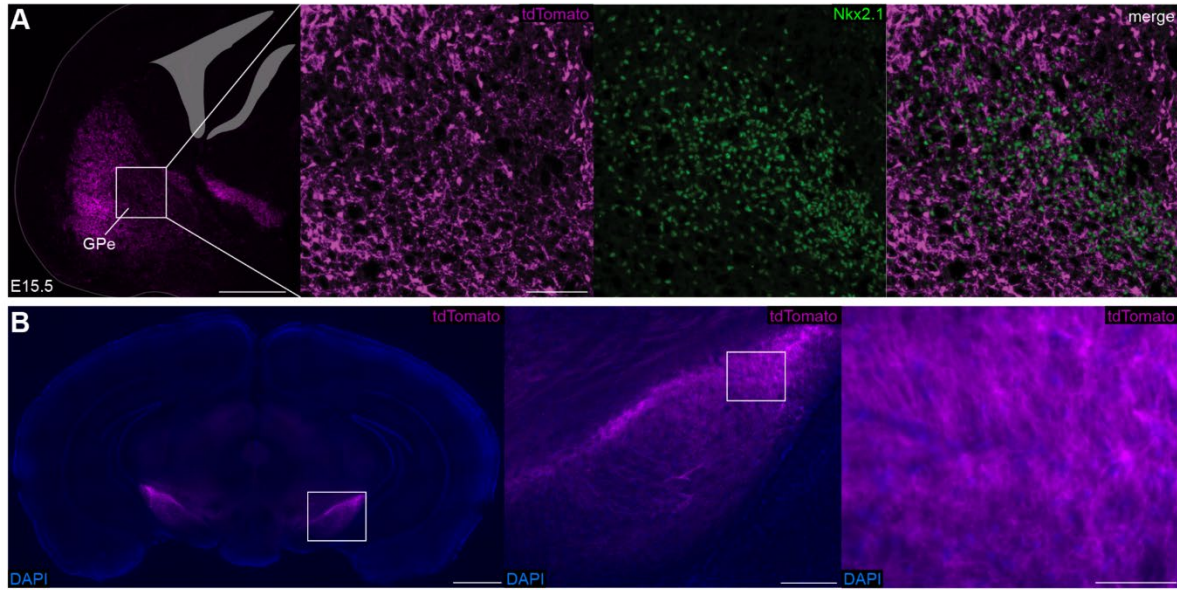
Figure 3S2. E10.5 tamoxifen administration does not lead to labeling of Nkx2.1+ external globus pallidus neurons or substantia nigra neurons in *hs599^CreER;*Ai14 mice. Related to Figure 1. (A) Left, E15.5 coronal hemisection of a *hs599^CreER*;Ai14 mouse administered tamoxifen at E10.5. Middle, magnification of TdTomato expression (magenta) and Nkx2.1 staining (green) in the developing external globus pallidus. Right, overlay of magnified images. Scale bars represent 500 µm in left and 100 µm in magnified images. **(B)** Left: Midbrain section from an *hs599^CreER*;Ai14 mouse containing the SNc and SNr. Middle and Right: Sequential enlargements of SNc and SNr showing tdTomato⁺ terminals, but not cell bodies. Scale bars from left to right represent 1 mm, 100 µm, and 50 µm.
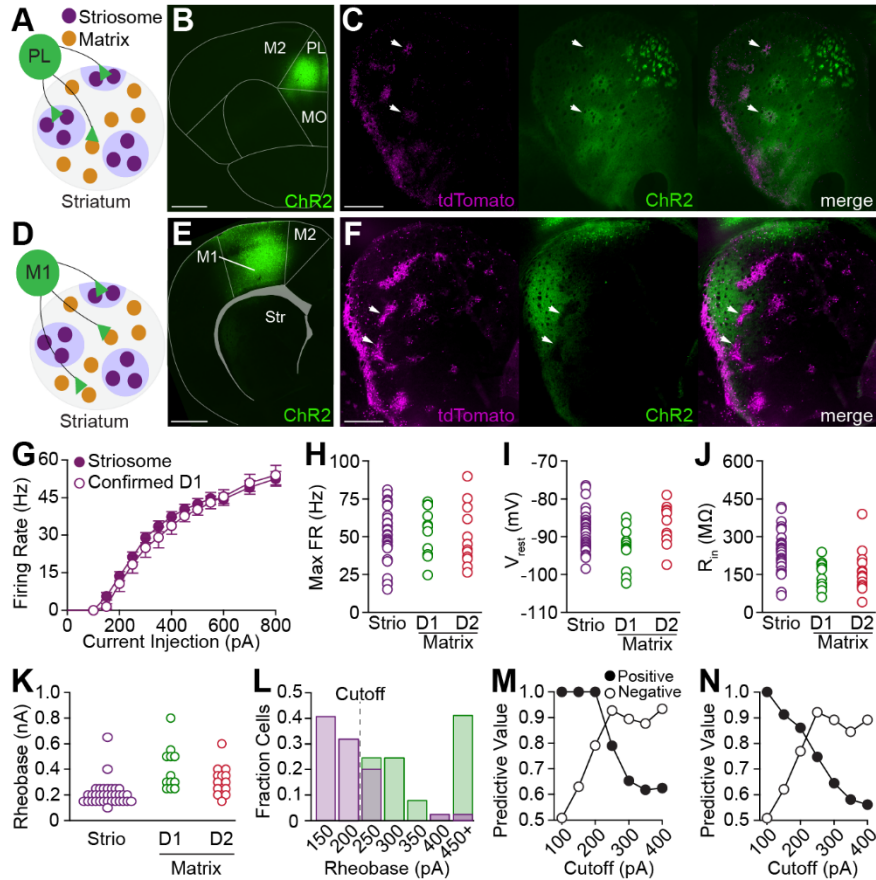
Figure 3S3. Differences in inputs and intrinsic excitability between striosome and matrix MSNs. Related to Figure 3. (A, D) Schematic of ChR2-eYFP in either **(A)** the prelimbic (PL) or **(D)** primary motor cortex (M1) of *hs599^CreER*;Ai14 mice. **(B,E)** Example of ChR2-eYFP (green) expression at the injection site for either **(B)** PL **(E)** or M1 (MO, medial orbitofrontal; M2, secondary motor cortex; str, striatum). Scale bars represent 1 μm. **(C,F)** Examples of the overlap between ChR2-eYFP⁺ corticostriatal terminals (green) and striosomes labeled by tdTomato (magenta) for mice injected in either **(C)** Pl or **(F)** M1. Scale bars represent 500 μm. **(G)** Current-frequency plot of instantaneous firing in response to various current injections for all recorded striosome MSNs and striosome MSNs confirmed to be direct pathway by biocytin-fill and post-hoc verification. **(H-J)** Comparison of **(H)** maximum firing rate **(I)** resting membrane potential, **(J)** input resistance, and **(K)** rheobase for direct pathway striosome, direct pathway matrix, and indirect pathway matrix MSNs. **(L)** Distribution of rheobases from striosome (purple) and direct pathway matrix MSNs (green) with an example discrimination cutoff at 200 pA. **(M-N)** Positive and negative predictive value for various cutoffs of rheobase for identifying direct pathway striosome MSNs from **(M)** direct pathway matrix MSNs or **(N)** all matrix MSNs.
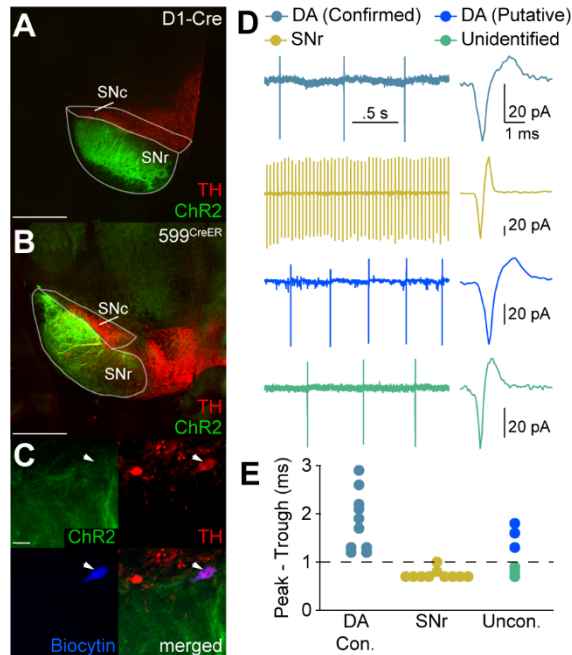
Figure 3S4. Identification of dopamine neurons in slice. Related to Figure 4. (A) Example of ChR2-eYFP[+] terminals (green) from a **(A)** D1-Cre;Ai32 or **(B)** *hs599^{CreER}*;Ai32 mouse in the SNr and SNc (as identified by staining for tyrosine hydroxylase (TH), red). Scales bars represent 1 mm. **(C)** Example of an SNc dopamine neuron recorded from a *hs599^{CreER}*;Ai32 mouse. ChR2-eYFP[+] terminals (green) are overlayed with TH (red) and biocytin staining (blue). Scale bar represents 10 μm. **(D)** Examples traces of cell-attached spiking from confirmed dopamine (dark blue), SNr (yellow), presumed dopamine (light blue), and unclassified (green) neurons. **(E)** Peak to trough amplitude for confirmed dopamine neurons (DA con.), SNr neurons, and unconfirmed neurons (Uncon.). The dotted line represents the threshold value for positive identification as a putative dopamine neuron.

3.9 References

Banghart, M.R., Neufeld, S.Q., Wong, N.C., and Sabatini, B.L. (2015). Enkephalin disinhibits mu opioid receptor rich striatal patches via delta opioid receptors. Neuron *88*, 1227–1239.

Bloem, B., Huda, R., Sur, M., and Graybiel, A.M. (2017). Two-photon imaging in mice shows striosomes and matrix have overlapping but differential reinforcement-related responses. ELife *6*, e32353.

Brown, J., Bullock, D., and Grossberg, S. (1999). How the basal ganglia use parallel excitatory and inhibitory learning pathways to selectively respond to unexpected rewarding cues. J. Neurosci. Off. J. Soc. Neurosci. *19*, 10502–10511.

Chieng, B., Azriel, Y., Mohammadi, S., and Christie, M.J. (2011). Distinct cellular properties of identified dopaminergic and GABAergic neurons in the mouse ventral tegmental area. J. Physiol. *589*, 3775–3787.

Crittenden, J.R., Lacey, C.J., Weng, F.-J., Garrison, C.E., Gibson, D.J., Lin, Y., and Graybiel, A.M. (2017). Striatal Cholinergic Interneurons Modulate Spike-Timing in Striosomes and Matrix by an Amphetamine-Sensitive Mechanism. Front. Neuroanat. *11*.

Cui, G., Jun, S.B., Jin, X., Pham, M.D., Vogel, S.S., Lovinger, D.M., and Costa, R.M. (2013). Concurrent Activation of Striatal Direct and Indirect Pathways During Action Initiation. Nature *494*, 238–242.

Davis, M.I., and Iii, H.L.P. (2011). Nr4a1-eGFP Is a Marker of Striosome-Matrix Architecture, Development and Activity in the Extended Striatum. PLOS ONE *6*, e16619.

Dodson, P.D., Larvin, J.T., Duffell, J.M., Garas, F.N., Doig, N.M., Kessaris, N., Duguid, I.C., Bogacz, R., Butt, S.J.B., and Magill, P.J. (2015). Distinct developmental origins manifest in the specialized encoding of movement by adult neurons of the external globus pallidus. Neuron *86*, 501–513.

Eblen, F., and Graybiel, A.M. (1995). Highly restricted origin of prefrontal cortical inputs to striosomes in the macaque monkey. J. Neurosci. *15*, 5999–6013.

Flandin, P., Kimura, S., and Rubenstein, J.L.R. (2010). The progenitor zone of the ventral medial ganglionic eminence requires Nkx2-1 to generate most of the globus pallidus but few neocortical interneurons. J. Neurosci. Off. J. Soc. Neurosci. *30*, 2812–2823.

Friedman, A., Homma, D., Gibb, L.G., Amemori, K., Rubin, S.J., Hood, A.S., Riad, M.H., and Graybiel, A.M. (2015). A Corticostriatal Path Targeting Striosomes Controls Decision-Making under Conflict. Cell *161*, 1320–1333.

Friedman, A., Homma, D., Bloem, B., Gibb, L.G., Amemori, K., Hu, D., Delcasso, S., Truong, T.F., Yang, J., Hood, A.S., et al. (2017). Chronic Stress Alters Striosome-Circuit Dynamics, Leading to Aberrant Decision-Making. Cell *171*, 1191-1205.e28.

Fujiyama, F., Sohn, J., Nakano, T., Furuta, T., Nakamura, K.C., Matsuda, W., and Kaneko, T. (2011). Exclusive and common targets of neostriatofugal projections of rat striosome neurons: a single neuron-tracing study using a viral vector. Eur. J. Neurosci. *33*, 668–677.

Gerfen, C.R. (1985). The neostriatal mosaic. I. compartmental organization of projections from the striatum to the substantia nigra in the rat. J. Comp. Neurol. *236*, 454–476.

Gerfen, C.R., Baimbridge, K.G., and Miller, J.J. (1985). The neostriatal mosaic: compartmental distribution of calcium-binding protein and parvalbumin in the basal ganglia of the rat and monkey. Proc. Natl. Acad. Sci. *82*, 8780–8784.

Gerfen, C.R., Paletzki, R., and Heintz, N. (2013). GENSAT BAC Cre-recombinase driver lines to study the functional organization of cerebral cortical and basal ganglia circuits. Neuron *80*.

Gertler, T.S., Chan, C.S., and Surmeier, D.J. (2008). Dichotomous Anatomical Properties of Adult Striatal Medium Spiny Neurons. J. Neurosci. *28*, 10814–10824.

Gong, S., Zheng, C., Doughty, M.L., Losos, K., Didkovsky, N., Schambra, U.B., Nowak, N.J., Joyner, A., Leblanc, G., Hatten, M.E., et al. (2003). A gene expression atlas of the central nervous system based on bacterial artificial chromosomes. Nature *425*, 917–925.

Hernández, V.M., Hegeman, D.J., Cui, Q., Kelver, D.A., Fiske, M.P., Glajch, K.E., Pitt, J.E.,

Huang, T.Y., Justice, N.J., and Chan, C.S. (2015). Parvalbumin+ Neurons and Npas1+ Neurons Are Distinct Neuron Classes in the Mouse External Globus Pallidus. J. Neurosci. Off. J. Soc. Neurosci. *35*, 11830–11847.

Jiménez-Castellanos, J., and Graybiel, A.M. (1989). Compartmental origins of striatal efferent projections in the cat. Neuroscience *32*, 297–321.

Kawaguchi, Y., Wilson, C.J., and Emson, P.C. (1989). Intracellular recording of identified neostriatal patch and matrix spiny cells in a slice preparation preserving cortical inputs. J. Neurophysiol. *62*, 1052–1068.

Kelly, S.M., Raudales, R., He, M., Lee, J.H., Kim, Y., Gibb, L.G., Wu, P., Matho, K., Osten, P., Graybiel, A.M., et al. (2018). Radial Glial Lineage Progression and Differential Intermediate Progenitor Amplification Underlie Striatal Compartments and Circuit Organization. Neuron *99*, 345-361.e4.

Kincaid, A.E., and Wilson, C.J. (1996). Corticostriatal innervation of the patch and matrix in the rat neostriatum. J. Comp. Neurol. *374*, 578–592.

van der Kooy, D., and Fishell, G. (1987). Neuronal birthdate underlies the development of striatal compartments. Brain Res. *401*, 155–161.

Kravitz, A.V., and Kreitzer, A.C. (2012). Striatal Mechanisms Underlying Movement, Reinforcement, and Punishment. Physiol. Bethesda Md *27*.

Lévesque, M., and Parent, A. (1998). Axonal arborization of corticostriatal and corticothalamic fibers arising from prelimbic cortex in the rat. Cereb. Cortex *8*, 602–613.

Lieberman, O.J., McGuirt, A.F., Mosharov, E.V., Pigulevskiy, I., Hobson, B.D., Choi, S., Frier, M.D., Santini, E., Borgkvist, A., and Sulzer, D. (2018). Dopamine Triggers the Maturation of Striatal Spiny Projection Neuron Excitability during a Critical Period. Neuron *99*, 540-554.e4.

Lopez-Huerta, V.G., Nakano, Y., Bausenwein, J., Jaidar, O., Lazarus, M., Cherassse, Y., Garcia-

Munoz, M., and Arbuthnott, G. (2016). The neostriatum: two entities, one structure? Brain Struct. Funct. *221*, 1737–1749.

Madisen, L., Zwingman, T.A., Sunkin, S.M., Oh, S.W., Zariwala, H.A., Gu, H., Ng, L.L., Palmiter, R.D., Hawrylycz, M.J., Jones, A.R., et al. (2010). A robust and high-throughput Cre reporting and characterization system for the whole mouse brain. Nat. Neurosci. *13*, 133–140.

Madisen, L., Mao, T., Koch, H., Zhuo, J., Berenyi, A., Fujisawa, S., Hsu, Y.-W.A., Iii, A.J.G., Gu, X., Zanella, S., et al. (2012). A toolbox of Cre-dependent optogenetic transgenic mice for light-induced activation and silencing. Nat. Neurosci. *15*, 793–802.

Mason, H.A., Rakowiecki, S.M., Raftopoulou, M., Nery, S., Huang, Y., Gridley, T., and Fishell, G. (2005). Notch signaling coordinates the patterning of striatal compartments. Development *132*, 4247–4258.

Miyamoto, Y., Katayama, S., Shigematsu, N., Nishi, A., and Fukuda, T. (2018). Striosome-based map of the mouse striatum that is conformable to both cortical afferent topography and uneven distributions of dopamine D1 and D2 receptor-expressing cells. Brain Struct. Funct.

Nóbrega-Pereira, S., Gelman, D., Bartolini, G., Pla, R., Pierani, A., and Marín, O. (2010). Origin and molecular specification of globus pallidus neurons. J. Neurosci. Off. J. Soc. Neurosci. *30*, 2824–2834.

Pert, C.B., Kuhar, M.J., and Snyder, S.H. (1976). Opiate receptor: autoradiographic localization in rat brain. Proc. Natl. Acad. Sci. U. S. A. *73*, 3729–3733.

Planert, H., Berger, T.K., and Silberberg, G. (2013). Membrane Properties of Striatal Direct and Indirect Pathway Neurons in Mouse and Rat Slices and Their Modulation by Dopamine. PLOS ONE *8*, e57054.

Ragsdale, C.W., and Graybiel, A.M. (1988). Fibers from the basolateral nucleus of the amygdala

selectively innervate striosomes in the caudate nucleus of the cat. J. Comp. Neurol. *269*, 506–522.

Sadikot, A.F., Parent, A., Smith, Y., and Bolam, J.P. (1992). Efferent connections of the centromedian and parafascicular thalamic nuclei in the squirrel monkey: A light and electron microscopic study of the thalamostriatal projection in relation to striatal heterogeneity. J. Comp. Neurol. *320*, 228–242.

Silberberg, S.N., Taher, L., Lindtner, S., Sandberg, M., Nord, A.S., Vogt, D., Mckinsey, G.L., Hoch, R., Pattabiraman, K., Zhang, D., et al. (2016). Subpallial Enhancer Transgenic Lines: a Data and Tool Resource to Study Transcriptional Regulation of GABAergic Cell Fate. Neuron *92*, 59–74.

Smith, J.B., Klug, J.R., Ross, D.L., Howard, C.D., Hollon, N.G., Ko, V.I., Hoffman, H., Callaway, E.M., Gerfen, C.R., and Jin, X. (2016). Genetic-Based Dissection Unveils the Inputs and Outputs of Striatal Patch and Matrix Compartments. Neuron *91*, 1069–1084.

Visel, A., Taher, L., Girgis, H., May, D., Golonzhka, O., Hoch, R.V., McKinsey, G.L., Pattabiraman, K., Silberberg, S.N., Blow, M.J., et al. (2013). A high-resolution enhancer atlas of the developing telencephalon. Cell *152*, 895–908.

Watabe-Uchida, M., Zhu, L., Ogawa, S.K., Vamanrao, A., and Uchida, N. (2012). Whole-Brain Mapping of Direct Inputs to Midbrain Dopamine Neurons. Neuron *74*, 858–873.

Yang, H., de Jong, J.W., Tak, Y., Peck, J., Bateup, H.S., and Lammel, S. (2018). Nucleus Accumbens Subnuclei Regulate Motivated Behavior via Direct Inhibition and Disinhibition of VTA Dopamine Subpopulations. Neuron *97*, 434-449.e4.

Yoshizawa, T., Ito, M., and Doya, K. (2018). Reward-Predictive Neural Activities in Striatal Striosome Compartments. ENeuro *5*.

CHAPTER 4

Striatal Dopamine, But Not D2R Sensitivity, Predicts the Development of Tardive Dyskinesia

---

4.1 Abstract

Use of antipsychotic medications to treat psychiatric disorders is limited by their tendency to induce motor side effects such as tardive dyskinesia (TD). Characterized by involuntary orofacial movements that emerge over chronic treatment with antipsychotic medications, TD is hypothesized to result from aberrant striatal activity driven by increased sensitivity of D2-type dopamine receptor (D2R) signaling. However, how dopamine signaling and striatal activity change during the development of TD is unknown. Here, we use a mouse model of TD in combination with *ex vivo* electrophysiology and *in vivo* imaging to determine the cell types and activity patterns that mediate TD. Counter to traditional models, we find that development of involuntary movements does not depend on sensitization of D2Rs, but tightly correlates with increases in striatal dopamine and activity of neurons in the ventrolateral portion of the striatum. These results point to unexpected mechanisms underlying TD and specific striatal subpopulations for targeting therapeutic relief.

4.2 Introduction

Antipsychotic medications are the mainstay treatment for numerous psychiatric diseases, such as schizophrenia and bipolar disorder, yet chronic use can often induce a condition called tardive dyskinesia (TD). Characterized by involuntary movements of the mouth, face, and tongue, TD can impair basic motor functions such as speech, and lead to feelings of stigmatization, embarrassment, and social isolation (Factor et al., 2019). Furthermore, although TD typically develops after months to years of antipsychotic treatment, it can irreversible (Caroff et al., 2018). Though newer antipsychotic medications have a somewhat lower risk of TD, it is still common in long-term treatment (Carbon et al., 2017; Caroff, 2019), and without a cure, TD represents a persistent clinical issue in the treatment of psychiatric disorders. Despite these issues, little is known about the cell types and underlying patterns of neural activity that drive the disorder.

Several converging lines of clinical evidence suggest that TD results from the chronic disruption of dopaminergic signaling. First, almost all antipsychotic medications associated with TD are D2-type dopamine receptor (D2R) antagonists (Divac et al., 2014), and other D2R antagonists used for chronic gastrointestinal disorders also cause TD (Rao and Camilleri, 2010). Secondly, polymorphisms in the vesicular monoamine transporter (VMAT2), the protein responsible for packaging dopamine into vesicles, as well as the DRD2 and DRD3 genes that encode D2Rs and D3Rs, have been associated with modified risks of TD (Zai et al., 2018). Third, the only medications currently approved for the treatment of TD are VMAT2 inhibitors (Koch et al., 2020).

While data indicating which brain structures causally contribute to TD are limited, indirect evidence points to the striatum, the primary input nucleus of the basal ganglia. Critical for control of voluntary movement (Nelson and Kreitzer, 2014), the striatum receives dense dopaminergic projections from the midbrain and is highly enriched for dopamine receptors. These receptors are present on several circuit elements, including striatal output neurons. Direct pathway medium spiny neurons (dMSNs) express excitatory D1-type dopamine receptors (D1Rs) and are known

to facilitate movement, while indirect pathway medium spiny neurons (iMSNs) express inhibitory D2Rs and are sufficient to suppress movement (Gerfen et al., 1990; Kravitz et al., 2010). Based on hints from clinical phenomenology (Crane, 1973; Marsden and Jenner, 1980; Peralta and Cuesta, 2010), human imaging (Kapur, 1998), and biochemical findings in rodent models of TD (Burt et al., 1977; Rogue et al., 1991; Savasta et al., 1988), chronic antipsychotic treatment is hypothesized to lead to a homeostatic hypersensitization of D2R signaling on iMSNs, which may in turn result in an imbalance in dMSN/iMSN activity. However, studies in preclinical models of TD provide conflicting evidence (Jiang et al., 1990; Shirakawa and Tamminga, 1994; Bachus et al., 2012; Yael et al., 2013; Sebel et al., 2017). Furthermore, it is currently unknown how dopamine signaling and activity of striatal neurons change over the course of chronic antipsychotic treatment and development of TD.

Here, we test how changes in dopamine signaling and activity within dMSNs and iMSNs contribute to involuntary movements caused by chronic antipsychotic treatment in a mouse model of TD. Using a combination of slice electrophysiology, optogenetics, and fiber photometry, we demonstrate that development of TD is not associated with sensitization of D2R signaling within the striatum. Rather, we provide data showing that increases in striatal dopamine predict the development of TD, and orofacial dyskinesia is driven by excessive activation of dMSNs within the ventrolateral portion of the striatum. Together, these results provide a new mechanism for the development of TD and identify a specific populations of cells for therapeutic targeting.

4.3 Results

4.3.1 A Mouse Model of TD Recreates Key Disease Features.

We first validated a mouse model of tardive dyskinesia (TD) that recapitulates core features of the disease. We sought a model that develops orofacial dyskinesia (1) similar to that observed in patients, (2) in response to chronic, but not acute administration of antipsychotic medication, and (3) which persists even after antipsychotic medication is stopped. To achieve these criteria, we adapted a protocol (Crowley et al., 2012) in which mice were implanted with slow-release haloperidol pellets (sq., 5 mg over 60 days) and scored them for vacuous chewing movements (VCMs), spontaneous separations of the upper and lower jaws used as a proxy for the orofacial dyskinesia observed in patients (Figure 4.1A-C). Healthy mice showed low VCM rates (Figure 4.1D, 2.27±0.43 per 5 minutes) that were decreased by acute haloperidol (1 mg/kg) administration (Figure 4.1D, 0.47±0.18 per 5 minutes), likely due to the overall reduction and slowing of movement seen caused by the drug (Kharkwal et al., 2016). However, from 21-60 days of chronic haloperidol treatment, VCM rates increased compared to control and baseline levels (Figure 4.1E, F, ctrl=1.78±0.32 hal=4.8±0.56), and persisted weeks after treatment cessation (Figure 4.1E, F, ctrl=1.73±0.25 hal=5.96±0.70). Together, these results demonstrate that the chronic haloperidol mouse model recapitulates key clinical features of TD.

4.3.2 D2R Hypersensitivity on iMSNs is Not Required for Development of TD

We next investigated the cellular mechanisms that might underlie the development and expression of orofacial movements in the mouse model of TD. Prevailing hypotheses posit that TD results from hypersensitivity of D2 dopamine receptors (D2Rs) on striatal iMSNs, leading to reduced iMSN output that causes disinhibited movements. To test this hypothesis, we assessed the sensitivity of iMSNs to dopamine signaling at D2R by measuring potassium currents through G-protein-linked inwardly rectifying potassium channels (GIRKs). GIRKs are downstream of

D2R/Gi signaling in many cell types (Marcott et al., 2014). We overexpressed GIRKs (AAV1-Syn-GIRK-A2-mCherry) in control and haloperidol-treated D2R^{GFP} mice (Figure 4.2A, B), and targeted iMSNs for whole-cell recordings in *ex vivo* brain slices of the ventrolateral striatum a region known to receive orofacial motor input (Chen et al., 2021). This approach allowed us to measure relative D2R sensitivity on iMSNs by comparing inhibitory postsynaptic currents (IPSCs) induced by varying concentrations of dopamine (0, 3, 10, 100 μM) to responses at a maximal dose (200 uM, Figure 4.2C,D). The prevailing hypothesis would predict a higher sensitivity to dopamine in iMSNs from haloperidol-treated mice, but we did not observe a difference in the normalized response between control and haloperidol-treated animals to either 3 μM (ctrl=24.7±14.7% hal=51.8±17.7%) and 10 μM dopamine (Figure 4.2C-E, ctrl=45.1±7.0% pA hal=36.6±7.0%). We next tested whether bath application of dopamine could occlude the response to electrically-evoked dopamine release, and whether this differed between control and haloperidol-treated mice. Once again, we found no evidence of sensitization, with reduce effects of dopamine on IPSC amplitudes in haloperidol-treated mice (3 μM=100.5±6.0%, 10uM=52.7±13.8%) than control animals (Figure 4.2H, 3 μM=50.2±9.8%, 10uM=24.1±10.9%). Combined, these suggest that chronic haloperidol does not induce functional sensitization of D2Rs in either striatal iMSNs.

Although we could not detect functional sensitization of D2R signaling in *ex vivo* brain slices, sensitization could still take place *in vivo* and contribute to the development of TD. To address this possibility, we conditionally deleted D2Rs from iMSNs by breeding D2R$^{f/f}$ x A2a$^{Cre/-}$ mice (iMSN-D2R-KO) and monitored the development of VCMs over the course of chronic haloperidol treatment (Figure 4.3A). As expected, wild-type littermates developed increased VCMs (6.1±1.0) compared to their own pretreatment levels (1.7±0.5) and sham-treated animals (1.8±6.1), which persisted after drug discontinuation (Figure 4.3B-C). Surprisingly, chronic haloperidol treatment *also* increased VCMs in iMSN-D2R-KO mice (9.1±1.4) compared to their own baseline (2.1±0.5) levels and those seen in sham-treated animals (1.4±0.3) (Figure 4.3D-E). To confirm that D2R signaling was eliminated from iMSNs in these animals, we measured

160

electrically evoked dopamine-IPSCs in iMSN-D2R-KO mice and wild type littermates, using the GIRK approach described above. While electrically-evoked D2R IPSCs were detectable in the majority of iMSNs from WT mice (n=16/20, N=4), they were almost entirely absent in iMSN-D2R-KO animals (n=1/20, N=4, Figure 4.3F-G). Furthermore, whereas haloperidol acutely lowered reduced average velocity in the open field in wild type mice, iMSN-D2R-KO showed reduced locomotion at baseline and occlusion of haloperidol's acute effect on locomotion (Figure 4.3H). Taken together, these data indicate that D2R sensitization of iMSNs is not present, nor are iMSN D2R required for development of orofacial movements in the mouse model of TD.

4.3.3 D2R Sensitization on Other Striatal Cells is Not Required for Development of TD

Though our evidence suggested that D2R on iMSNs do not play a key role in the development of TD in the mouse model, D2R are expressed on other striatal circuit elements, including cholinergic interneurons and dopamine terminals (Soares-Cunha et al., 2016). Indeed, the D2R hypersensitivity hypothesis is largely based on biochemical and imaging studies reflecting overall striatal D2R receptor expression levels (Burt et al., 1977; Savasta et al., 1988; Rogue et al., 1991; Lévesque et al., 1995; D'Souza et al., 1997; Florijn et al., 1997; Remington and Kapur, 1999; Kapur et al., 2000), which are likely to include D2R expressed on these other cell types. We thus tested whether D2R receptors on these cell types are necessary for the development of VCMs by treating ChAT[Cre]xD2R[f/f] (ChAT-D2R-KO) and DAT[Cre]xD2R[f/f] (DAT-D2R-KO) animals with chronic haloperidol (Figure 4S1A). We observed no difference in the development of VCMs in either ChAT-D2R-KO (Sham=2.0±0.1, Hal =5.6±1.3) or DAT-D2R-KO (Sham=1.0±0.5, Hal=5.0±0.6) compared to wild type animals treated with haloperidol (Sham =1.2±0.2 and 1.7±0.2 , Hal=5.5±1.0 and 4.2±0.3, respectively, Figure 4S1A,C,E,G), nor in their persistence following drug washout (Figure 4S1B,D,F,H). These results indicate that D2R in three key striatal cell types (iMSNs, dopamine neurons, and cholinergic interneurons) are not necessary for the development of TD.

4.3.4 Excitability of iMSNs and dMSNs Is Reduced by Chronic Haloperidol Treatment

While we did not detect sensitization of D2Rs on iMSNs in response to chronic haloperidol treatment, it remained possible that the excitability of striatal iMSNs and dMSNs were altered to bias striatal output, resulting in excessive and/or involuntary movement. To address this possibility, we used whole-cell *ex vivo* slice recordings to assess the intrinsic excitability of dMSNs and iMSNs from sham- and haloperidol-treated mice (Figure 4.4A). We used D2-GFP mice (Gong et al., 2003) in order to target dMSNs (GFP negative) or iMSNs (GFP positive) from the same region of the VLS. To isolate the physiological correlates of VCMs from the acute effects of haloperidol on cellular properties, we performed these recordings x-y weeks after treatment ended, when haloperidol has washed out of the system, but VCMs persist. We found that that chronic haloperidol treatment led to a reduction in intrinsic excitability of dMSNs (Figure 4.4B, D). While no difference was observed in the input resistance (Sham=71.4±10.6, Hal=62.9±12.0 MΩ) or resting membrane potential (Sham=-90.8±1.3, Hal=-89.6±1.5 mV, Figure 4.4E-F), we observed a trending increase in the rheobase (Sham=630±49.0, Hal=813±101 pA, Figure 4.4G). A similar reduction in intrinsic excitability was observed in iMSNs from haloperidol-treated mice compared to sham controls (Figure 4.4C, H). Again, we found no difference in input resistance Sham=119.4±13.3, Hal=94.9±18.0 MΩ) or resting membrane potential (Sham=-88.0±1.4, Hal=-88.2±1.3 mV, Figure 4.4I-J), but again a trending increase in rheobase (Sham=330±20.0, Hal=386±37 pA, Figure 4.4K). The comparable decrease in intrinsic excitability across both pathways suggests TD does not result from an overall imbalance of dMSN and iMSN excitability.

4.3.5 Increases in Striatal Dopamine Predict Dyskinesia Severity

Given the lack of evidence for involvement of D2R sensitization in the development of TD, we next explored alternative mechanisms that may drive dyskinesia. Other forms of striatal-dependent dyskinesias have been linked to dopamine (Bastide et al., 2015; Hallett, 2015; Ribot et al., 2019). Moreover, ex vivo and anesthetized recordings suggest that while acute haloperidol

administration increases striatal dopamine, chronic treatment leads to an overall reduction (Lane and Blaha, 1987). It is currently unknown how chronic antipsychotic treatment changes dopamine release in awake, behaving animals and whether such changes might relate to TD development. To address this gap, we expressed the fluorescent dopamine sensor dLight1.1 in the lateral striatum of control animals and those treated chronically with haloperidol. We assessed fluorescent signals as well as behavioral outcomes, including VCMs (Figure 4.5A and Figure 4S2A-B). We first validated that dLight fluorescence scales with dopamine release in *ex vivo* striatal slices (Figure 4S2C). Consistent with published work using fast-scan cyclic voltammetry to measure dopamine release (Bergstrom, 2012), we observed that acute haloperidol increased dLight signal across several measures (Figure 4S2E-I), including transient frequency (Mean $\Delta=0.21\pm0.02$, Figure 4S2G), transient amplitude (Mean $\Delta=0.29\pm0.04\%$ $\Delta F/F$, Figure 4S2H), and overall fluorescence (Mean $\Delta=4.42\pm0.49\%$ $\Delta F/F$, Figure 4S2F, I). Despite this dramatic increase in striatal dopamine, acute haloperidol did not increase VCMs (Pre= 2.8 ± 0.8, Post=2.9 ± 0.9, Figure 4S2J). In response to chronic treatment, as in previous cohorts, mice developed a persistent increase in VCMs (13.3 ± 1.6) compared to sham-treated animals (6.2 ± 1.8, Figure 4.5B,C). In parallel, the frequency of dopamine transients was increased in haloperidol-treated (0.65 ± 0.05 Hz) as compared to sham-treated mice (0.38 ± 0.05 Hz, Figure 4.5D-E). No difference in dopamine transient amplitude was detected between sham ($2.6\pm0.1\%$ $\Delta F/F$) and haloperidol-treated animals ($2.8\pm0.001\%$ $\Delta F/F$, Figure 4.5F-G).

Both acute and chronic haloperidol increased a measure of striatal dopamine *in vivo*, but did only chronic haloperidol led to increased VCMs. This observation suggests that transiently increased striatal dopamine alone is not sufficient to drive orofacial movements. However, chronic elevations in striatal dopamine may promote development of TD, and acute elevations may relate to this vulnerability. We tested whether haloperidol-induced changes in striatal dopamine, on both chronic and acute timescales, might predict the development of VCMs over time. Indeed, we found that average dopamine transient frequency in individual animals predicted average VCM

rates across weeks (Figure 4.5H). Furthermore, we found that increases in dopamine in response to acute administration of haloperidol (prior to chronic treatment) also predicted VCM rates months later (Figure 4.5I). Thus, while transient increases in striatal dopamine may not be sufficient to drive orofacial dyskinesia, they are a strong correlate of the development of TD during chronic haloperidol treatment.

4.3.6 Reductions in Dopamine Reduce Dyskinesia Severity

Given the correlation between striatal dopamine and development of VCMs, we next asked whether reducing dopamine levels would alleviate VCM severity. Mice expressing dLight1.1 in the ventrolateral striatum were acutely administered tetrabenazine (10 mg/kg), a VMAT2 inhibitor known to deplete synaptic dopamine (Roberts et al., 1986; Grigoriadis et al., 2017). Previous *ex vivo* studies using fast-scan cyclic voltammetry have shown that tetrabenazine reduces striatal dopamine release (Reches et al., 1983), but this drug has not been administered while measuring striatal dopamine in freely-moving animals. We observed a reduction in average dopamine levels (Figure 4.6A-B, Mean=-2.7±0.1% $\Delta F/F$) transient frequency (Figure 4.6C, Mean= Mean=-.15±0.02 Hz), and transient amplitude (Figure 4.6D, Mean=0.19±0.01% $\Delta F/F$) in response to tetrabenazine treatment. Furthermore, we found that tetrabenazine reduced VCM frequency (Figure 4.6E, Pre=7.4±1.9 Post=3.0±1.1), indicating that reductions in dopamine are sufficient to ameliorate VCM severity. These data suggest that elevated striatal dopamine may in part drive expression of VCMs.

4.3.7 Activation of dMSNs in the Ventrolateral Striatum Drives Orofacial Dyskinesia

The involuntary movements of TD are often restricted to the face and upper extremities. One explanation for this phenomenon, given the somatotopic mapping of sensorimotor information within the striatum (Hintiryan et al., 2016), is that the orofacial movements of TD involve striatal neurons within an anatomically defined subregion. Based on recent work studying

licking movements, we suspected the ventrolateral striatum (VLS) might contain MSNs involved in driving orofacial movements similar to those seen in TD (Chen et al., 2021; Hintiryan et al., 2016). To test this possibility, we injected Cre-dependent channelrhodopsin (AAV-DIO-ChR2-eYFP) in the VLS (Figure 4.7A-B) or dorsomedial striatum (DMS, Figure 4.7E-F) of D1[Cre] mice, then scored them in the open field for changes in VCMs and general location. We found that bilateral, continuous stimulation of VLS dMSNs (30 sec, 1 mW) induced immediate and robust VCMs (OFF=1.0±0.2, ON=56±0.5, Figure 4.7C), but no change in overall movement velocity (OFF=2.8±1.1 cm/s, ON=1.3±0.01 cm/s, Figure 4.7D). Conversely, stimulation of DMS dMSNs did not increase VCMs (OFF=0.8±0.1, ON=1.0±0.3, Figure 4.7G), but did increase movement velocity (OFF=2.0±0.6, ON=3.5±0.6 cm/s, Figure 4.76H). These data indicate that activation of dMSNs in the ventrolateral striatum is sufficient to induce VCMs and points to a striatal subpopulation that could drive the orofacial movements of tardive dyskinesia.

4.4 Discussion

Here, we attempt to identify the structures, cell types, and patterns of activity involved in the development of TD. Contrary to prevailing hypotheses, we find that TD does not result from increased dopaminergic signalling at D2Rs on iMSNs. Instead, we find that chronic haloperidol treatment increases striatal dopamine in a manner that is predictive of TD severity. Furthermore, we demonstrate that activating dMSNs in the ventrolateral striatum is sufficient to drive orofacial movements qualitatively similar to those observed with chronic haloperidol treatment. Together, these findings point towards hyperdopaminergic signaling onto ventrolateral dMSNs as a potential underlying cause of TD.

The hypothesis that TD results from sensitization of striatal D2Rs initially arose from clinical observations. Discontinuation of antipsychotic treatment was observed to acutely exacerbate involuntary movements in some patients, while increasing the dose or switching to a more potent D2R antagonist provided temporary relief (Marsden and Jenner, 1980; Peralta and Cuesta, 2010; Peralta et al., 2010). Consistent with clinical observation, antipsychotic treatment in rodents was shown to upregulate D2R express within the striatum (Burt et al., 1977; Savasta et al., 1988; Rogue et al., 1991; Lévesque et al., 1995; D'Souza et al., 1997; Florijn et al., 1997). However, studies in post-mortem tissue from rodents and patients also demonstrated that D2R levels return to baseline once treatment is discontinued (Blin et al., 1989; Reynolds et al., 1992), despite persistent orofacial dyskinesia. Our finding that deletion of D2Rs from iMSNs, dopaminergic terminals, and cholinergic interneurons fails to prevent the development of VCMs indicates that upregulation of D2Rs within the striatum is not required for development or expression of TD. However, blockade of D2Rs may still play a role in TD. Previous work revealed that chronic haloperidol or deletion of D2Rs from iMSNs induces aberrant striatal plasticity in which LTD is converted to LTP (Centonze et al., 2004). Additionally, one outstanding question not addressed here is whether TD results from disruption of D2R signaling in a single population or whether multiple populations play a role. Our observation that deletion of D2Rs from any one

population failed to increase VCMs on its own suggests that blockade on multiple subpopulations may be required for development of TD.

The hyper-dopaminergic hypothesis of schizophrenia posits that the disease results from excessive dopamine signaling and that antipsychotic medications alleviate positive symptoms through blockade of dopamine signaling. The reality is likely far more complex, as studies of how antipsychotics affect dopamine transmission have been variable. Studies in anesthetized rodents suggest that while acute haloperidol administration increases striatal dopamine, chronic treatment leads to an overall reduction (Lane and Blaha, 1987; See, 1991; Moore et al., 1998). In awake and freely behaving mice, we find that acute and chronic haloperidol treatment increase dopamine, with the latter being persistent after drug withdrawal. In addition to the added component of behavior, one explanation for the difference in our observation from previous ones may be that our approach integrates not just the release probability of dopamine, but also the pattern of dopamine signaling over time. Higher rates of dopamine transients could raise overall dopamine levels while leaving terminals partially depleted, resulting in reduced evoked dopamine. Further mechanistic study is needed in combination with *in vivo* measurements to test this hypothesis.

We also find that changes in dopamine in response to acute or chronic haloperidol are highly predictive of the development of VCMs. In combination with our finding that activation of ventrolateral dMSNs is sufficient to drive orofacial movements, this result suggests that such movements may arise as a result of excessive dopaminergic signaling onto dMSNs. Our preliminary results suggest that excitability of dMSNs is reduced with chronic haloperidol treatment, which is inconsistent with this hypothesis. However, these *ex vivo* experiments do not integrate the instantaneous effect of dopamine, which has been shown to rapidly modulate dMSN excitability (Lahiri and Bevan, 2020). Likewise, changes in excitability do not integrate how alterations in glutamatergic signaling (a key driver of MSN firing) might affect firing rates in vivo. Studies currently in progress aim at identifying how the activity of dMSNs and iMNs changes in

response to haloperidol treatment and the development of TD. Indeed, understanding the cellular and circuit mechanisms of TD will require additional studies that directly link behavior with alterations in neural signaling and activity.

4.5 Experimental Procedures

Animals: Adult mice of either sex (age >6 weeks) from six transgenic lines were used in this study. For conditional knockout of D2R receptor expression from specific cell types, Drd2$^{loxP/loxP}$ mice were crossed initially to either A2A$^{Cre/-}$, ChAT$^{Cre/-}$, or DAT$^{Cre/-}$ mice to create F1 breeders that were heterozygous for each transgene (e.g. A2A$^{Cre/-}$: Drd2$^{loxP/-}$). F1 breeders were then crossed to unrelated Drd2$^{loxP/loxP}$ mice to generate F2 conditional knockout animals or littermate controls for experimentation (e.g. A2A$^{Cre/-}$: Drd2$^{loxP/loxP}$ or Drd2$^{loxP/loxP}$). Mice were considered wildtype if they lacked Cre expression. A2A$^{Cre/-}$ mice were used alongside D1$^{Cre/-}$ mice for calcium imaging in indirect and direct pathway MSNs, respectively. Drd2$^{eGFP/-}$ mice were used for identification of direct and indirect pathway neurons in slice. All animals were housed 1-5 per cage and maintained on a 12 hr light/dark cycle with food and water provided *ad libitum*. All experimental procedures were carried out with the approval of the Institutional Animal Care and Use Committee at the University of California, San Francisco and complied with the local and national ethical and legal regulations regarding research using mice.

Surgical Procedures: In all procedures, mice were anesthetized with an intraperitoneal injection of ketamine-xylazine (15-30 mg total dose) and placed in a stereotaxic frame (Kopf Instruments). Anesthesia was then maintained using isoflurane (1 %, inhaled). For measurement of GIRK-mediated IPSCs, a stereotax-mounted drill was used to create bilateral burr holes above the striatum. A 33 gauge blunt needle was then slowly inserted at each site and 500 nL of AAV9-hSyn-TdTomato-T2A-mGIRK2-1-A22A-WPRE-bGH(Marcott et al., 2014; Silm et al., 2019) (diluted 1:3 with sterile saline, courtesy of Chris Ford and Robert Edwards) injected at 50 nL/min using a Hamilton Microinjector at the following coordinates (from Bregma in mm): (AP: +0.25 ML: ±2.7 DV: -3.3). Needles were left in place for 5 min post injection and slowly removed before the scalp was sutured.

For photometry recordings of striatal dopamine, 500 nL of AAV5-CAG-dLight1.1 (diluted 1:3, Addgene) was injected at 50 nL/min using a Micro4 injector (World Precision Instruments) and 33 gauge blunt needle at the following coordinates (from Bregma in mm): (DLS: AP: +0.8 ML: -2.1 DV: -2.4, VLS: AP: +0.25 ML: -2.5 DV: -3.5). The needle was left in place for 10 min, then slowly withdrawn. Afterwards, the surface of the skull was scored with a scalpel and covered with dental cement (Metabond). A 400 µm silica/polymer fiber-optic cannula (3-5mm in length, Doric Lenses) was then was lowered 0.2 mm above the viral injection site at a rate of 0.1 mm/min. A 4 pin (2x2) female Mill-Max connector coated in dental cement was placed over the contralateral hemisphere for selfie-cam attachment. Both the connector and optical fiber were then secured to the skull using dental acrylic (Ortho-Jet). The scalp was then sutured around the implant and the animal allowed to recover from anesthesia.

Implants for photometry recordings of calcium activity in dMSNs and iMSNs were performed as described above. 300 nL of AAV1-Syn-Flex-GCAMP6s-WPRE-SV40 (diluted 1:8 in sterile saline, Addgene) was injected at 50 nL/min into the striatum of A2aCre or D1Cre at the following coordinates (mm from Bregma): (AP: +0.25 ML: -2.8 DV: -3.5).

For optogenetic activation of MSNs, 500 nL of AAV5-EF1a-DIO-hChR2(H134R)-eYFP-WPRE-hGH (Addgene) was injected bilaterally as described above at the following coordinates (mm from Bregma): (DMS: AP: +0.25 ML: ±1.5 DV: -2.3, VLS: AP: +0.25 ML: ±2.7 DV: -3.3). Hand-made 200 µm optical fiber-ceramic ferrule assemblies (components, Thor Labs) were then implanted 0.1mm above the injection site and secured using dental cement and dental acrylic.

For chronic haloperidol treatment, slow-release haloperidol pellets (5 mg, 60 day, Innovative Research of America) were implanted subcutaneously between the shoulder blades. After anesthesia was induced, a small incision (~7 mm) was made posterior to the shoulders. A small subcutaneous pocket was created by gently inserting and opening scissors through the incision. Forceps were used to insert a pellet ~10 mm above the incision, which was then sutured and covered with surgical glue. For sham implants, forceps were inserted, but no pellet was

implanted. Mice were then singly housed and kept on a heating pad daily for 7-10 days until the incision site was fully healed.

Slice Electrophysiology: Mice were deeply anesthetized with ketamine-xylazine (100-200 mg total dose, IP) and perfused with a carbogenated slicing solution containing (in mM): 250 glycerol, 2.5 KCl, 1.2 NaH_2PO_4, 10 HEPES, 21 $NaHCO_3$, 5 D-glucose, 2 $MgCl_2$, 2 $CaCl_2$. Next, animals were decapitated and the brain dissected, mounted on a chuck, and sliced in ice-cold slicing solution. Serial 275 µm coronal slices of striatum were then cut using a vibrating microtome (Leica) and transferred to warm (34°C) artificial cerebrospinal fluid (ACSF) containing (in mM): 125 NaCl, 26 $NaHCO_3$, 2.5 KCl, 1.25 NaH_2PO_4, 12.5 D-glucose, 1 $MgCl_2$, 2 $CaCl_2$. Slices were incubated for 30-50 min and subsequently kept at room temperature (~23°C) for 2-8 hours.

During recordings, slices were continually superfused with carbogenated ACSF at 30-33°C. Differential interference contrast optics on an Olympus BX51WI microscope with a 40x immersion objective lens were used to target neurons for whole-cell patch recordings using borosilicate glass electrodes (2-5MΩ). Pipette internal solution contained the following (in mM): 115 K-methylsulfonate, 20 NaCl, 1.5 MgCl2, 10 HEPES(K), 10 BAPTA-tetrapotassium, ATP, GTP, and phosphocreatine (pH 7.4, ~275 mOsm). For cell-filling and morphological reconstruction of recorded cells, 1 mg/mL biocytin (Sigma) was also added to the internal solution.

For experiments measuring GIRK-mediated IPSCs, D2R-mediated signaling was isolated by including the following antagonists to the ACSF (in µM): 0.3 CPG 35348, DhβE, 5 NBQX, 10 nomifensine, 50 picrotoxin, 1 SCH 23390, and 0.2 scopolamine. GIRK[+] iMSNs were identified using GFP (473) and TxRed (562 nm) filters (Chroma) and held at -70 mV. GIRK-mediated IPSCs were evoked using an A365 stimulus isolator (World Precision Instruments), and a monopolar glass stimulating electrode placed within the field of view to deliver a single 60-70 µA pulse of 300 µsec duration.

For measurement of intrinsic excitability, GIRK⁻ iMSNs and dMSNs were patched and held at -70mV for 5 minutes. Recordings were then switched to current clamp, and 550 msec square-wave current injections (-200pA to 2000 pA) were injected in 100 pA steps. Firing rate was calculated as the number of spikes over the duration of the current injection.

All recordings were conducted using a MultiClamp 700B amplifier (Molecular Devices) and digitized using an ITC-18 A/D board (HEKA). Igor Pro 6.0 software (Wavemetrics) and custom acquisition routines (mafPC, courtesy of M.A. Xu-Friedman) were used for acquisition. Both voltage clamp and current-clamp recordings were filtered at 5 kHz and digitized at 10 kHz.

Open field Behavior: To quantify the effect of manipulations on gross locomotion, mice were placed in a Plexiglas cylinder 25 cm in diameter and allowed to freely explore for 30 minutes. An overhead camera and Ethovision 10.0 software (Noldus) or DeepLabCut (Mathis et al., 2018) were used to track the animal's position and velocity. For acute pharmacological manipulations, an intraperitoneal injection was preceded by a 30 minute baseline and followed by 90 minutes of post-injection recording. Average baseline velocity was calculated from 0-25 minutes. Average post-injection velocity was calculated from 45-105 minutes.

Selfie-cam Recordings: High-resolution video of orofacial movements in freely behaving mice was achieved using methods adapted from (Meyer et al., 2018). In summary, a small head mount was implanted on the skull (see Surgical Procedures) on which a small arm made from 3D-printed parts could be connected for each behavioral session. The arm held a CMOS camera connected to a video cable, and was adjusted to point at the mouse's face. Briefly, a Raspberry Pi 4 Model B (4 Gb) and custom Python code were used to record video from a Raspberry Pi Spy Camera (Part: 1937, Raspberry Pi Foundation) and relay TTL pulses to data acquisition devices with the capture of each frame. The focal length of the CMOS camera was adjusted by unscrewing the outer lens. The camera was head-mounted using custom, 3D-printed plastic holder glued to a female 6 pin (3x2) Mill-Max connector. A male-male 4 pin (2x2) Mill-Max connector was used to

bridge the selfie-cam holder with skull-attached head mount. Mice were habituated to both the selfie-cam and optical cables for at least two 30 minute sessions prior to data acquisition.

Live Dyskinesia Scoring: Vacuous chewing movements (VCMs) were scored online using conventional methods or offline review of selfie-cam video (see below). For conventional scoring, 5 mice were placed in a 5 separate one liter glass beakers and allowed to habituate for 5-10 min. A rater blinded to genotype and drug treatment then scored VCMs in each mouse for 1 minute, and repeated this process 5 times, rating a total of 5 minutes per animal. An orofacial movement was counted as a single VCM if 1) the lower and upper jaws visibly separated, 2) nothing was visible in the mouth, 3) the event did not take place within 3 sec of grooming, 4) the event did not take place within 3 sec of licking the wall or floor of the beaker. Prior to data collection, all animals were habituated to glass beakers 2-3 times for 10-15 minutes each.

Offline Dyskinesia Scoring: For offline quantification of VCMs from selfie-cam recordings, videos were scored by a rater blinded to drug treatment. Raters used Behavioral Observation Research Interactive Software (BORIS) to mark individual VCM events and grooming bouts from 15 minutes of continuous video. An individual orofacial movement was considered a VCM using the same requirements as described for live scoring. To obtain precise timestamps of VCMs for alignment, Avidemux software was used to identify frames of peak jaw separation. Timestamps were then aligned to photometry signals using custom MatLab code.

Optogenetics: Mice were tethered bilaterally with optical patch cables (200 μm) and a selfie cam/video cable, then placed in the open field arena for 8 minute sessions. After a two-minute baseline period, mice received 30 seconds of continuous stimulation with 473 nm blue light (1 mW), followed by 30 seconds of no stimulation. After 3 more repetitions of stimulation, mice were left in the open field for an additional two minutes. Each animal underwent three sessions, during

which light stimulation was provided to the left, right, or bilateral striatum. Movement velocity was calculated using Ethovision 10.0 (Noldus) during stimulation on and off periods, while VCMs were scored by review of selfie-cam video. Changes in velocity were calculated from bilateral stimulation sessions.

Pharmacology: For acute administration, haloperidol (Sigma) was dissolved in glacial acetic acid and then added to 0.1 M sodium bicarbonate solution at concentration of 0.1mg/mL. Mice were administered 1.0 mg/kg IP injections, with 0.1 M sodium bicarbonate solution used as vehicle. Tetrabenazine (Tocris) was dissolved in a 20% DMSO, 10% Tween20, 70% normal saline solution at a concentration of 0.1mg/mL. Tetrabenazine was administered IP at 1 or 10 mg/kg. The same solution without tetrabenazine was used as vehicle.

Fiber Photometry: In vivo optical imaging of striatal dopamine and intracellular calcium was performed as described previously (Gunaydin et al., 2014) using an RZ5P fiber photometry processor (TDT) and Synapse software (TDT) that controlled a two-channel LED driver (Doric Lenses). The LED driver controlled 465 and 405 nm LEDs (DORIC) that were sinusoidally modulated at 210 and 330 Hz, respectively. Excitation and emission light were passed through a Fluorescence Mini Cube (Doric Lenses) and 400 μm fiber-optic cable with motorized commutation to the fiber optic cannula. Emitted μfluorescence was collected onto a Visible Femtowatt Photoreceiver Module (DC, low) at a sampling rate of ~1017 Hz.

All recordings took place in the open field (Plexiglas cylinder, 25 cm diameter). Prior to recording, mice were habituated with light pulses for 10 minutes to reduce further fiber bleaching. During recordings, video was recorded from three cameras: one above the arena (for gross locomotion and position, 20 Hz), one in front of the arena (for posture and rearing, 20 Hz), and a selfie-cam (for high resolution detection of orofacial movements, 90 Hz). Videos were

synchronized to photometry data using TTL-pulses delivered with each frame to the RZ5P fiber photometry processor and collected using Synapse software.

Histology: For validation of viral expression and fiber placement, animals were deeply anesthetized with ketamine-xylazine (100-200 mg, IP) and transcardially perfused with 4% paraformaldehyde (PFA) in PBS. Brains were then dissected and placed in 4% PFA at 4°C for 24 hours before transfer to a 30% sucrose solution. Coronal sections (35 µm) were prepared on a freezing microtome (Leica). Sections were washed 2-3 times and stored in PBS at 4°C before being mounted onto glass slides using a DAPI mounting medium (Vectashield). A Nikon 6D conventional wide-field microscope was used to take stitched multi-channel fluorescence images of whole brain sections at 4-10x.

Quantification and Statistical Analysis

Statistics: All data are presented as the mean ± SEM, with N referring to the number of animals and n to the number of cells. Statistical tests have not yet been applied as the predetermined n/N has not been reached in the majority of experiments.

Inclusion/exclusion Criteria: Fiber photometry experiments were included/excluded from analysis based on a fiber location and fluorescence signal. We set the minimum threshold for fluorescence signal detection based on photometry recordings from mice with no fluorophore expression. Mice were also excluded based on post-mortem histology if the fiber track or fluorophore expression were detected outside of the striatum.

For all experiments involving chronic haloperidol treatment, mice were excluded if the empty pellet could not be recovered at the time of sacrifice. A total of 2 animals were excluded for this reason.

Photometry Analysis: Photometry data was analyzed in Matlab using code provided by TDT and custom code. First, 465 nm and 405 nm signals were smoothed with a 200 msec window. Next, the 405 nm channel was fit linearly to the 465 nm using the first 30 minutes of the recordings session (full recording period for weekly sessions and baseline period for acute pharmacological experiments). The fitted 405 nm signal was then subtracted from 465 nm signal and the remainder divided by the average of the fitted 405 nm signal to obtain ΔF/F. All subsequent analyses were performed using the ΔF/F trace.

For detection of dLight1.1 and GCAMP6s transients, we used an amplitude threshold based on substituting the fitted 405 nm channel for the 465 nm channel to calculate ΔF/F. For each recording session from every animal, local minima and maxima were identified and the amplitude of all transient increases extracted. The 95% confidence interval of transient increases was used as a threshold for identifying transients in the ΔF/F trace. To validate this approach in dLight recordings, we compared the cumulative distribution functions of transient amplitudes for the 465 and 405 nm channels before and after acute administration of haloperidol. While no change was detected in the 405 nm channel, haloperidol caused a rightward shift in transient amplitude which was apparent even within the 95% confidence interval.

For individual sessions, the average transient amplitude was calculated as the mean of all transients detected above threshold. Transient frequency was calculated as the total number of identified transients over the analyzed time period.

Slice Analysis: Amplitude of GIRK-mediated currents were analyzed manually in Igor (Mathworks). For exogenous application of dopamine, holding potential was measured continuously every 10 seconds, and IPSC amplitude was calculated by subtracting the average holding in the 30 seconds prior to wash on from the peak holding current reached 2-5 minutes after wash on initiation. For intermediate doses, this value was then normalized to that of the subsequent IPSC in response to a maximal dopamine dose. Electrically evoked IPSCs were also

quantified manually by measuring the change from ~10 milliseconds prior to stimulation to the peak of the IPSC. Amplitudes were normalized to the average IPSC amplitude prior to application of exogenous dopamine.

Intrinsic excitability was measured as the average instantaneous firing rate across spiking. Firing rates, resting membrane potential, and rheobase were all calculated using custom code in Igor. Input resistance was calculated manually using a -5 mV voltage step in current clamp and Ohm's Law.

4.6 Author Contributions and Acknowledgements

4.7 Figures

Figure 4.1: Chronic haloperidol treatment recapitulates key features of tardive dyskinesia in mice.
(A) Experimental timeline of chronic haloperidol treatment and behavioral quantification for a mouse model of tardive dyskinesia. **(B)** Example of mouse at with jaw at rest. **(C)** Example of mouse making a vacuous chewing movement (VCM). **(D)** Quantification of VCMs in wild type mice prior (Pre, grey circle, N=30) and after acute haloperidol (Acute Hal., purple circle, N=30). **(E)** Quantification of VCMs before (Pre), during, and after treatment with chronic haloperidol (purple circles, N=32-35) or sham surgery (black circles, N=29-34). **(F)** Summary of average VCMs in and sham-treated (black circles, N=39) and haloperidol treated (purple circles, N= 34) mice while on drug (weeks 3-7) and during washout (weeks 13-15). Data are presented as mean with individual data points or mean ± S.E.M.
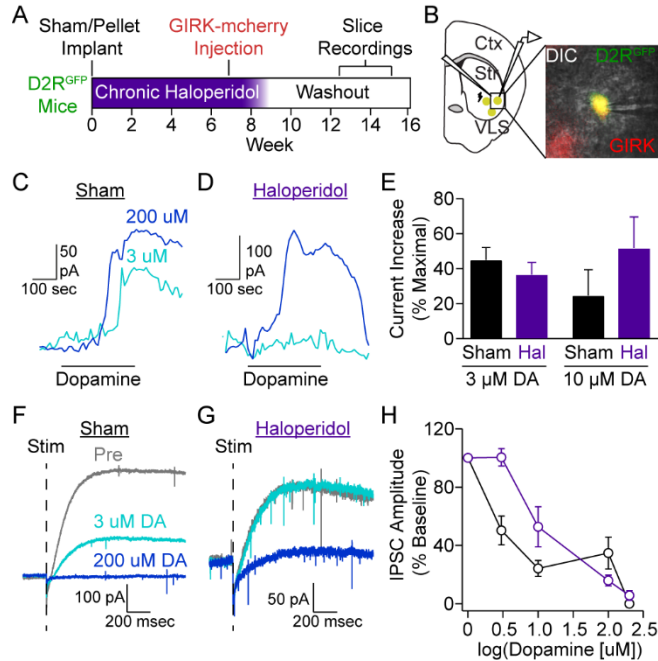
Figure 4.2: Chronic haloperidol treatment does not sensitize D2R signaling on striatal iMSNs or dopaminergic terminals. (A) Experimental timeline for determining how chronic haloperidol treatment effects D2R sensitivity in iMSNs and dopaminergic terminals. **(B)** Schematic and example image of slice recording from GIRK+ (red) and GFP+ (green) iMSNs during dopamine application and electrical stimulation. Double-positive cells show in yellow. **(C)** Example of GIRK-mediated IPSC from a sham-treated animal in response to 5 minute application of 3 μM (teal) and 200 μM (blue) dopamine. **(D)** Same as (C), but from an animal chronically treated with haloperidol. **(E)** Quantification of normalized peak IPSC amplitude in response to either 3 μM (left, n=3) or 10 μM (right, n=3) dopamine in either sham-treated (black, N=3) or haloperidol treated (purple, N=3) mice. Values were normalized to peak response at 200 μM dopamine. **(F)** Example of GIRK IPSC in response to electrically evoked dopamine at baseline (Pre, grey) and in the presence of 3 μM (teal) and 200 μM (blue) dopamine. **(G)** Same as (F), but from an animal chronically treated with haloperidol. **(H)** Quantification of normalized GIRK-mediated IPSC amplitude in the presence of 3, 10, 100, and 200 μM dopamine (n=2-3) for sham (black N=3) and haloperidol-treated (purple, N=3) mice. Data are presented as mean ± S.E.M.
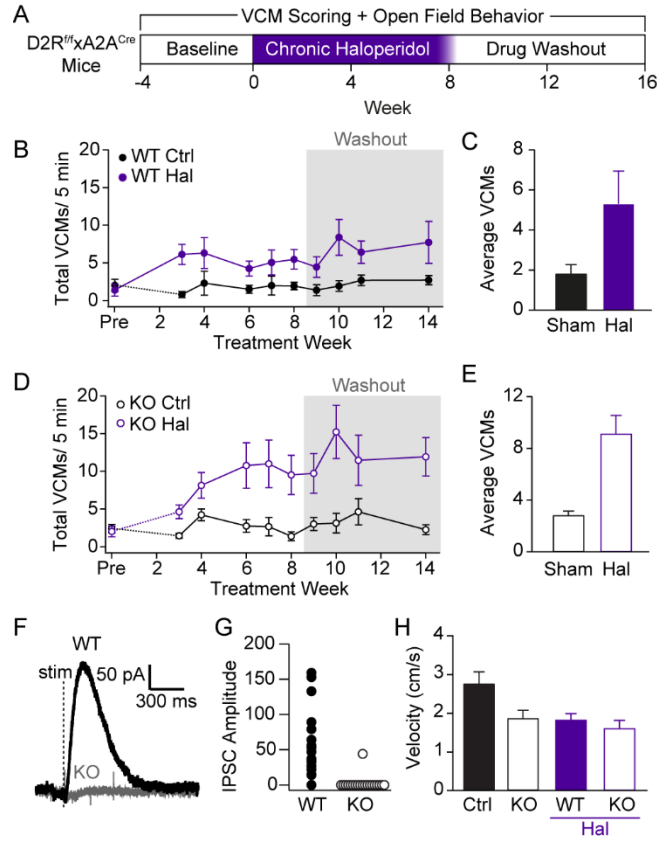
Figure 4.3: Knockout of D2Rs from striatal iMSNs does not prevent the development of VCMs in response to chronic haloperidol treatment. (A) Experimental timeline of haloperidol treatment and behavioral scoring in wild type and iMSN-D2R-KO mice. **(B)** Quantification of VCMs in sham (Ctrl, closed black N=16) or haloperidol-treated (Hal, closed purple N=15) wild type mice before (Pre), during haloperidol treatment (weeks 3-8), and after treatment (grey box, weeks 9-14). **(C)** Summary of average VCMs in sham and haloperidol-treated during washout (weeks 10-14). **(D)** Same as in (B), but for sham (Ctrl, open black, N=9) and haloperidol-treated (Hal, open purple, N=15) iMSN-D2R-KO mice. **(E)** Same as in (C) but for iMSN-D2R-KO mice. **(F)** Example traces of GIRK-mediated IPSC in response to electrically evoked dopamine in wild type (black) and iMSN-D2R-KO mice. **(G)** Quantification of IPSC amplitude in wild type (n=20, N=4) and iMSN-D2R-KO mice (n=20, N=4). **(H)** Average open field velocity in wild type (Ctrl N=13, WT Hal=15) and iMSN-D2R-KO (open bars, N=9 per group).
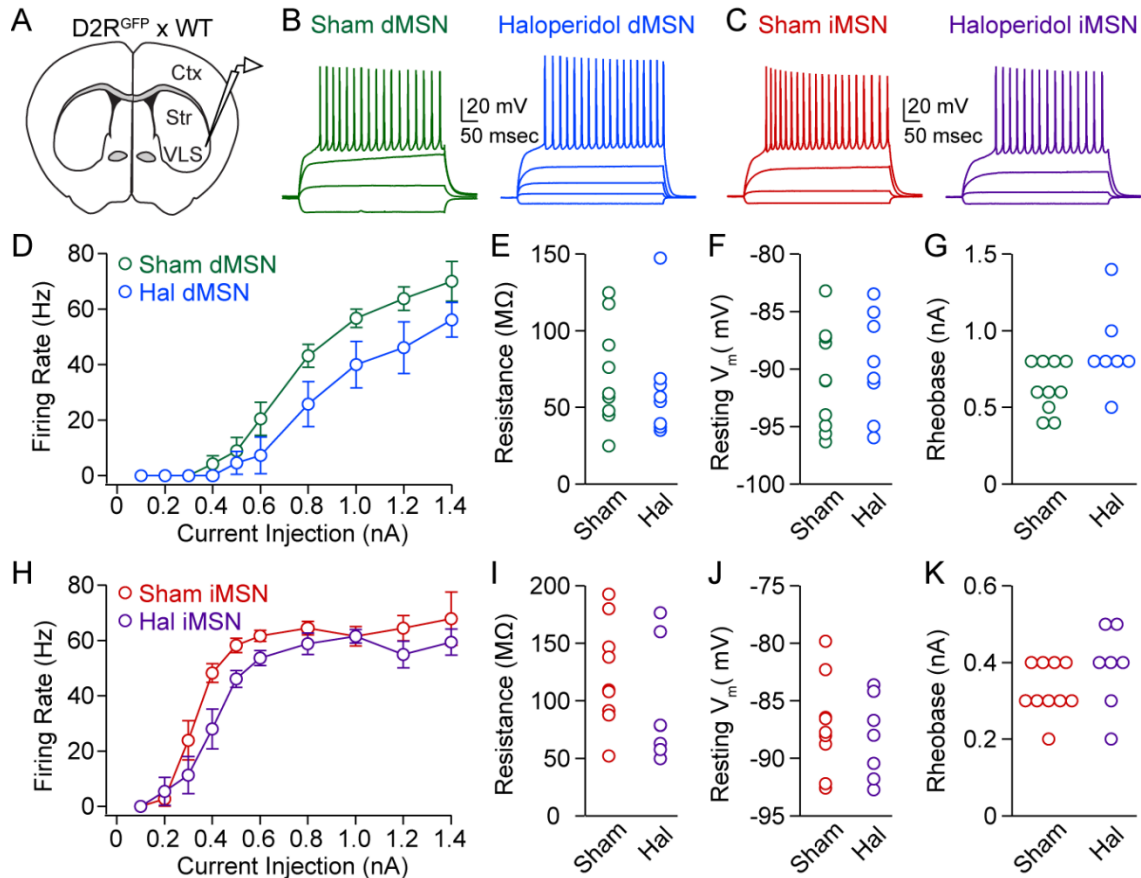
Figure 4.4: Chronic haloperidol treatment leads to persistent decreases in intrinsic excitability of direct and indirect pathway MSNs. (A) Schematic of slice configuration for recording intrinsic excitability of iMSNs and dMSNs from D2R^{GFP} mice receiving sham or chronic haloperidol treatment. **(B)** Examples of voltage changes and spiking in response to -100, 100, 300, and 500 pA current steps. dMSNs from sham and haloperidol-treated mice are shown in green and blue respectively. **(C)** Same as (B), but iMSNs from sham and haloperidol-treated mice as shown in red and purple, respectively. **(D)** Instantaneous firing rates of dMSNs in response to current injections of various amplitudes for sham (n=10, N=4) and haloperidol treated animals (n=6, N=4). **(E)** Input resistance for dMSNs from sham (n=10) and haloperidol-treated mice (n=8). **(F)** Resting membrane potential for dMSNs from sham (n=10) and haloperidol-treated mice (n=8). **(G)** Rheobase for dMSNs from sham (n=10) and haloperidol-treated mice (n=8). **(H)** Instantaneous firing rates of iMSNs in response to current injections of various amplitudes for sham (n=10, N=4) and haloperidol treated animals (n=7, N=4). **(I)** Input resistance for iMSNs from sham (n=10) and haloperidol-treated mice (n=8). **(J)** Resting membrane potential for iMSNs from sham and haloperidol-treated mice. **(K)** Rheobase for iMSNs from sham and haloperidol-treated mice.
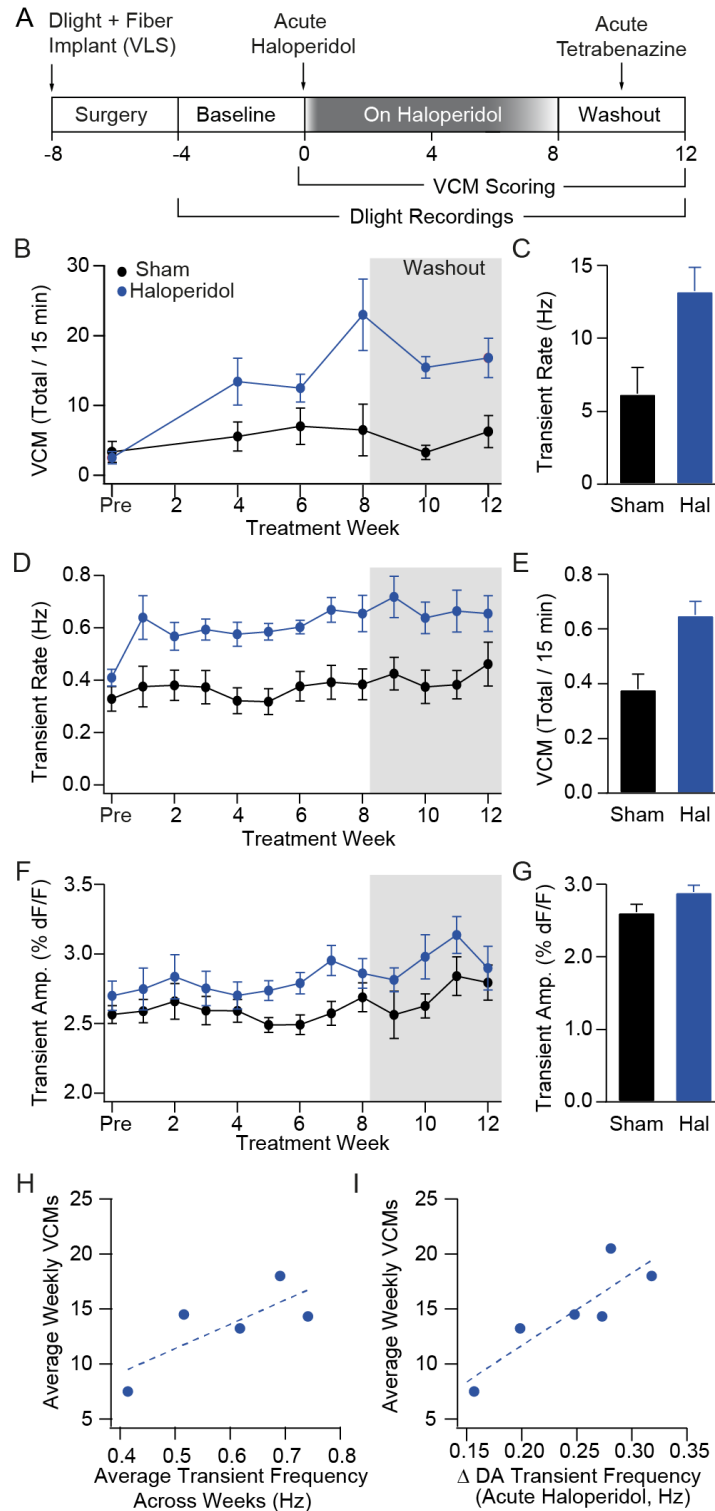
Figure 4.5: Striatal dopamine predicts the development of VCMs. (A) Experimental timeline for measuring dopamine changes in relation to TD. **(B)** Average VCM score across weeks for sham (black, N=6-7) and haloperidol-treated mice (blue, N=7-8). **(C)** Quantification of average VCMs during the washout period (weeks 10-12). **(D)** Average dopamine transient rate across weeks for sham and haloperidol-treated mice. **(E)** Quantification of average dopamine transients during the washout. **(F)** Average transient amplitude across weeks for sham and haloperidol-treated mice. **(G)** Quantification of average dopamine

transient amplitude during the washout period. **(H)** Correlation between average VCMs across weeks and average transient frequency for haloperidol treated mice. **(I)** Correlation between average VCMs across weeks and the change in transient rate in response to an initial acute dose of haloperidol.
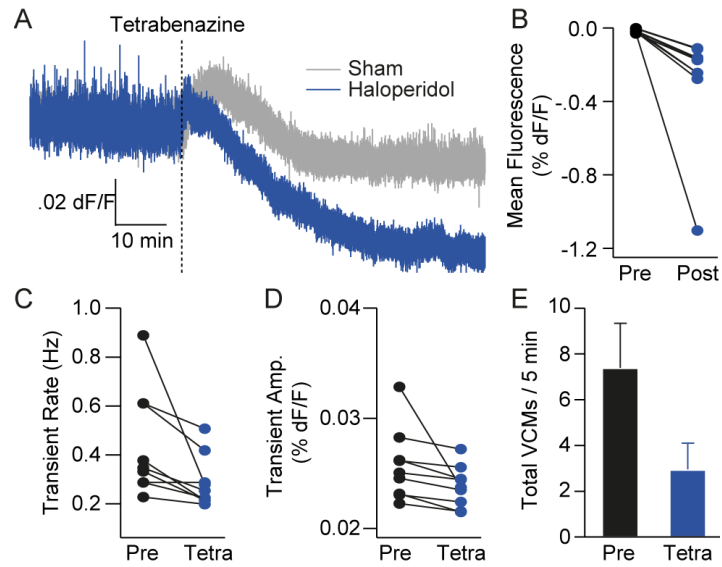
Figure 4.6: Tetrabenazine reduces striatal dopamine and VCMs. (A) Average traces of dLight1.1signal aligned to injection of tetrabenazine (10 mg/kg) for sham (grey, N=3) and haloperidol treated (blue, N=3) mice. **(B)** Change in overall dLight1.1 signal intensity from baseline (Pre) to 30-90 after injection of tetrabenazine (Post, N=9). **(C)** Change in dopamine transient rate following tetrabenazine for the same periods as described in (B). **(D)** Change in dopamine transient amplitude following tetrabenazine for the same periods as described in (B). **(E)** Total VCMs in mice treated with haloperidol before and after administration of tetrabenazine (N=10).
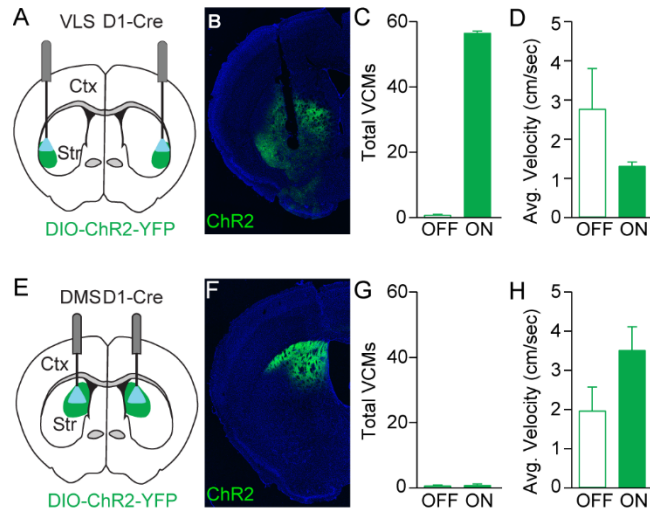
Figure 4.7: Activation of dMSN in the VLS, but not DMS, is sufficient to induce vacuous chewing movements. (A) Schematic of optogenetic targeting of dMSN in the VLS. **(B)** Example histology of ChR2 expression and fiber track in the VLS. **(C)** Total VCMs 30 seconds before (OFF) and during (ON) continuous dMSN stimulation in the VLS (N=3). **(D)** Average velocity during the same periods as described in (C). **(E)** Schematic of optogenetic targeting of dMSN in the DMS. **(F)** Example histology of ChR2 expression and fiber track in the DMS. **(G)** Total VCMs during the conditions as described in (C), but for continuous dMSN stimulation in the DMS (N=3). **(H)** Average velocity during the same periods as described in (C). All data are presented as the mean ± S.E.M.

4.8 Supplemental Figures
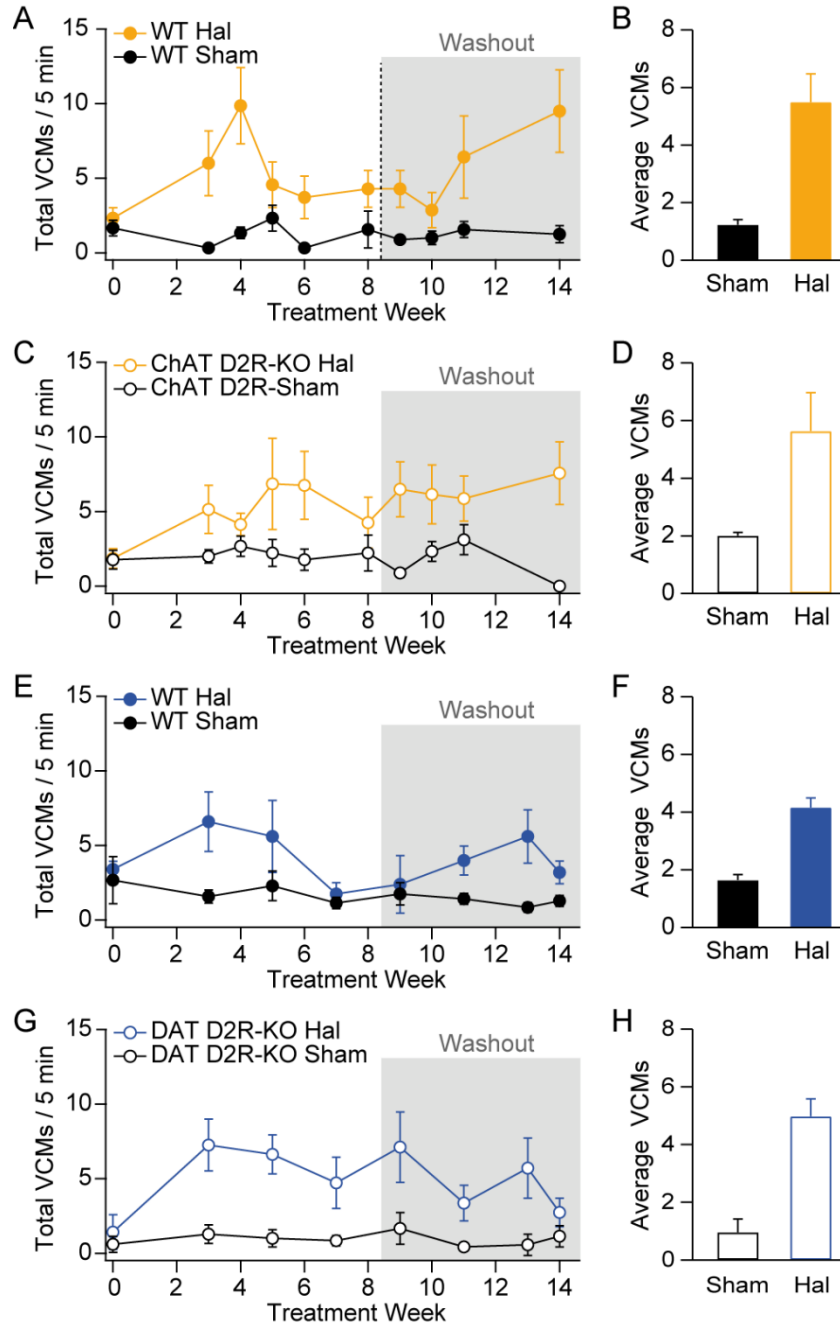
Supplemental Figure 4.1: Knockout of D2Rs from striatal iMSNs does not prevent the development of VCMs in response to chronic haloperidol treatment. (A) VCMs in sham (Sham, closed black N=9) and haloperidol-treated wild type mice (Hal, closed yellow N=7) before (week 0), during treatment (weeks 3-8), and during washout (weeks 10-14). **(B)** Summary of average VCMs in sham and haloperidol during the washout period. **(C)** Same as described in (A), but for sham (open black, N=9) and haloperidol treated (open yellow, N=8) ChAT-D2R-KO mice. **(D)** Summary of average VCMs in sham and haloperidol during the washout period for ChAT-D2R-KO mice. **(E)** Average VCMs in sham (Sham, closed black N=7) and haloperidol-treated wild type mice (Hal, closed blue N=4) across weeks. **(F)** Same as described in (B), but for comparison to DAT-D2R-KO mice. **(G)** Average VCMs in sham (Sham, closed black N=7) and haloperidol-treated DAT-D2R-KO mice (Hal, closed blue N=8) across weeks. **(H)** Summary of average VCMs in sham and haloperidol during the washout period for DAT-D2R-KO mice.
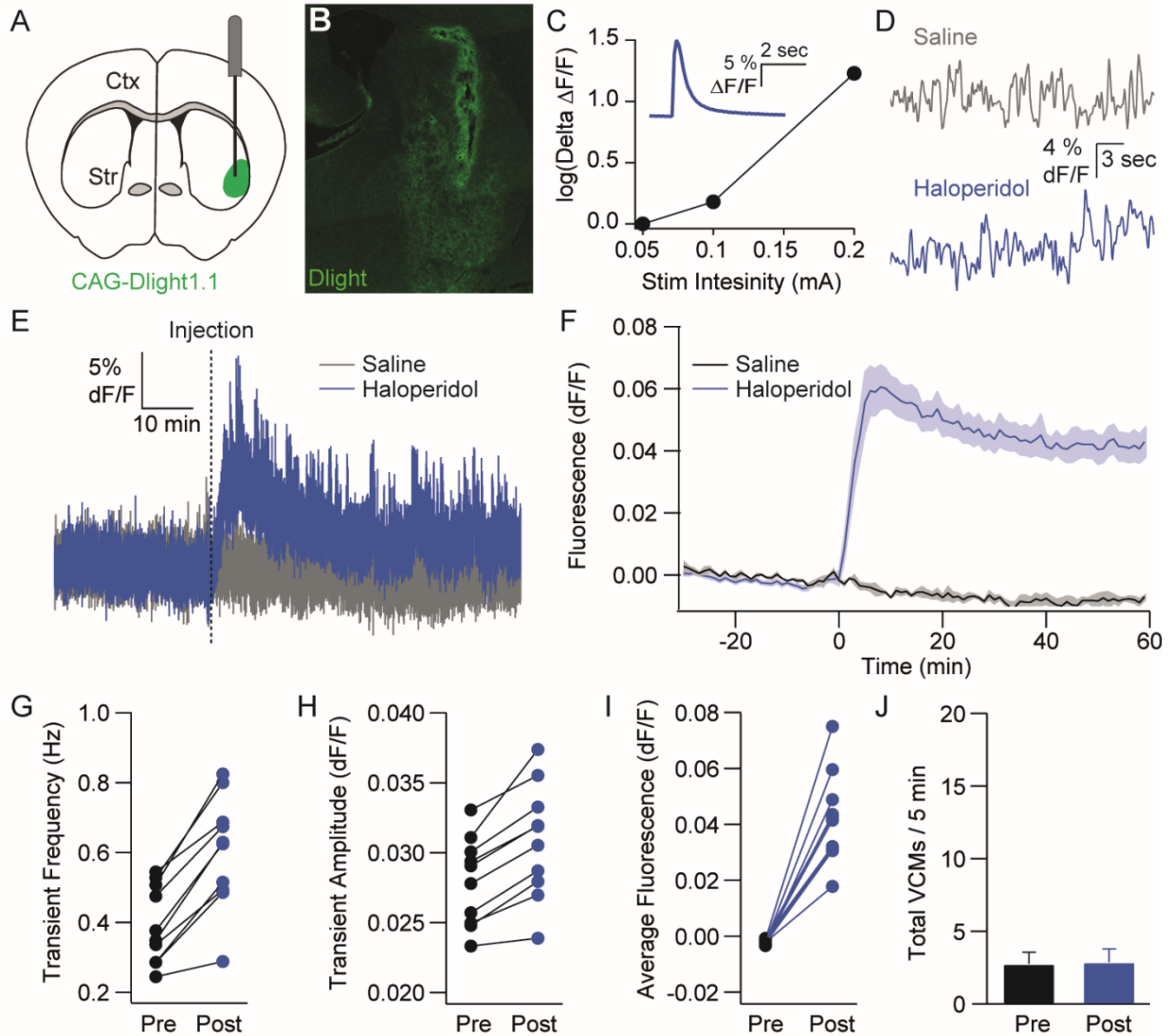
Supplemental Figure 4.2: Acute haloperidol administration increases striatal dopamine, but does not induce VCMs. (A) Schematic of dLight1.1 and fiber placement with the striatum. **(B)** Example histology of dLight expression and fiber track. **(C)** Example of increases in dLight signal intensity recording in slice in response to increases stimulation intensities. **(D)** Example of dLight signal using fiber photometry in mice injected I.P. with saline or haloperidol. **(E)** Example response of dLight signal in response to saline (grey) or haloperidol (blue) injection. **(F)** Summary of dLight signal change in response to saline or haloperidol N=10). **(G)** Dopamine transient frequency before (Pre, black) and after (Post, blue) haloperidol injection. **(H)** Dopamine transient amplitude before and after haloperidol injection. **(I)** Average dopamine signal intensity and after haloperidol injection. **(J)** VCMs before and after haloperidol injection (N=10). Data are presented as points for individual animals or the mean ± S.E.M.

4.9 References

Bachus, S.E., Yang, E., McCloskey, S.S., and Minton, J.N. (2012). Parallels between behavioral and neurochemical variability in the rat vacuous chewing movement model of tardive dyskinesia. Behav. Brain Res. *231*, 323–336.

Bastide, M.F., Meissner, W.G., Picconi, B., Fasano, S., Fernagut, P.-O., Feyder, M., Francardo, V., Alcacer, C., Ding, Y., Brambilla, R., et al. (2015). Pathophysiology of L-dopa-induced motor and non-motor complications in Parkinson's disease. Prog. Neurobiol. *132*, 96–168.

Bergstrom, B.P. (2012). Using In Vivo Voltammetry to Demonstrate Drug Action: A Student Laboratory Experience in Neurochemistry. J. Undergrad. Neurosci. Educ. *10*, A113–A117. Blin, J., Baron, J.C., Cambon, H., Bonnet, A.M., Dubois, B., Loc'h, C., Mazière, B., and Agid, Y. (1989). Striatal dopamine D2 receptors in tardive dyskinesia: PET study. J. Neurol. Neurosurg. Psychiatry *52*, 1248–1252.

Burt, D.R., Creese, I., and Snyder, S.H. (1977). Antischizophrenic drugs: chronic treatment elevates dopamine receptor binding in brain. Science *196*, 326–328.

Carbon, M., Hsieh, C.-H., Kane, J.M., and Correll, C.U. (2017). Tardive Dyskinesia Prevalence in the Period of Second-Generation Antipsychotic Use: A Meta-Analysis. J. Clin. Psychiatry *78*, 20738.

Caroff, S.N. (2019). Overcoming barriers to effective management of tardive dyskinesia. Neuropsychiatr. Dis. Treat. *15*, 785–794.

Caroff, S.N., Ungvari, G.S., and Cunningham Owens, D.G. (2018). Historical perspectives on tardive dyskinesia. J. Neurol. Sci. *389*, 4–9.

Centonze, D., Usiello, A., Costa, C., Picconi, B., Erbs, E., Bernardi, G., Borrelli, E., and Calabresi, P. (2004). Chronic haloperidol promotes corticostriatal long-term potentiation by targeting dopamine D2L receptors. J. Neurosci. Off. J. Soc. Neurosci. *24*, 8214–8222.

Chen, Z., Zhang, Z.-Y., Zhang, W., Xie, T., Li, Y., Xu, X.-H., and Yao, H. (2021). Direct and indirect

pathway neurons in ventrolateral striatum differentially regulate licking movement and nigral responses. Cell Rep. *37*, 109847.

Crane, G.E. (1973). Persistent dyskinesia. Br. J. Psychiatry J. Ment. Sci. *122*, 395–405.

Crowley, J.J., Kim, Y., Szatkiewicz, J.P., Pratt, A.L., Quackenbush, C.R., Adkins, D.E., van den Oord, E., Bogue, M.A., Yang, H., Wang, W., et al. (2012). Genome-wide association mapping of loci for antipsychotic-induced extrapyramidal symptoms in mice. Mamm. Genome Off. J. Int. Mamm. Genome Soc. *23*, 322–335.

Divac, N., Prostran, M., Jakovcevski, I., and Cerovac, N. (2014). Second-Generation Antipsychotics and Extrapyramidal Adverse Effects. BioMed Res. Int. *2014*, e656370.

D'Souza, U., McGuffin, P., and Buckland, P.R. (1997). Antipsychotic regulation of dopamine D1, D2 and D3 receptor mRNA. Neuropharmacology *36*, 1689–1696.

Factor, S.A., Burkhard, P.R., Caroff, S., Friedman, J.H., Marras, C., Tinazzi, M., and Comella, C.L. (2019). Recent developments in drug-induced movement disorders: a mixed picture. Lancet Neurol. *18*, 880–890.

Florijn, W.J., Tarazi, F.I., and Creese, I. (1997). Dopamine receptor subtypes: differential regulation after 8 months treatment with antipsychotic drugs. J. Pharmacol. Exp. Ther. *280*, 561–569.

Gerfen, C.R., Engber, T.M., Mahan, L.C., Susel, Z., Chase, T.N., Monsma, F.J., and Sibley, D.R. (1990). D1 and D2 dopamine receptor-regulated gene expression of striatonigral and striatopallidal neurons. Science *250*, 1429–1432.

Gong, S., Zheng, C., Doughty, M.L., Losos, K., Didkovsky, N., Schambra, U.B., Nowak, N.J., Joyner, A., Leblanc, G., Hatten, M.E., et al. (2003). A gene expression atlas of the central nervous system based on bacterial artificial chromosomes. Nature *425*, 917–925.

Grigoriadis, D.E., Smith, E., Hoare, S.R.J., Madan, A., and Bozigian, H. (2017). Pharmacologic Characterization of Valbenazine (NBI-98854) and Its Metabolites. J. Pharmacol. Exp. Ther. *361*, 454–461.

Gunaydin, L.A., Grosenick, L., Finkelstein, J.C., Kauvar, I.V., Fenno, L.E., Adhikari, A., Lammel, S., Mirzabekov, J.J., Airan, R.D., Zalocusky, K.A., et al. (2014). Natural neural projection dynamics underlying social behavior. Cell *157*, 1535–1551.

Hallett, M. (2015). Tourette Syndrome: Update. Brain Dev. *37*, 651–655.

Hintiryan, H., Foster, N.N., Bowman, I., Bay, M., Song, M.Y., Gou, L., Yamashita, S., Bienkowski, M.S., Zingg, B., Zhu, M., et al. (2016). The mouse cortico-striatal projectome. Nat. Neurosci. *19*, 1100–1114.

Jiang, L.H., Kasser, R.J., Altar, C.A., and Wang, R.Y. (1990). One year of continuous treatment with haloperidol or clozapine fails to induce a hypersensitive response of caudate putamen neurons to dopamine D1 and D2 receptor agonists. J. Pharmacol. Exp. Ther. *253*, 1198–1205.

Kapur, S. (1998). A new framework for investigating antipsychotic action in humans: lessons from PET imaging. Mol. Psychiatry *3*, 135–140.

Kapur, S., Zipursky, R., Jones, C., Shammi, C.S., Remington, G., and Seeman, P. (2000). A Positron Emission Tomography Study of Quetiapine in Schizophrenia: A Preliminary Finding of an Antipsychotic Effect With Only Transiently High Dopamine D2 Receptor Occupancy. Arch. Gen. Psychiatry *57*, 553–559.

Kharkwal, G., Brami-Cherrier, K., Lizardi-Ortiz, J.E., Nelson, A.B., Ramos, M., Del Barrio, D., Sulzer, D., Kreitzer, A.C., and Borrelli, E. (2016). Parkinsonism Driven by Antipsychotics Originates from Dopaminergic Control of Striatal Cholinergic Interneurons. Neuron *91*, 67–78.

Koch, J., Shi, W.-X., and Dashtipour, K. (2020). VMAT2 inhibitors for the treatment of hyperkinetic movement disorders. Pharmacol. Ther. *212*, 107580.

Kravitz, A.V., Freeze, B.S., Parker, P.R., Kay, K., Thwin, M.T., Deisseroth, K., and Kreitzer, A.C. (2010). Regulation of parkinsonian motor behaviours by optogenetic control of basal ganglia circuitry. Nature *466*, 622–626.

Lahiri, A.K., and Bevan, M.D. (2020). Dopaminergic Transmission Rapidly and Persistently

> Enhances Excitability of D1 Receptor-Expressing Striatal Projection Neurons. Neuron
> *106*, 277-290.e6.

Lane, R.F., and Blaha, C.D. (1987). Chronic haloperidol decreases dopamine release in striatum

> and nucleus accumbens in vivo: depolarization block as a possible mechanism of action.
> Brain Res. Bull. *18*, 135–138.

Lévesque, D., Martres, M.P., Diaz, J., Griffon, N., Lammers, C.H., Sokoloff, P., and Schwartz,

> J.C. (1995). A paradoxical regulation of the dopamine D3 receptor expression suggests
> the involvement of an anterograde factor from dopamine neurons. Proc. Natl. Acad. Sci.
> U. S. A. *92*, 1719–1723.

Marcott, P.F., Mamaligas, A.A., and Ford, C.P. (2014). Phasic dopamine release drives rapid

> activation of striatal D2-receptors. Neuron *84*, 164–176.

Marsden, C.D., and Jenner, P. (1980). The pathophysiology of extrapyramidal side-effects of

> neuroleptic drugs. Psychol. Med. *10*, 55–72.

Mathis, A., Mamidanna, P., Cury, K.M., Abe, T., Murthy, V.N., Mathis, M.W., and Bethge, M.

> (2018). DeepLabCut: markerless pose estimation of user-defined body parts with deep
> learning. Nat. Neurosci. *21*, 1281–1289.

Meyer, A.F., Poort, J., O'Keefe, J., Sahani, M., and Linden, J.F. (2018). A Head-Mounted Camera

> System Integrates Detailed Behavioral Monitoring with Multichannel Electrophysiology in
> Freely Moving Mice. Neuron *100*, 46-60.e7.

Moore, H., Todd, C.L., and Grace, A.A. (1998). Striatal Extracellular Dopamine Levels in Rats

> with Haloperidol-Induced Depolarization Block of Substantia Nigra Dopamine Neurons. J.
> Neurosci. *18*, 5068–5077.

Nelson, A.B., and Kreitzer, A.C. (2014). Reassessing models of basal ganglia function and

> dysfunction. Annu. Rev. Neurosci. *37*, 117–135.

Peralta, V., and Cuesta, M.J. (2010). The effect of antipsychotic medication on neuromotor

abnormalities in neuroleptic-naive nonaffective psychotic patients: a naturalistic study with haloperidol, risperidone, or olanzapine. Prim. Care Companion J. Clin. Psychiatry *12*, PCC.09m00799.

Peralta, V., Campos, M.S., De Jalón, E.G., and Cuesta, M.J. (2010). Motor behavior abnormalities in drug-naïve patients with schizophrenia spectrum disorders. Mov. Disord. *25*, 1068–1076.

Rao, A.S., and Camilleri, M. (2010). Review article: metoclopramide and tardive dyskinesia. Aliment. Pharmacol. Ther. *31*, 11–19.

Reches, A., Burke, R.E., Kuhn, C.M., Hassan, M.N., Jackson, V.R., and Fahn, S. (1983). Tetrabenazine, an amine-depleting drug, also blocks dopamine receptors in rat brain. J. Pharmacol. Exp. Ther. *225*, 515–521.

Remington, G., and Kapur, S. (1999). D2 and 5-HT2 receptor effects of antipsychotics: bridging basic and clinical findings using PET. J. Clin. Psychiatry *60 Suppl 10*, 15–19.

Reynolds, G.P., Brown, J.E., McCall, J.C., and Mackay, A.V. (1992). Dopamine receptor abnormalities in the striatum and pallidum in tardive dyskinesia: a post mortem study. J. Neural Transm. Gen. Sect. *87*, 225–230.

Ribot, B., Aupy, J., Vidailhet, M., Mazère, J., Pisani, A., Bezard, E., Guehl, D., and Burbaud, P. (2019). Dystonia and dopamine: From phenomenology to pathophysiology. Prog. Neurobiol. *182*, 101678.

Roberts, M.S., McLean, S., Millingen, K.S., and Galloway, H.M. (1986). The pharmacokinetics of tetrabenazine and its hydroxy metabolite in patients treated for involuntary movement disorders. Eur. J. Clin. Pharmacol. *29*, 703–708.

Rogue, P., Hanauer, A., Zwiller, J., Malviya, A.N., and Vincendon, G. (1991). Up-regulation of dopamine D2 receptor mRNA in rat striatum by chronic neuroleptic treatment. Eur. J. Pharmacol. *207*, 165–168.

Savasta, M., Dubois, A., Benavidès, J., and Scatton, B. (1988). Different plasticity changes in D1

and D2 receptors in rat striatal subregions following impairment of dopaminergic transmission. Neurosci. Lett. *85*, 119–124.

Sebel, L.E., Graves, S.M., Chan, C.S., and Surmeier, D.J. (2017). Haloperidol Selectively Remodels Striatal Indirect Pathway Circuits. Neuropsychopharmacology *42*, 963–973.

See, R.E. (1991). Striatal dopamine metabolism increases during long-term haloperidol administration in rats but shows tolerance in response to acute challenge with raclopride. Neurosci. Lett. *129*, 265–268.

Shirakawa, O., and Tamminga, C.A. (1994). Basal ganglia GABAA and dopamine D1 binding site correlates of haloperidol-induced oral dyskinesias in rat. Exp. Neurol. *127*, 62–69.

Silm, K., Yang, J., Marcott, P.F., Asensio, C.S., Eriksen, J., Guthrie, D.A., Newman, A.H., Ford, C.P., and Edwards, R.H. (2019). Synaptic Vesicle Recycling Pathway Determines Neurotransmitter Content and Release Properties. Neuron *102*, 786-800.e5.

Soares-Cunha, C., Coimbra, B., Sousa, N., and Rodrigues, A.J. (2016). Reappraising striatal D1- and D2-neurons in reward and aversion. Neurosci. Biobehav. Rev. *68*, 370–386.

Yael, D., Zeef, D.H., Sand, D., Moran, A., Katz, D.B., Cohen, D., Temel, Y., and Bar-Gad, I. (2013). Haloperidol-induced changes in neuronal activity in the striatum of the freely moving rat. Front. Syst. Neurosci. *7*, 110.

Zai, C.C., Maes, M.S., Tiwari, A.K., Zai, G.C., Remington, G., and Kennedy, J.L. (2018). Genetics of tardive dyskinesia: Promising leads and ways forward. J. Neurol. Sci. *389*, 28–34.

CHAPTER 5

Conclusions

5.1 Conclusions

The work presented here provides new insights into basal ganglia circuitry and explores how dysfunction within these circuits contributes to loss of motor control. First, we explore the how several models of basal ganglia function contribute to our understanding Parkinson's disease, then weigh the evidence underlying these different models (Chapter 2). Next, we demonstrate that striosome and matrix represent at least two functionally distinct circuits within the striatum. While matrix neurons receive greater sensorimotor input from the cortex and project to traditional basal ganglia output nuclei, striosome neurons receive greater limbic information and send substantial inhibition to SNc dopamine neurons (Chapter 3). Lastly, we investigate the cellular and circuit mechanisms of tardive dyskinesia, providing evidence that this disorder is mediated by hyperdopaminergic signaling onto direct pathways neurons in the ventrolateral striatum (Chapter 4).

This work highlights the utility of the classical model in understanding the basal ganglia, while underscoring the need to expand through additional models that integrate the circuit's full complexity. Our finding that striosome neurons receive greater input from the prelimbic cortex and act as the predominant source of striatal inhibition to SNc dopamine neurons shines light on a striatal pathway whose function *in vivo* is largely under studied. As discussed in an earlier chapter, recent work suggests that striosomes play a role in cost-benefit decision making. Future work may attempt to isolate how striosome output to dopamine neurons is involved in this process. Additionally, it is possible that striosome and matrix will play a role in understanding diseases of the basal ganglia. Work in progress aims to examine how activity of dopamine neurons may relate to their pattern of degeneration in diseases such as Parkinson's disease. Striosomes may

represent a powerful regulator of SNc activity, forming a negative feedback loop that could prevent excessive dopaminergic activity. If elevated activity of dopamine neurons contributes to their degeneration, breakdown of this potential negative feedback provided by striosomes could play an important role in such a process.

In recent years, advances in technology have been instrumental in developing our understanding of cell types and their functions. Single-cell sequencing has allowed identification of new cell types, whose connectivity can now be dissected using modern tracing tools, and whose function can be probed using a variety of optical and chemogenetic tools. This general approach has led to a surge of discovery within the basal ganglia. Our work on striosomes points toward an untapped potential in substituting developmental definitions of cell types into this pipeline. It may be possible that many other cell types differentiate their connectivity from the neighbors at particular points in time before adopting overlapping molecular identities that would make them indistinguishable in an adult animal. Developmental studies will likely shed light on how information is parallelized within the basal ganglia and may expedite discovery of additional cell types.

Lastly, this work reaffirms the need to connect patterns of neural activity to behavior in order to understand diseases such as tardive dyskinesia. Despite decades of research into the effects of antipsychotics on neural activity and the testing of numerous pharmacological interventions to ameliorate tardive dyskinesia, no clear model has emerged to explain the disorder. While our findings diverge from prevailing models of dysfunction in tardive dyskinesia, they are still largely in line with predictions from the parallel circuit and classical models. Given the multiple avenues in the classical model for modulating behavior, we propose that the linking neural activity directly to the involuntary movements is the missing glue required to bind the work from previous studies together into a coherent understanding.

In conclusion, this work demonstrates the utility of approaching the basal ganglia with both an evidence-based model of its function and an open mind towards its potential. Leaps and

bounds have been made over the past century in understanding the basal ganglia, but here at

the end of a PhD, it has never been clearer that we are only at the beginning.

Publishing Agreement

It is the policy of the University to encourage open access and broad distribution of all theses, dissertations, and manuscripts. The Graduate Division will facilitate the distribution of UCSF theses, dissertations, and manuscripts to the UCSF Library for open access and distribution. UCSF will make such theses, dissertations, and manuscripts accessible to the public and will take reasonable steps to preserve these works in perpetuity.

I hereby grant the non-exclusive, perpetual right to The Regents of the University of California to reproduce, publicly display, distribute, preserve, and publish copies of my thesis, dissertation, or manuscript in any form or media, now existing or later derived, including access online for teaching, research, and public service purposes.

DocuSigned by:

Matthew McGregor

A062448CC16A4D8...   Author Signature

3/10/2022

Date